N70-29173

Report No. [redacted]30
Part IV

TWO PHASE FLOW AND HEAT TRANSFER IN POROUS BEDS UNDER VARIABLE BODY FORCES

CR-102708

Final Report
Part IV
By Admiral S. Piper and Harold R. Henry

Part I N70-18908

Part III N70-27074

Part II T70-01264

Project Director:

Harold R. Henry, Ph.D.
Professor of Engineering Mechanics
University of Alabama

Submitted to

George C. Marshall Space Flight Center
National Aeronautics and Space Administration
Huntsville, Alabama

Contract No. NAS8-21143
University of Alabama No. 22-6560

December 1969
Bureau of Engineering Research
University of Alabama

SQT. 61944

N70-29743

TWO PHASE FLOW AND HEAT TRANSFER IN POROUS BEDS UNDER VARIABLE BODY FORCES - PART IV

S. Piper, et al.

University of Alabama
University, Alabama

December 1969

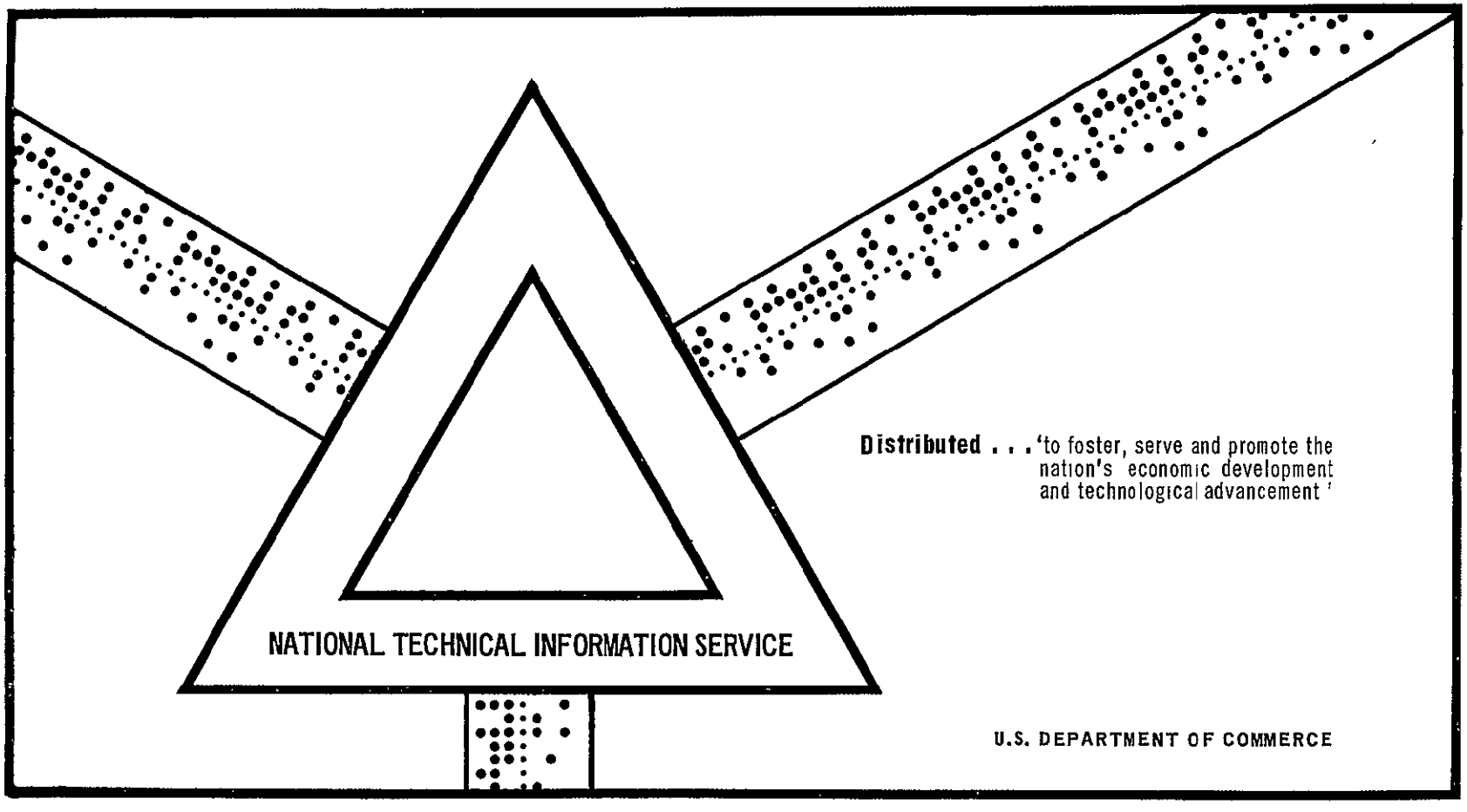

CR-102708

Report No. 113-30
Part IV

TWO PHASE FLOW AND HEAT TRANSFER IN POROUS BEDS UNDER VARIABLE BODY FORCES

Final Report
Part IV
By Admiral S. Piper and Harold R. Henry

Project Director:

Harold R. Henry, Ph.D.
Professor of Engineering Mechanics
University of Alabama

Submitted to

George C. Marshall Space Flight Center
National Aeronautics and Space Administration
Huntsville, Alabama

Contract No. NAS8-21143
University of Alabama No. 22-6560

December 1969
Bureau of Engineering Research
University of Alabama

TABLE OF CONTENTS

LIST OF FIGURES

PREFACE

This is Part IV of a seven part final report under Contract No. NAS8-21143 between the George C. Marshall Space Flight Center and the University of Alabama. This report includes the results of a systems analysis of the transients occurring in an assumed model of the proposed flight experiment for boiling and vapor bubble studies. The technique of digital simulation is employed in the analysis.

The basic equations of fluid mechanics and heat transfer are determined for each component making up the assumed flight experiment model. This includes the fluid flow circuit, the heat exchangers for boiling and condensation, the pump and the motor. These equations are solved simultaneously for a limited range of variables by digital simulation using a high speed computer.

The results indicate that digital simulation can be a useful tool in determining the total system characteristics. This is expecially useful in determining start up or shut down transients as well as transients resulting from catastrophic events such as value failure.

CHAPTER I

INTRODUCTION

Early liquid propellant rockets experienced difficulty in maintaining a steady flow of fuel to the rocket engines. The trouble in these early rockets was due to the turbulent flow conditions existing at the interface between the fuel feed lines and the propellant tanks. Fine mesh screens and thin porous blankets were found to be effective in reducing these undesirable effects. Recently the more efficient cryogenic liquid fuels are being used. A characteristic of these cryogenic liquid fuels is a tendency to boil or vaporize in the propellant tanks during flight. This vapor collects on the above mentioned screens and obstructs the flow of the liquid fuel to the engines. A possible solution to this problem may be replacing the screens with coarsely packed porous beds.

Therefore, in order to gain more fundamental knowledge in the area of two-phase flow through porous beds, the National Aeronautics and Space Administration in Huntsville, Alabama awarded the University of Alabama the contract to design a flight experiment to determine the behavior of two-phase vapor-liquid and/or gas-liquid flow through porous beds in a low gravity environment. This thesis is concerned specifically with that part of the experiment in which the second phase (vapor) is obtained by heating the

liquid (water) to boiling by using electrical-thermal elements within the porous bed.

An idealized mathematical model of the proposed system is developed. The resulting system of differential and algebraic equations is digitally simulated using the International Business Machine (IBM) System/360 Continuous System Modeling Program (CSMP). The objective of the simulation is to study and evaluate the modeling of the system; however, this thesis does not give an exhaustive study of the system but shows representative results obtainable using the simulation.

In Chapter II the proposed system is divided into several subsystems and the equations of motion are developed for each subsystem. Chapter III begins with a discussion of some of the salient features of CSMP as they pertain to this thesis and concludes with the development of the simulation program including a flow-diagram. Within Chapter IV the discussion and display of the simulation results are given. In Chapter V, the final chapter in the thesis, concluding remarks with regard to the digital simulation and results obtained from the simulation are given.

CHAPTER II

DEVELOPMENT OF THE SYSTEM EQUATIONS

In this development, the mathematical models derived are for an idealized system. An idealized system implies the ultimate in functional capability and is not limited by either physical or economic factors. The idealized model conveys the functional sense in which the system is to be used and is sufficiently complete, while avoiding attention to fine details.

The development of the "equations of motion" for the fluid system is now given. The expression "equations of motion" is used for both differential and algebraic equations within the system. Assumptions and/or approximations made, are stated during each mathematical development.

This system is a "mixed system" in that electrical, mechanical, fluid and thermodynamic quantities appear together and are, of course, interrelated. A diagram of the entire system is given in Figure 1. The system is discussed in this chapter under the following headings:

Motor and Speed Control

Positive-Displacement Pump

Preheater and Control

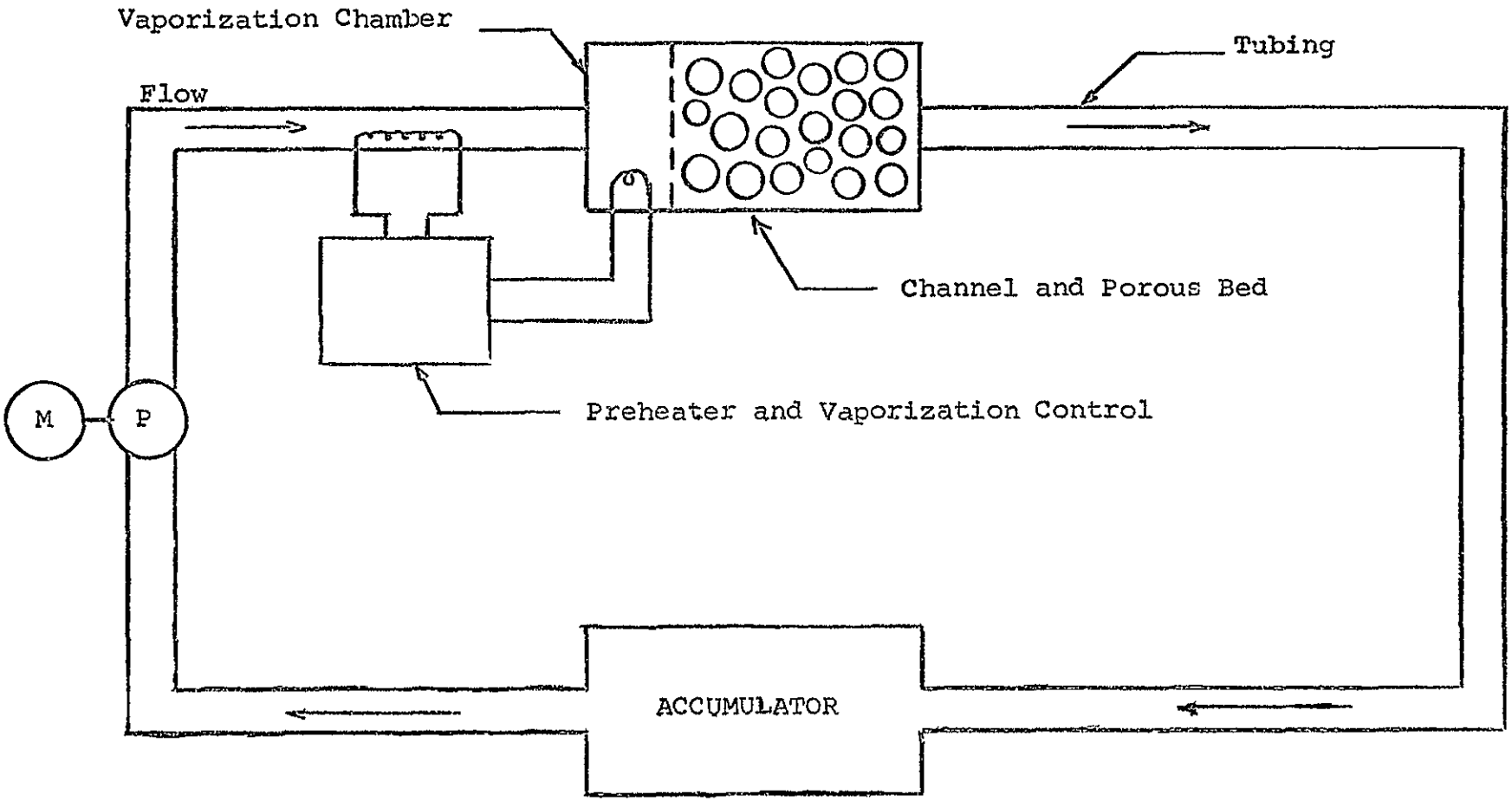

FIGURE 1. SCHEMATIC DIAGRAM OF THE FLUID SYSTEM.

Vaporization Chamber and Condensation

Channel and Porous Bed

Accumulator and Vaporization Control

Pressure Equations

Motor and Speed Control

A linear DC-motor using field voltage as a means to vary speed is used. It is assumed the motor is supplied with a constant armature current.

This means for regulating the speed of the DC-motor is realized through the use of state-variable feedback.

Conventional methods of synthesizing a linear control system usually call for some type compensation network to be designed to achieve the performance characteristic needed to perform the system's designated task. Through the use of state-variable feedback, the task of synthesizing a compensating network is reduced to that of determining the appropriate feedback coefficients. This is done using simple algebra and block diagram manipulations. The designer selects the time response and then Laplace transforms it into a rational fraction of the complex variable s. The system is depicted in standard block diagram form where all the state variables are fed back through the appropriate transducers to the input of the system. In following the above procedure, a system can be made to conform to given time domain specifications as long as those specifications can be translated into

the appropriate mathematics.[1]

The state-variable synthesis technique is now demonstrated:

$$\dot{L}\overset{\circ}{i}_f + Ri_f = V_f \tag{1}$$

$$J\overset{\circ}{W} + BW = T - T_L - T_D \tag{2}$$

$$V_f = K_a \text{ ERROR} \tag{3}$$

$$T = K_m i_f \tag{4}$$

$$\text{ERROR} = \text{REF} - k_1 W - k_2 i_f \tag{5}$$

Equations (1) and (2) have been time scaled so that the unit of time employed in this development is minutes.

t = time in minutes

i_f = the field current of motor (amp)

$\overset{\circ}{i}_f$ = di_f/dt (amp/min)

$\dot{L}$ = the field inductance (henrys)/60

R = the field resistance (ohms)

$\overset{\circ}{W}$ = the derivative of angular velocity with respect to time

J = the polar moment of enertia of the motor plus the pump ($lbf\text{-}in^2/386.4$)

lbf = pounds force

B = viscous friction of the motor plus the pump (lbf-in-min)

---

[1]Superscripts denote references given at the end of this thesis.

T = the electromagnetic torque of the motor (lbf-in)

T_L = the torque needed to overcome the fluids resistance to flow

T_D = any arbitrary disturbance torque applied to motor shaft (lbf-in)

V_f = the applied field control voltage (volts)

K_a = the DC-amplifier gain

K_m = the electromagnetic torque constant of the DC-motor (lbf-in/amp)

REF = the applied reference DC-voltage to the motor speed control (volts)

k_1 = feedback coefficient (volts-min/rad)

k_2 = feedback coefficient (ohms)

A block diagram representation of the Laplace transformed electrical and mechanical Equations 1 through 5 is given in Figure 2.

The motor and the mechanical load forms a second-order system. A second-order system which is slightly underdamped is assumed to be adequate. Second-order systems have been thoroughly studied and there exist normalized plots[2] for different undamped natural frequencies (W_n) and damping factors ($\mathcal{Z}_n$). Therefore, the desired time response was easily transformed into a rational fraction of the complex variable s and is given by:

$$\theta(s) = W_n^2 / (s^2 + 2\mathcal{Z}_n W_n s + W_n^2) \qquad (6)$$

where the coefficients W_n and $\mathcal{Z}_n$ completely determine the response of Equation 6 to a unit-step input.

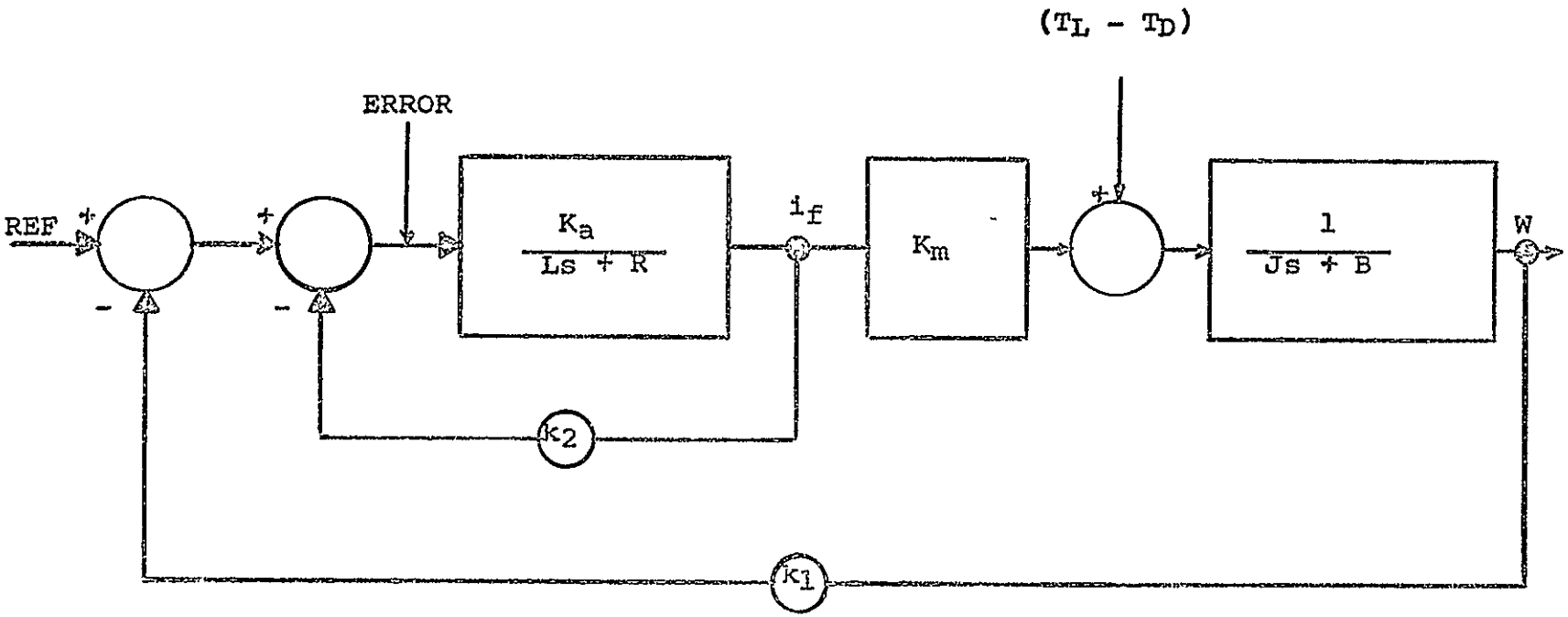

FIGURE 2. BLOCK DIAGRAM OF THE MOTOR SPEED CONTROL SYSTEM.

In order to consider the system shown in Figure 2 to be a single-input, single-output system, the torques T_L and T_D are set to equal to zero.

The block diagram of the speed control system in Figure 2 is now manipulated into a convenient form so the feedback coefficients may be determined. This is accomplished in two steps. See Figures 3(a) and (b).

Equating the results of Figure 3(b) to Equation 6 gives the results in Equation 7. The feedback coefficients k_1, k_2 and the gain K_a may be determined directly by equating like coefficients of the left and right sides of Equation 7.

$$W_n^2/(s^2 + 2\mathcal{Z}_n W_n s + W_n^2) = \frac{K_a K_m/L' J}{s^2 + (R/L' + B/J + k_2 K_a J)s + (K_a K_m k_1 + RB/LJ + k_2 K_a B)} \tag{7}$$

where:

W_n = the known undamped natural frequency of a second-order system (rad/min)

$\mathcal{Z}_n$ = the known damping factor of a second-order system

After k_1, k_2 and k_a are determined, the motor speed control system as shown in Figure 2 in mathematically equivalent to Equation 6 from the input, output viewpoint.

Positive-Displacement Pump

Before beginning the development of the positive-displacement pump, it is well to note a couple of general

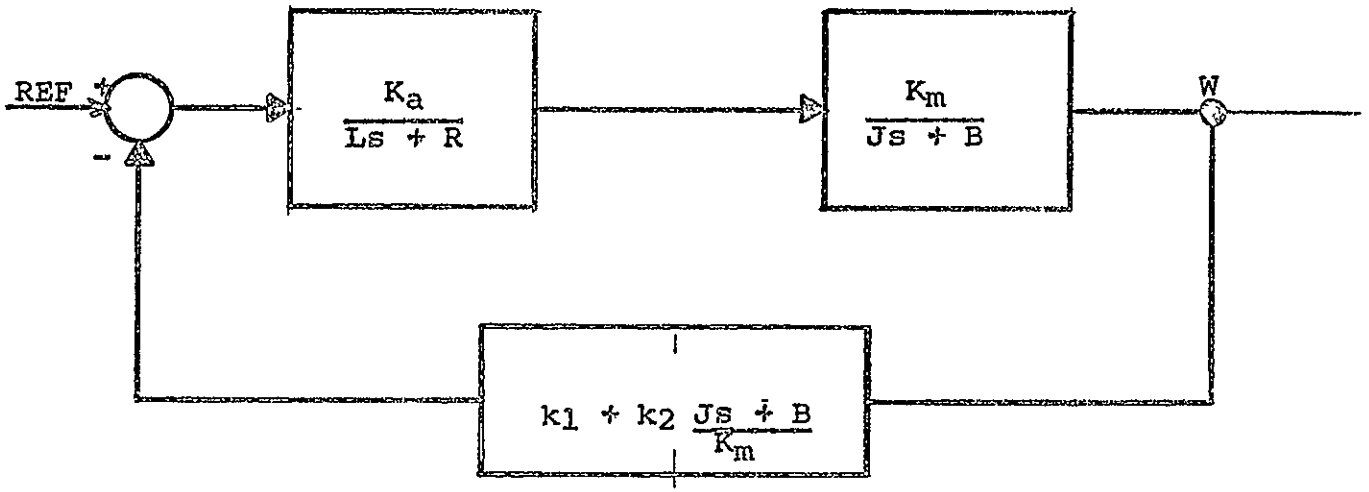

(a)

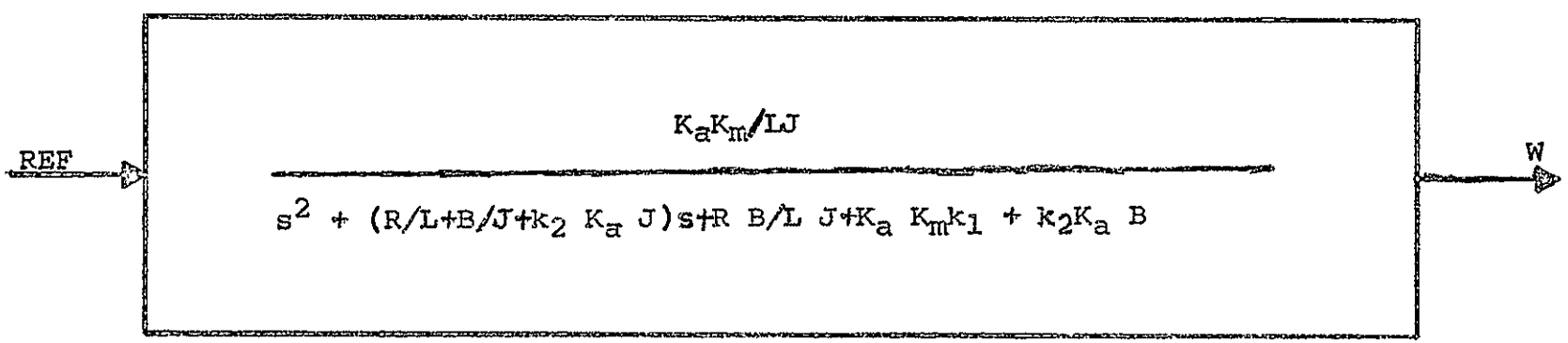

(b)

FIGURE 3. BLOCK DIAGRAM REDUCTION OF SPEED-CONTROL SYSTEM.

characteristics of this type of device.

Probably the most distinguishing feature of this device is that the quantity of liquid displaced per revolution of the shaft is approximately a constant. Another important characteristic is that the pressure developed by the pump is a function of the fluid circuit.

This mechanical-fluid device is analogous to the constant current generator from electrical circuit theory if pressure is the analog of voltage and fluid flow is the analog of current.[1]

An ideal positive-displacement pump is defined as having no power losses due to friction and leakages and, consequently, has an efficiency of 100%. In practice, 80% efficiency is readily obtained and, therefore, as a first approximation, the system analyst will often use the ideal pump as the model for the actual device.[3]

Consider now the equations for the ideal positive-displacement pump:

$$\text{Mechanical Power In} = \text{Fluid Power Out}$$

$$T_L W = \Delta P Q \tag{8}$$

The torque, T_L (lbf-in), is required to overcome the back pressure of the fluid circuit in order to produce a given flow rate. The back pressure existing in a fluid circuit is a function of the physical parameters of the circuit.

The angular speed of the pump shaft is W. Since the motor is directly coupled to the pump, the motor speed and the pump speed are the same (rad/min). The differential pressure drop across the pump is ΔP (lbf/in^2).

The volumetric flow rate (Q) is normally expressed linearly in terms of the displacement constant (D_D) and the angular speed of the pump shaft.

$$Q = D_D W \tag{9}$$

Factors affecting the accuracy of Equation 9 are:[4]

1. Pump speed
2. Pressure at discharge and pressure on suction side
3. Viscosity of fluid
4. Amount of entrained air or non-condensable gases in fluid

of the above mentioned factors, the two most important for this system are numbers (2) and (4).

The pump used is assumed capable of delivering five gal/min into a back-pressure of at least an order of magnitude higher than is expected to occur during the experiment. The effects of large pressure differentials across the pump are to increase the amount of slip flow which decreases the efficiency of the device. Slip flow is defined as the flow in the reverse direction through a pump due to large pressure differentials.[5]

If two-phase flow were to occur through the pump, its exact effect would be difficult to predict, but it may be

concluded that the volumetric constant of the pump would effectively be reduced. This conclusion is drawn from an intuitive concept that since displacement volume would be shared by fluid and vapor, there would naturally be less fluid delivered per revolution. Therefore, to deliver the same flow the pump speed would have to be increased.

As implied from the above discussion, the entrainment of vapor through the pump is a highly undesirable phenomenon. It is assumed that this phenomenon does not occur. The validity of this assumption is checked with the simulation.

Preheater and Control

The first law of thermodynamics is sufficient to describe the process of heating flowing water in a tube, a typical cross-section of the preheater which is shown in Figure 4.

$$\begin{pmatrix}\text{rate of change of energy} \\ \text{within the control volume}\end{pmatrix} =$$

$$\begin{pmatrix}\text{rate of heat flow-in + rate that heat} \\ \text{is added by the heaters}\end{pmatrix} -$$

$$\begin{pmatrix}\text{rate of heat flow-out + rate of heat} \\ \text{transferred by convection}\end{pmatrix}$$

It is assumed the tubing and water are at the same temperature. Also transfer of energy from one section of water to another by conduction is neglected since the flow rates are much larger than the heat conduction rates. Heat conduction would be significant if the system was operated

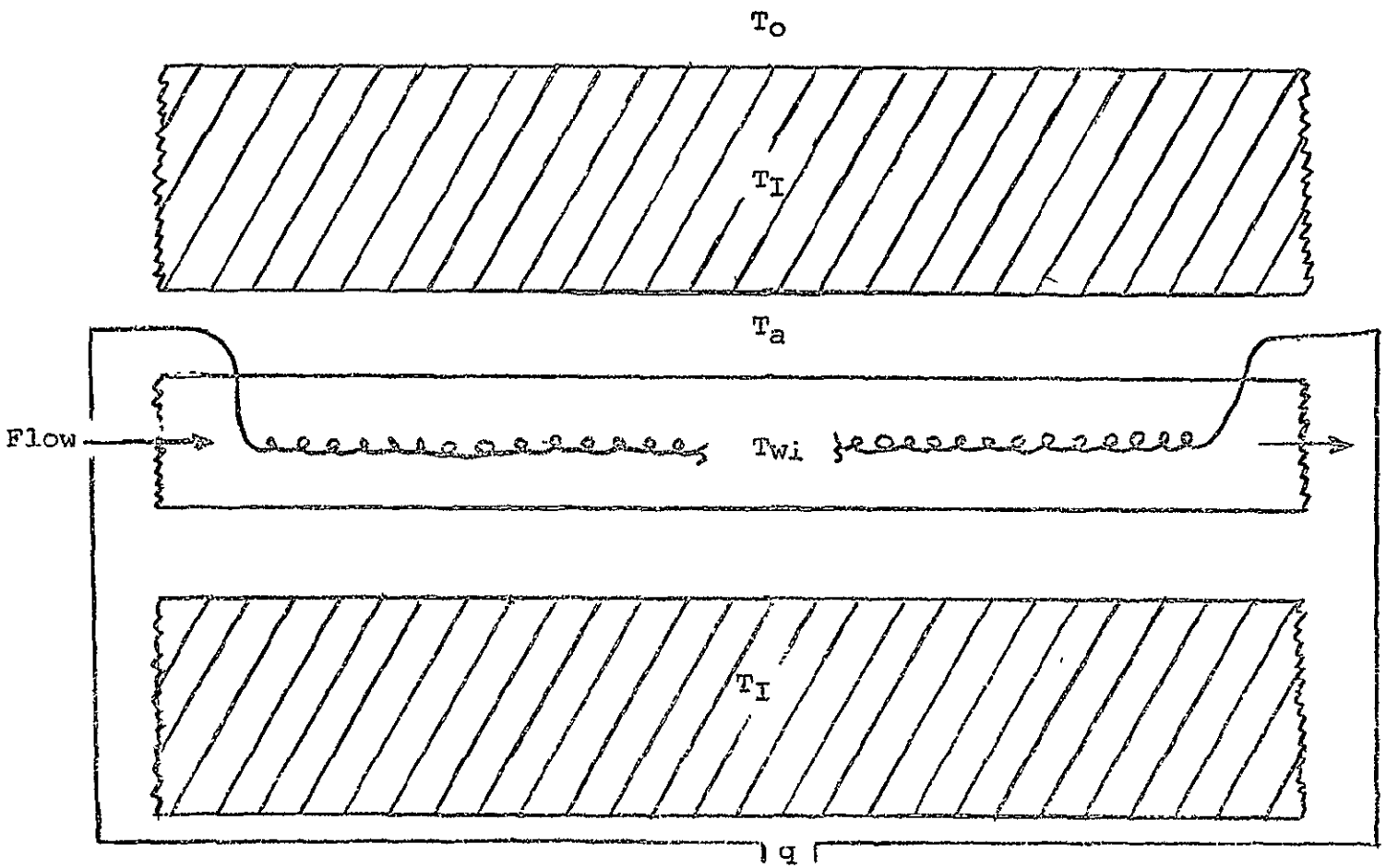

FIGURE 4. CROSS-SECTIONAL VIEW OF THE PREHEATER SECTION.

statically (no flow), with the heaters on since conduction would be the only thermal coupling between sections. But by the very nature of the experiment, the system will always operate dynamically.

The equations of motion of the preheater are given as follows:

$$P_w V_w C_w \dot{T}_{wi} = P_w C_w Q\ (T_{w(i-1)} - T_{wi}) + UA(T_a - T_{wi}) + Q1 \quad (10)$$

$$P_a V_a C_a \dot{T}_a = UA(T_{wi} - T_a) + U_1 A_1 (T_I - T_a) \quad (11)$$

$$P_I V_I C_I \dot{T}_I = U_1 A_1 (T_a - T_I) + U_2 A_2 (T_o - T_I) \quad (12)$$

where:

$\dot{T}$ = dT/dt

P_w = the density of water (lbm/in^3)

V_w = the volume of water in the ith section (in^3)

C_w = the specific heat of water (BTU/lbm$^\circ$F)

Q = the volumetric flow-rate of water (in^3/min)

U = the heat transfer coefficient between the tubing and air (BTU/in^2 min $^\circ$F)

A = the heat transfer area for the tubing and air (in^2)

$Q1$ = the heater input (BTU/min)

P_a = the density of air (lbm/in^3)

V_a = the volume of air in the ith section (in^3)

C_a = the specific heat of air (BTU/lbm $^\circ$F)

U_1 = the heat transfer coefficient between air and insulation material (BTU/in^2 min $^\circ$F)

A_I = the heat transfer area between the insulation and air (in^2)

P_I = the density of the insulation (lbm/in^3)

V_I = the volume of the ith section of insulation (in^3)

C_I = the specific heat of insulation (BTU/lbm ^oF)

T_o = ambient temperature (^oF)

The preheater control is an "on-off" or "bang-bang" type. In this particular case, the heat-input (Q1) in the preheater section is either completely on or completely off. Implementation of the "on-off" control is through the control law. The control law in this case consists of several logical statements which are:

If $T_{wi} \geq$ (Reference Temperature - DX) then Q1 = 0.0

If $T_{wi} \leq$ (Reference Temperature - DX-BAN) then Q1 = Qmax

If $T_{wi} <$ (Reference Temperature - DX), and T_{wi} is positive in sign, then Q1 = Qmax

If $T_{wi} <$ (Reference Temperature - DX) but > (Reference Temperature - DX-BAN), and $\overset{o}{T}_{wi}$ is megative in sign, then Q1 = 0.0

An arbitrary increment of temperature, DX, separates the upper limit of the BAN and the Reference Temperature (saturation temperature as determined by the absolute pressure in the ith section of the tubing). To account for inaccuracies in the control system, the increment, DX, was included to ensure the temperature T_{wi} would not reach the reference temperature.

The arbitrary increment of temperature is BAN in which the heat-input (Q1) can be off. Whether the heat-input (Q1) is off within the BAN increment is determined by the sign of the derivative of the water temperature ($dT_{wi}/dt = \overset{o}{T}_{wi}$) within the ith section of tubing. The width of this temperature increment is set by the requirements on the amount of vaporization needed to successfully accomplish the flight experiment.

A time response like that shown in Figure 5 is representative for the preheater control system.

If vaporization occurs in the preheater section, Equation 10 must be replaced by another equation in order to account for this change of phase. The derivation and explanation of this phenomenon is given in a later section.

Vaporization Chamber and Condensation

The saturation temperature (boiling point of water) is a function of both pressure and temperature. Formation of vapor bubbles is considered negligible at temperatures below saturation temperature. At saturation temperature, the vapor pressure tends to exceed the local absolute pressure which results in the development of vapor bubbles. Enough vapor bubbles are formed to prevent the temperature of the water to rise above the boiling point. Therefore, the temperature of the boiling water remains constant until either all the liquid is vaporized or there is a change in the absolute pressure.

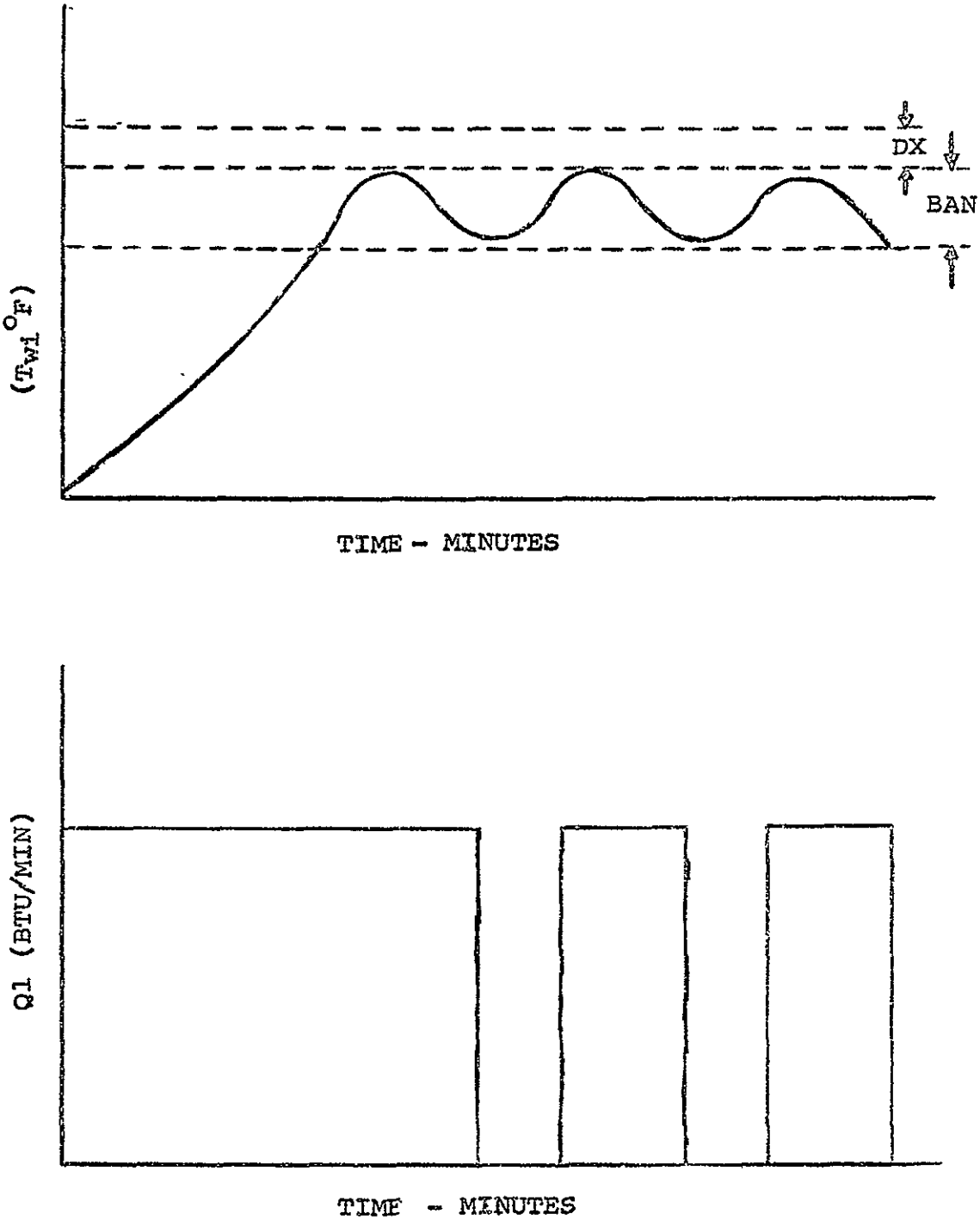

FIGURE 5. TIME RESPONSE OF THE PREHEATER CONTROL.

In this presentation all the boiling is assumed to occur in the "vaporization chamber" even though localized vaporization due to extreme pressure gradients may take place.

An energy balance is written for the cross-section of the vaporization chamber in Figure 6.

$$\begin{pmatrix}\text{rate of energy stored}\\ \text{within the liquid}\end{pmatrix} =$$

$$\begin{pmatrix}\text{rate of heat flow-in + rate}\\ \text{that heat is added by the heaters}\end{pmatrix} -$$

$$\begin{pmatrix}\text{rate of heat flow-out + vapor boil-up rate}\end{pmatrix}$$

$$d/dt(P_wV_wC_wT_{wc}) = -\lambda v + P_wC_wQ(T_w-T_{wc}) + UA(T_o - T_{wc}) \tag{13}$$

Upon comparing Equation 10 and 13, two differences are noted. First, in Equation 13, the derivative of the entire term on the left side is taken since the volume of water is changing with vaporization. Second, the term λv appears on the right side of Equation 13. This term accounts for the loss of heat due to vaporization where v is called vapor boil-up rate and λ is the latent heat of the vapor.

Performing the differentiation of Equation 13 gives

$$P_wC_wT_{wc}\dot{V}_w + P_wC_wV_w\dot{T}_{wc} = + Q2 + P_wC_wQ(T_w - T_{wc}) + UA(T_o - T_{wc}) - \lambda v. \tag{14}$$

Substituting $P_w\dot{V}_w = - v$ into Equation 14 gives

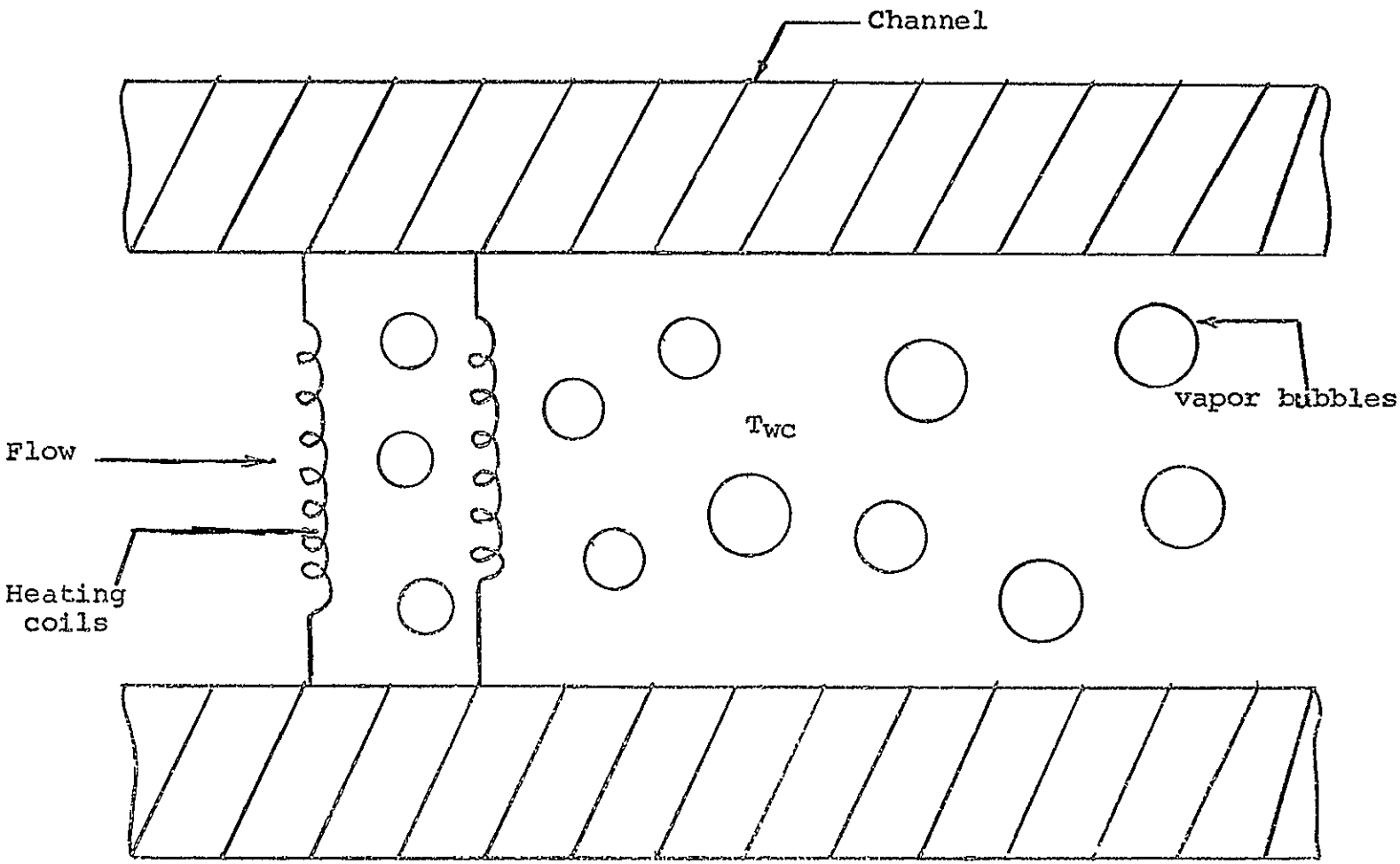

FIGURE 6. CROSS-SECTION OF VAPORIZATION CHAMBER.

$$v = P_w C_w Q/(\lambda - C_w T_{wc}) \quad (T_w - T_{wc}) \quad +$$

$$UA_3/(\lambda - C_w T_{wc}) \quad (T_o - T_{wc}) \quad - \qquad (15)$$

$$P_w C_w V_w \dot{T}_{wc}/(\lambda - C_w T_{wc}) + Q2/(\lambda - C_w T_{wc}).$$

Now Equation 15 gives the rate of vaporization in terms of fluid temperature and the heat input Q2. The method of controlling the vaporization will be given in Section VI.

Condensation is the negative of vaporization and is dependent upon the heat losses in those sections in which vaporization occurs. Recalling the assumption that all the vaporization occurs locally within the vaporization chamber, but condensation will occur in sections of the system which contains vapor bubbles. It is assumed that vapor bubbles cannot exist in those sections in which the surrounding fluid temperature is below saturation. These assumptions are discussed in a later section with regard to a modified definition of thermodynamic quality. The equations describing condensation within the system are of the same form as the vaporization expression, Equation 15. There is a condensation equation for each section of the system in which vapor bubbles exist. A typical expression is

$$CONDEN = P_w C_w Q/(\lambda - C_w T_{wc}) \quad (T_{wc} - T_w) \quad + \qquad (16)$$

$$UA_3(T_{wc} - T_o)/(\lambda - C_w T_w)$$

where the terms in Equation 16 are similar to those in Equation 15.

Channel and Porous Bed

The porous bed consists of small glass spheres packed in the channel. How well the porous media is packed can be expressed by the so called "porosity of the bed." Figure 7 shows a section of the bed displaying the porous media. Porosity ($\emptyset$) is defined as the ratio of the pore volume to the total volume.[6]

The overall objective of this experiment is to determine the behavior of two-phase vapor-liquid flow through porous beds in low gravity environment. Therefore, to the fluid dynamist and the thermodynamist, the phenomenon occurring within the channel and porous bed is the focal point of their work. But to the system analyst, the channel and porous bed form but a link of an entire system. In keeping with the system's point of view, the equations of motion for this section are derived by simplifying the problem as much as possible.

Equation 17, which had been developed by another investigator, is used as a starting place in this development.[7]

$$dP/dX = \alpha(u\ V_L/d^2 + (\beta u\ V_L/d^2)\ Re \qquad (17)$$

Equation 17 allows one to calculate the pressure at any point along the length of the porous bed as a function of the experimental parameters α, β, and the Reynolds Number (Re) for the flow. Reynolds Number in the channel is defined to be the ratio of the product of fluid density,

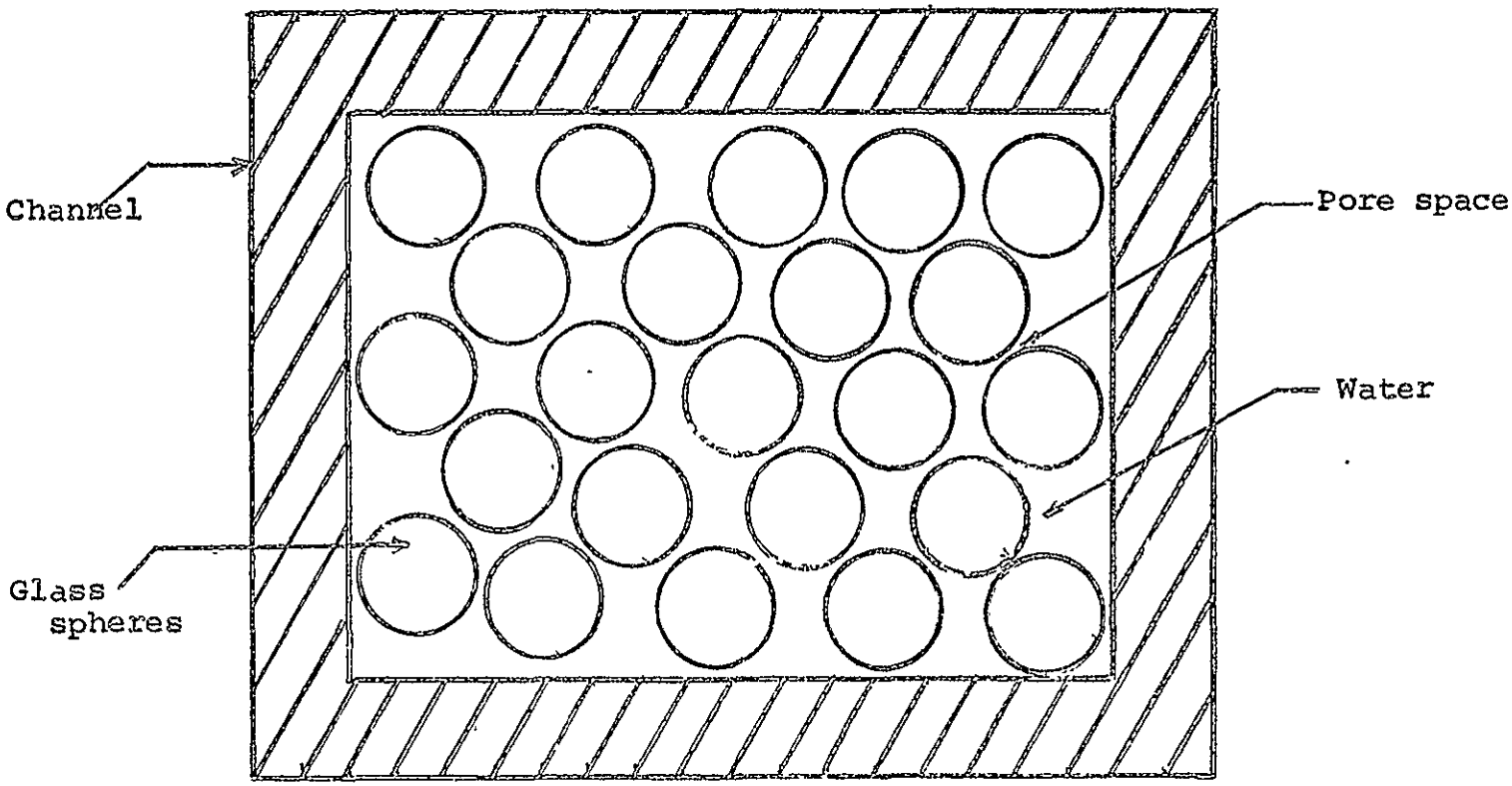

FIGURE 7. CROSS-SECTIONAL VIEW OF CHANNEL SHOWING POROUS MEDIA.

the diameter of one sphere, and the average fluid velocity to the fluid viscosity. The other parameters in Equation 17 are d, the diameter of a sphere, V_L, the velocity of the water, and u, the viscosity of the water. The temperature and pressure are no longer independent properties of water once saturation is reached. So, if the pressure is known, the temperature of the saturated water is automatically determined. With the dependence of temperature upon pressure along with results of Equation 17, the temperature variation of saturated water in the porous bed can be determined. During times when the water within the porous bed is not saturated, then an equation of the form of Equation 15 without the terms λ v and Q2 is applicable for the unsaturated water.

In order to make the analysis of the channel and porous bed complete, expressions for the temperature of the porous media and channel as they are coupled to the water temperature must be developed.

The porous media is assumed to be equally distributed in a cross-section and along the length of the bed. From the knowledge of the volume of the bed, porosity of the bed, density of porous media, and diameter of one sphere, the total surface area and the total mass of the porous media can be calculated. If the bed is divided into n sections, then the surface area of the porous media in the nth section is the total surface area divided by n, the number of sections. Similarly, the mass of the porous media in the nth section

is the total mass of the porous media divided by the number of sections. The surface area of the porous media is needed in order to calculate the heat transfer from the water to the porous media or vice versa. In order to calculate the heat capacity of the porous media, the mass of the porous media is required.

The following procedure is used to obtain the area and mass of a section:

$$V_S = (1-\phi)V_C \tag{18}$$

$$M_S = P_{pm}\, V_S \tag{19}$$

$$B_n = (1-\phi)V_C/4/3\pi r_b^3 \tag{20}$$

$$B_a = 3(1-\phi)V_C/r_b \tag{21}$$

where:

V_S = the volume of porous media in channel (in^3)

V_C = the volume of channel (in^3)

M_S = mass of porous media in channel (lbm)

P_{pm} = the density of the porous media (lbm/in^3)

B_n = the number of spheres in channel

r_b = the radius of a sphere (in)

B_a = the total surface area of the glass sphere (in^2)

Now the mass of the porous media in section n is

$$M_{S(n)} = P_{pm}V_S/n. \tag{22}$$

The surface area of the porous media in section n is

$$B_{a(n)} = 3(1-\emptyset)\ V_c/r_b\ n. \tag{23}$$

Now the energy equations can be written for the nth section of the porous media, the water in the nth section of the porous bed, and the nth section of the channel. See Figure 8.

The energy balance for the nth section of the channel can be expressed as follows:

$$\begin{pmatrix}\text{rate of accumulation of energy}\\ \text{within section n of channel}\end{pmatrix} =$$

$$\begin{pmatrix}\text{energy transferred from the water to the channel -}\\ \text{energy transferred from the channel to the air}\end{pmatrix}$$

$$P_c V_c C_c \dot{T}_{c(n)} = U_3 A_3 (T_{w(n)} - T_{c(n)}) + U_4 A_3 (T_o - T_{c(n)}). \tag{24}$$

where:

P_c = the density of channel material (lbm/in^3)

C_c = the specific heat of the channel material ($BTU/lbm-^oF$)

V_c = the shell volume of the nth section of the channel (in^3)

U_3 = the heat transfer coefficient between the water and channel (BTU/in^2-min-^oF)

A_3 = the heat transfer surface area (in^2)

U_4 = the heat transfer coefficient between the channel and air (BTU/in^2-min-^oF)

The energy balance for the nth section of the porous media is

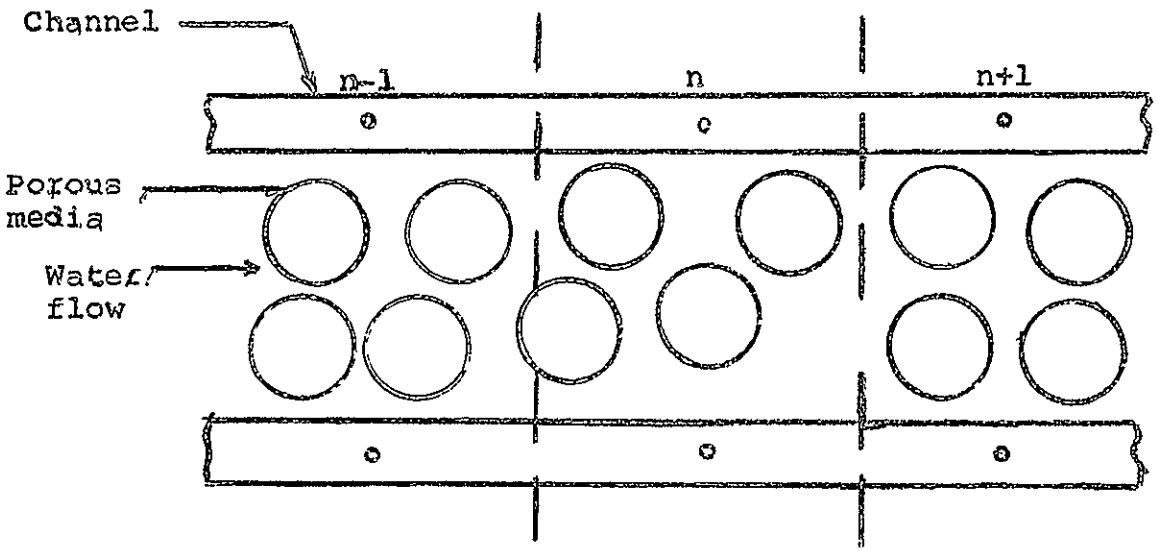

FIGURE 8. NTH SECTION OF CHANNEL AND POROUS BED.

$$\begin{pmatrix}\text{rate of accumulation of energy}\\ \text{within the nth section of porous media}\end{pmatrix} =$$

$$\begin{pmatrix}\text{energy transferred from the water}\\ \text{to the porous media in section n}\end{pmatrix}$$

$$P_g V_g C_g \dot{T}_g = U_5 A_4 (T_{w(n)} - T_{g(n)}) \qquad (25)$$

where:

P_g = the density of the porous media (lbm/in^3)

V_g = the volume of the porous media in the nth section (in^3)

C_g = the specific heat of the porous media ($BTU/lbm-^oF$)

U_5 = the heat transfer coefficient between the porous media and water (BTU/in^2-min-^oF)

A_4 = the heat transfer surface area for water and the porous media (in^2)

Equation 26 describes the temperatures behavior of the water at the nth section of the channel. The development of Equation 26 is similar to Equation 10 and will not be given.

$$\begin{pmatrix}\text{rate of accumulation of energy in the}\\ \text{nth section of water in the porous bed}\end{pmatrix} =$$

$$\begin{pmatrix}\text{heat-in due to flow + heat transfer from the}\\ \text{porous media + heat transferred from channel}\end{pmatrix} -$$

$$\begin{pmatrix}\text{heat-out due to flow}\end{pmatrix}$$

$$P_{wf(n)} V_{wf(n)} C_{wf(n)} \dot{T}_{wf(n)} =$$

$$P_{wf(n)} C_{wf(n)} Q (T_{wf(n-1)} - T_{wf(n)}) + \qquad (26)$$

$$U_5 A_4 (T_{g(n)} - T_{wf(n)}) + U_3 A_3 (T_{c(n)} - T_{wf(n)}).$$

The symbols in Equation 26 are similar to those which have been previously defined.

A summary of the results obtained in this section is now given. The channel was subdivided into several sections. The porous media was assumed to be evenly distributed throughout the channel. Then the total surface area and total mass of the porous media was determined. The surface area of any section is equal to the total surface area divided by the number sections, n. The mass of the porous media in any section is determined similarly. The time-dependent equations for temperatures of the channel, of porous media, and of the water were written. Thus the mathematical model for the process within this section was obtained.

Equations 24, 25, and 26 are valid as long as the water temperature is below saturation. After saturation has been reached, Equation 26 is replaced by Equation 27 with Equations 24 and 25 remaining the same. The appropriate equation was employed according to logical rules programmed into the simulation and is discussed in Chapter III.

$$T_{wf}(n) = F(P_n) \tag{27}$$

The function, $F(P_n)$, expresses the relation between the temperature, $T_{wf}(n)$, in the nth section of the channel and the absolute pressure, P_n, in the nth section of the channel when saturation has occurred. The function

$F(P_n)$ is constructed from data taken from thermodynamic tables of saturation pressure and temperature.

Accumulator and Vaporization Control

The accumulator and vaporization control are presented together because in this system they are integrally related.

Accumulators are widely used in fluid systems to smooth transients such as line shock, valve surges, and pump flow-ripple. Any time a positive-displacement pump is used, as in this system, there will be some flow ripple. The amount of ripple depends upon the particular pump.[8]

A simple example of an accumulator is an open tank with a piston or weight sitting on top of the fluid. See Figure 9. The piston is free to move up and down depending upon the level of water in the tank.

$$\begin{pmatrix}\text{rate of accumulation}\\ \text{of water in tank}\end{pmatrix} = \begin{pmatrix}\text{Flow-in} - \text{Flow-out}\end{pmatrix}$$

$$\overset{o}{V} = Q_{in} - Q_{out} \tag{28}$$

The pressures at the entrance and exit of the accumulator as given in Figure 9 are:

$$P_4 = W_p/A_p + \gamma_w h' \tag{29}$$

$$P_5 = W_p/A_p + \gamma_w h \tag{30}$$

where:

W_p = the weight of the piston (lbf)

A_p = the area of the piston (in^2)

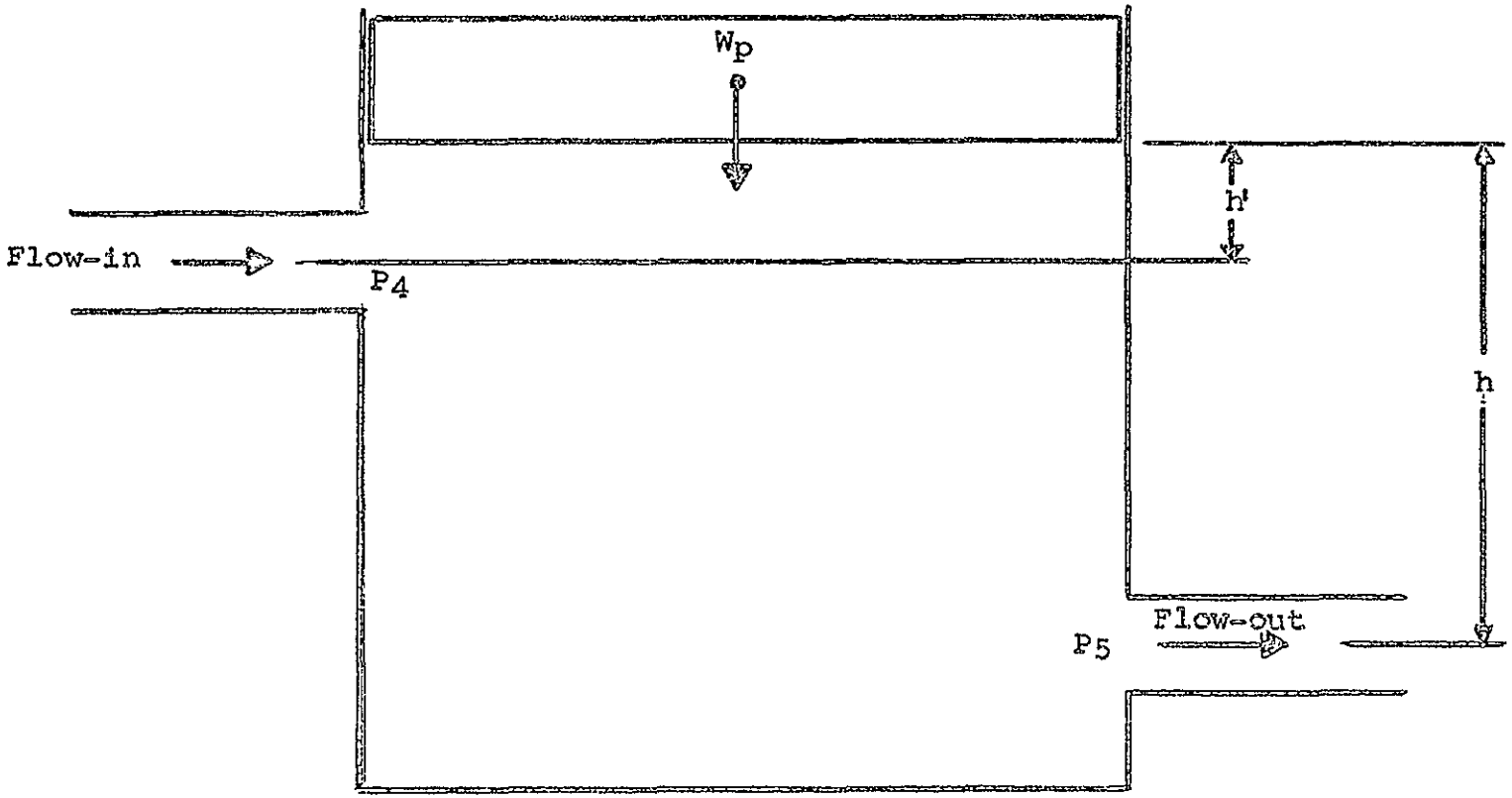

FIGURE 9. A PISTON-TYPE ACCUMULATOR.

h' = the height of the piston above the input flow (in)

h = the height of the piston above the output flow (in)

γ_w = the specific weight of water (lbf/in^3)

The volume of the accumulator as shown in Figure 9 is $V = A_p\, h$. Assuming that A_p and W_p remain constant, then Equation 31 follows by differentiating Equation 30 with respect to time.

$$\begin{aligned} \dot{P}_5 &= \gamma_w / A_p \, \dot{V} \\ &= \gamma_w / A_p \, (Q_{in} - Q_{out}) \end{aligned} \tag{31}$$

Equation 31 can be integrated to give the absolute pressure of the accumulator as a function time. If vaporization occurs in the system, then Equation 31 is modified to account for this effect.

In this experiment, all foreign gases will be purged and the fluid circuit completely filled with water. This is done to ensure the bubbles formed are composed entirely of water vapor. When vaporization occurs and the vaporization minus the condensation is a positive quantity, the resultant effect on the system is an increase in the volume of the accumulator. It is assumed that water is essentially incompressible. The system is assumed to have an accumulator which has a component equation similar to Equation 31 and is given by:

$$P_{ac} = K_{ac} V_{ac} \tag{32}$$

$$\overset{o}{P}_{ac} = K_{ac} \overset{o}{V}_{ac} \tag{33}$$

$$\overset{o}{V}_{ac} = 1/P_{wc} (Q_{in} - Q_{out}) + SPV\ (VAPOR\text{-}CONDEN) \tag{34}$$

where:

K_{ac} = the pressure-volume constant ($lbf\text{-}min/in^5$)

P_{wc} = the density of the water in the accumulator (lbm/in^3)

SPV = the specific volume of saturated vapor (in^3/lbm)

Therefore, ultimately, a net increase in the accumulator volume will manifest itself as a change in the absolute pressure around the fluid circuit.

The vaporization control is motivated by two factors. First, results from initial simulation runs showed that the "On-Off" preheater control has marked effects on the vaporization during the "off" period of the preheater control. That is, the vaporization level will follow the variations in temperature of the water in the preheater section. Ideally a vaporization control will tend to smooth out the above mentioned variations in vaporization level.

The second motivating factor is the need to continuously measure either quantitatively or qualitatively the thermodynamic quality of the two-phase vapor liquid. Quality is defined as[9]

$$SG = \frac{\text{Mass of Vapor}}{\text{Mass of Liquid}} \tag{35}$$

A modified definition of quality is also used in this development. The denominator of Equation 35 is the total mass of liquid in the system where the denominator of the modified quality is the mass of the liquid between the vaporization chamber and the accumulator. The numerator term remains the same. The motivation for the alternate definition is that the experiment is to be designed so that vapor exists only between the vaporization chamber and the accumulator. When the term QUAL1 is used later in this thesis, it will denote the quality as defined by Equation 35, while the term QUAL2 denotes the modified quality as defined above.

The coupling between the vaporization control and quality measurement is not obvious. The mass of vapor in the system at any time is given by

$$\text{Mass of Vapor} = \int_0^t (\text{Vaporization} - \text{condensation})\, dt. \quad (36)$$

Equation 36 can be integrated directly since vaporization is given in closed form by Equation 15 and condensation is given in closed form by Equation 16. Since in practice, vaporization and condensation are not readily measurable; therefore, another method of obtaining the mass of the vapor is needed. Equation 34 depends upon the flow-in, the flow-out, and the vaporization minus the condensation. The flow-in, flow-out, and volume, V_{ac}, can be easily measured. The absolute pressure of the accumulator, P_{ac}, can be measured accurately

and it thus seems plausible to calibrate a system to give mass of vapor in terms of absolute accumulator pressure or volume. So any control scheme that used P_{ac} as one of the control parameters would in a sense be a thermodynamic quality control system. In the simulation it is assumed the liquid flow-in equals the liquid flow-out of the accumulator, since the overall vapor content is small as compared to the liquid.

The proposed vaporization control is a pressure control system with the vaporization being controlled indirectly. It is noted there is no active way to control condensation other than manipulate the physical parameters of the system. A block diagram of the vaporization control system is given in Figure 10. The values for the feedback coefficients A_1 and A_2 and the gain K_{av} can be obtained from the simulation.

Pressure Equations for Fluid Circuit

In this development it is assumed that pressure losses or pressure drops can occur in the tubing connecting the components themselves. Losses due to fittings, curature of the tubing, and instrumentation are neglected as first approximation in this anaylsis.

Tube pressure drop equations have been derived experimentally and are functions of the length (L) and diameter (D) of the tubing, viscosity (v) of the liquid and Reynolds Number (Re) of the flow. Equation 37 describes the pressure drop (ΔP_t) in the tubing and it also accounts

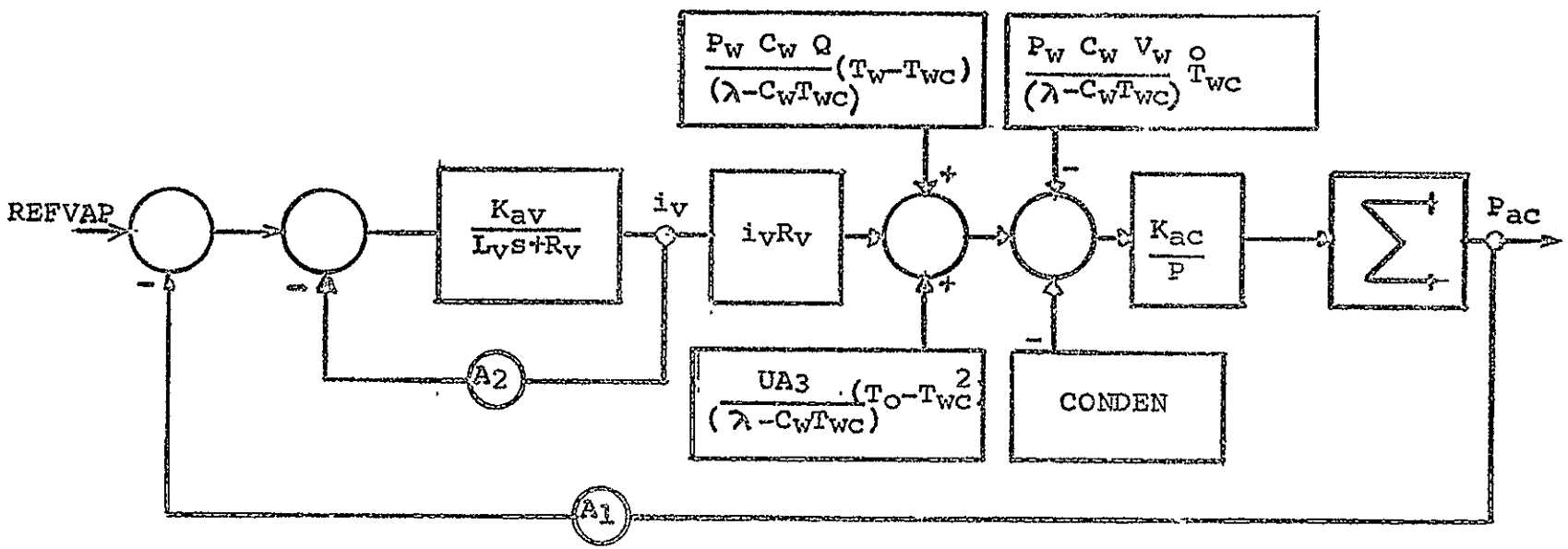

FIGURE 10. VAPORIZATION CONTROL.

for entrance and exit losses. The entrance and exit losses are those incurred when the water is flowing from a smaller diameter tube into a larger diameter tube or vice versa.[10]

$$\Delta P_t = 128\ u\ L\ Q/\pi D^4\ (1+.0434\ D/L\ Re) \qquad (37)$$

Referring to Figure 9, and Equations 29 and 30, the pressure drop, P_{45}, from entrance to exit of the accumulator is given by

$$P_{45} = P_4 - P_5 \qquad (38)$$

$$P_{45} = \gamma_w(h' - h) \qquad (39)$$

where $(h' - h)$ is the difference in height from entrance to exit. It is assumed the height difference in the accumulator is negligible.

Most of the equations presented thus far have been differential equations with time the independent variable, but the pressure equations, with one exception, are strictly steady-state. The exception being that the absolute pressures around the fluid circuit are affected by the pressure $P_{ac}(t)$ which is a function of time.

Equation 17 gives the pressure drop across the channel. Note that Equation 17 and 37 are of the same basic mathematical form.

The fluid circuit is idealized into the schematic as shown in Figure 11. From this schematic, the pressure drops and the absolute pressures, as referenced to the accumulator

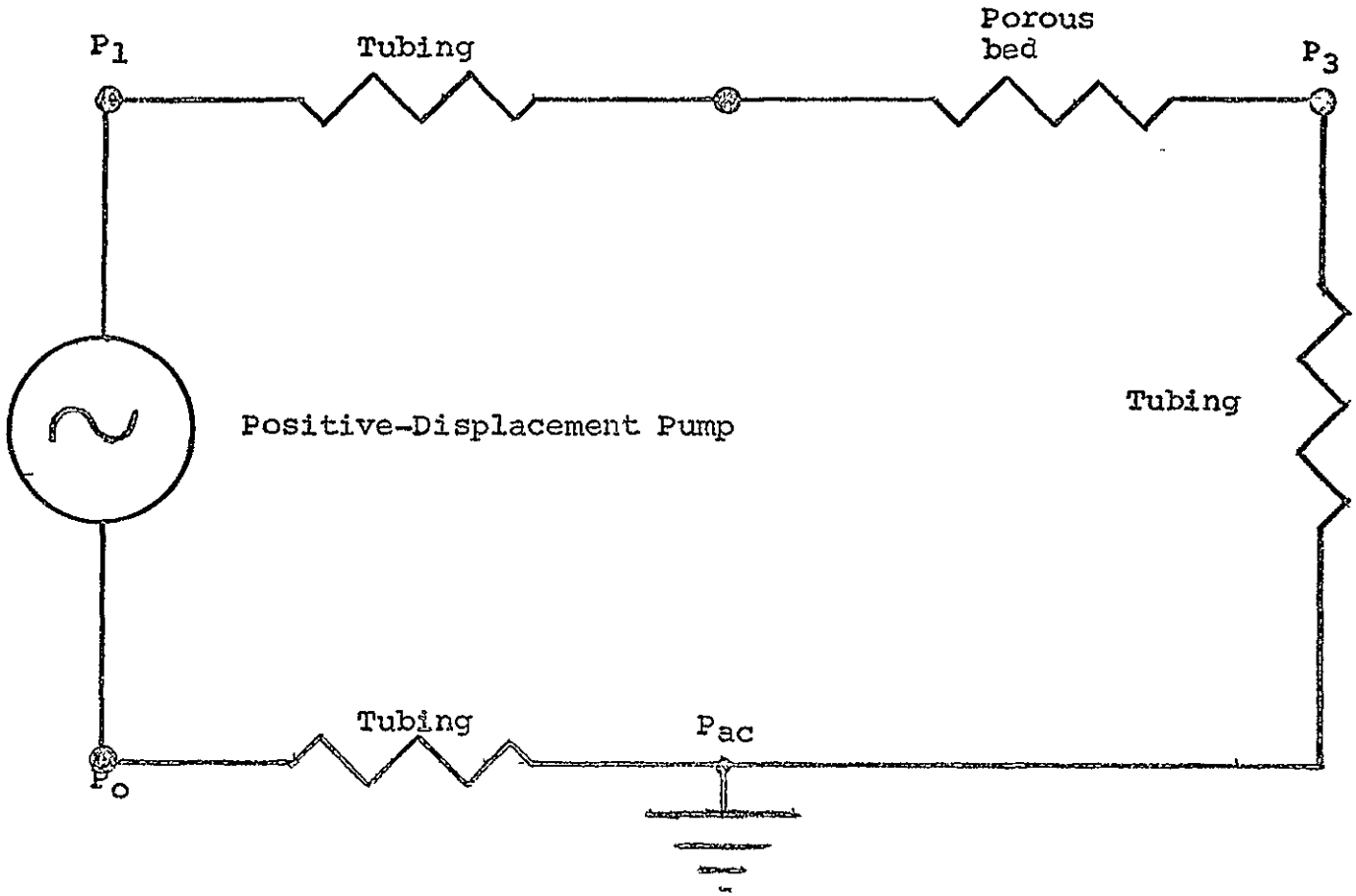

FIGURE 11. PRESSURE SCHEMATIC OF FLUID CIRCUIT.

pressure, may be calculated for various parts of the fluid circuit.

$$P_{10} = P_{12} + P_{23} - P_{3ac} + P_{aco} \quad (40)$$

$$P_{2ac} = P_{23} + P_{3ac} \quad (41)$$

$$P_1 = P_{12} + P_{23} + P_{3ac} + P_{ac} \quad (42)$$

$$P_2 = P_{23} + P_{3ac} + P_{ac} \quad (43)$$

$$P_3 = P_{3ac} + P_{ac} \quad (44)$$

$$P_o = -P_{oac} + P_{ac} \quad (45)$$

where:

P_{10} = the total pressure drop around the fluid circuit (lbf/in^2)

P_{2ac} = the pressure differential between locations 2 and ac in fluid circuit

P_1 = the absolute pressure at location 1 in the fluid circuit (lbf/in^2)

P_2 = the absolute pressure at location 2 in the fluid circuit (lbf/in^2)

P_3 = the absolute pressure at location 3 in the fluid circuit (lbf/in^2)

P_o = the absolute pressure at location 0 in the fluid circuit (lbf/in^2)

CHAPTER III

DEVELOPMENT OF THE SIMULATION PROGRAM

Originally, the selection of digital simulation was a personal preference of the author but since the system as described in the previous chapter requires the use of 51 integrators and 58 function generators, digital simulation was necessary because of the limited amount of analog equipment available. An IBM developed program called "Continuous System Modeling Program" (CSMP) which runs on the IBM System 360/ Model-50 computer was used for the entire simulation.

No attempt to compare digital and analog simulation or to compare other digital simulation techniques with CSMP will be made since the author's practical experience in the general area of machine computation is not broad enough to make such critical comments. Rather, a summary of the essentials on how to run a typical CSMP program will be given. For those desiring a more functional knowledge of CSMP, the IBM literature on this program is a good source.[11]

Before beginning the discussion of the development of the simulation program of this thesis, a brief description of CSMP will be given. The purpose of this

description is not detail instruction in the use of CSMP but to make familiar those features of CSMP as related to this thesis.

CSMP is essentially a program for solving a system of ordinary differential equations. A system of equations of the most general class or ordinary differential equations, i.e., non-linear with time varying coefficients can be programmed. Therefore, it is apparent that CSMP is capable of solving a large class of engineering problems. CSMP will have particular significance to those people concerned with design and analysis of dynamic systems.

It is assumed in the following discussion of the essentials of programming a problem for CSMP that the mathematical modeling of the system has been done and a set of differential and algebraic equations of the form of Equations 46 and 47 are to be programmed.

$$\overset{o}{X}_{ij} = F(t, X_{ij}, U_{ik}) \tag{46}$$

$$0 = A(t)_{ij} X_{ij} + K_{ij} \tag{47}$$

$$i = 1, 2, \ldots, n$$

$$j = 1, 2, \ldots, m$$

$$k = 1, 2, \ldots, p$$

where:

t = independent variable

X_{ij} = dependent variable

U_{ik} = forcing functions

$A(t)_{ij}$ = time-varying or constant coefficients

K_{ij} = constants or parameters which could stand alone in a mathematical expression

A general outline of a CSMP program is given in Figure 12. The remainder of this discussion will refer to elements within this figure. Figure 12 contains six sections of which all or some of the six sections will appear in every CSMP program. A CSMP program will always contain a set of CSMP control cards and the cards END, STOP, AND ENDJOB. The other sections may or may not be included in a particular program depending upon the particular problem at hand.

Frequently, a program will contain parameters which are defined in terms of more basic system parameters and constants. Rather than perform these calculations before the program is run, they may be calculated within the INITIAL section. Calculations performed within the INITIAL section will be performed only once at the beginning of the simulation. In fact any calculation which needs to be performed only once at the beginning of the simulation can be done in the INITIAL section.

Sometimes certain calculations are needed only at the end of the simulation. This may be achieved within the TERMINAL section of the CSMP program. An example of the use of the TERMINAL option would be parameter optimization in which it may be desirable to return to the main simulation program and rerun the simulation with the updated

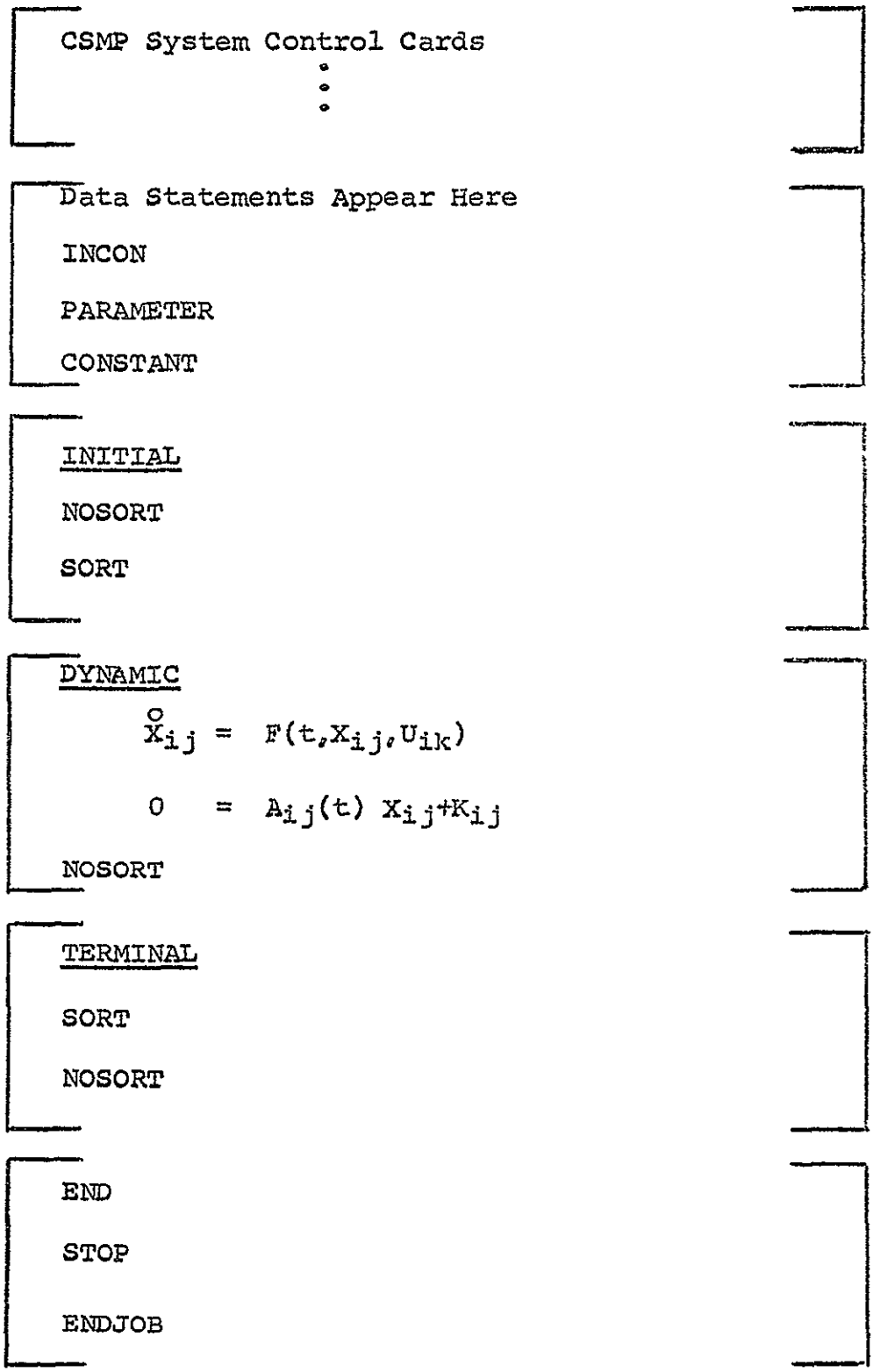

FIGURE 12. BASIC STRUCTURE OF A CSMP PROGRAM

parameter values. When the RE-RUN option is used, the program will return to the INITIAL section (if one is included) where the new parameter value, as calculated in the terminal section, will update the simulation. The entire simulation will be rerun using the updated parameter value.

A DYNAMIC section will probably be included in every simulation as the system differential equations are integrated within this section. This section is the most flexible within the program and can accommodate a wide variety of dynamic systems, i.e., a wide range of mathematical formulations.

An important feature of the CSMP program is the SORT and NOSORT options. If a section of coding contains no Fortran branching or logical tests then the SORT option can be employed. Within a SORT section, the program automatically places the statements in the best possible sequence to ensure an accurate solution. Incorrect sequencing of the structure statements introduces a phase lag that could seriously affect the stability and accuracy of the solution. Within a NOSORT section, the burden of correctly sequencing the structure statements lies with the programmer. The advantage of utilizing the NOSORT option is that the full power of standard Fortran programming is available.

The discussion now returns to the development of the simulation program for the system equations developed in the previous chapter.

The simulation program was developed in six steps. These steps given in chronological order are:

1. Separate or decouple the system equations into three independent sections: Electrical, Pressure and Thermodynamic.
2. Assume constant values for all coefficients of the differential equations.
3. Make appropriate runs on each section to check them out.
4. Consolidate the three sections and make appropriate runs to check out system.
5. Relax the constraint of step two where applicable and make appropriate runs.
6. With steps one through five completed, make simulation runs with all systems functioning.

The above six steps are not intended to imply any generality of method but to convey the method of approach taken in this problem. In general, if the system to be simulated is large, it is recommended that it be simplified and broken down into smaller subsystems as much as possible. This procedure is invaluable in the initial check-out and debugging phase of the program.

The only equation coding problems occurred in what could be called "equation control." Equation control is defined in this discussion to be the switching-in and switching-out of the appropriate set of equations during the simulation.

The fluid-thermodynamic portions of the system operate either in the unsaturated state or the saturated state. In Chapter II, the fluid-thermodynamic equations of motion were developed. Though the exact details of these equations will vary depending upon the particular section of the system under investigation, they will be of the general form.

$$P\ V\ C\ \overset{\circ}{T}_i = P\ C\ Q\ (T_{(i-1)} - T_i) + U\ A\ (T_o - T_i) + q \tag{48}$$

$$T_i = F\ (\_i) \tag{49}$$

The above symbols are analogous to those defined in Chapter II.

Equation 48 is valid as long as the water temperature is below saturation, but once saturation is reached, Equation 49 is valid. The water temperature will vary around the fluid circuit (see Figure 1) from an unsaturated state before the preheater to fully saturated and boiling within the vaporization chamber. With saturated water and vapor bubbles leaving the vaporization chamber and moving through the porous bed, heat transfer losses could cause the water temperature to drop below saturation. In order to ensure that this condition is detected, a saturation test is made at the beginning of each of ten sections of the porous bed. Saturation tests are also made in each section of tubing, within the accumulator, and in the preheater and vaporization chamber. Equation control is needed to implement the saturation test, and from the results of the saturation test, employ the

appropriate equation in the simulation.

As implied from the above discussion, the saturation test is actually two tests. One test is made to determine when water makes the transition from the "unsaturated to the saturated state" (UTSS), and a second test has to be made to determine when the transition is made in reverse direction, i.e., from the "saturated state to the unsaturated state" (SSTU).

The UTSS test is accomplished by comparing the actual water temperature with the saturation temperature as computed by a function generator which has as its input the absolute pressure as calculated during the simulation. The pertinent Fortran statements for the UTSS test are given below. These are followed with an explanation of the coding.

```
117     RO  =  AFGEN(TF1S,P2S)
122     IF(T1.GE.RO.)  GO  TO  8

  8     CONTINUE
128     XU  =  RO - T1
129     T1  = MODINT(T100,XU,XU,T1D)
```

The above sequence of coding will implement the UTSS test. It works as follows. Assume that temperature T1 (Statement Number 129) has reached saturation temperature. The variable, RO, is the generated reference saturation temperature. When $T1 \geq RO$ then the program goes to

Statement Number 8 and then proceeds to Statement Number 128. The control variable, XU, will have a value of zero at saturation. Statement Number 129 makes use of a special CSMP function, MODINT, which is a "mode-controlled integrator" (MCI). The MCI functions as a regular integrator if the algebraic sign of the control variable, in this case XU, is positive. If the algebraic sign of the control variable becomes negative or zero, the MCI will hold the value of the last output until the control variable sign becomes positive. Thus when a saturation condition exists, the control variable, XU, is zero and so the MCI will hold the last temperature output as is desired.

Two methods of making the SSTU test were developed to work with the unforced and forced temperature differential equations. Equation 48 is a typical forced temperature differential equation. If the forcing function, q, is zero then Equation 48 becomes unforced and takes the following form:

$$P\ V\ C\ \dot{T}_i = P\ C\ Q(T_{(i-1)} - T_i) + U\ A(T_o - T_i) \qquad (50)$$

The above symbols are analogous to those defined in Chapter II.

The first method applies to Equation 50 and utilizes the knowledge that once saturation is reached the temperature remains constant and, therefore, the derivation of temperature with respect to time of Equation 50 must equal zero. Equation 50 then becomes an algebraic equation, Equation 51, and can be solved explicitly for the water temperature T_i. It was found

that Equation 51 and Equation 49 compared within three degrees and so Equation 51 could be used to detect a change from a saturated state to the unsaturated state. Also it appears that the expressions used for the heat-transfer coefficient of Equation 26 are correct, based on the results of the comparison. The pertinent Fortran statements which exemplify the first method of making the SSTU test are given below. This is followed with an explanation of the coding.

$$T_i = P\ C\ Q\ T_{(i-1)}/(P\ V\ C+U\ A) + U\ A\ T_o\ /(P\ V\ C+U\ A) \qquad (51)$$

The above symbols are analogous to those defined in Chapter II.

```
117     RO   =  AFGEN(TF1S,P2S)
                 .
                 .
122     IF(T1.GE.RO)  GO  TO  8
                 .
                 .
                 .
  8     CONTINUE
                 .
                 .
                 .
124     IF(T1       .LT.RO )T1 = T1S
                 .
                 .
                 .
  9     CONTINUE


128     XU   =  RO - T1
129     T1   =  MODINT(T100,XU,XU,T1D)
```

The explanation of the above sequence of coding which implements the first method of the SSTU test is now given. It is assumed that the temperature T1 has been in a

saturated state and enough heat transfer has taken place so that T1S is just dropping below RO, i.e., temperature T1 is making the transition from saturation to unsaturation. The sequence of events begins with Statement Number 124 and with T1S less than RO. Since the conditional expression of Statement Number 124 has been satisfied, then the value of temperature T1 is replaced by the value of temperature T1S. Therefore, the control variable XU, as calculated in Statement Number 128, has a positive algebraic sign which causes the MCI of Statement Number 129 to switch from the hold-mode to normal integration. With the return of the MCI to normal integration operation, the first method of the SSTU test is complete.

The development of a second method of making a SSTU test was motivated by the inability of the first method to function with equations of the form of Equation 48. When Equation 48 is manipulated into the form of Equation 51, it was found that there was an intolerable difference between Equation 52 and the true saturation temperature given by Equation 49. The symbols used in Equation 52 are similar to those defined in Chapter II. Equation 52 has a large discontinuity at the time of switching. It is highly

$$T_i = P\ C\ Q\ T_{(i-1)}/P\ V\ C+U\ A) + U\ A\ T_o/(P\ V\ C+U\ A) + q/(P\ V\ C+U\ A) \quad (52)$$

improbable that all the water in a particular section would reach saturation and instantaneously completely vaporize

into super-heated steam. This would require an impulse of power which is incongruent with the physical system. An explanation which used physical and mathematical arguments will be given. The general solution to Equation 48 would contain the complementary or transient solution and the particular or steady-state solution. A mathematical steady-state condition is usually denoted by the derivative terms vanishing and the solution taking the form of the forcing function. The vanishing of the derivative term in Equation 48, at saturation, is imposed by the physical constraints of the process and not due to a steady-state condition in the usual mathematical sense. Thus the value of the dependent variable jumped from the imposed steady-state value to that imposed by the forcing function. The second method of making the SSTU test was made to be independent of equations of the form of Equation 52. The pertinent Fortran coding which implements the second method of performing the SSTU test is given below. An explanation of the coding is then given.

```
 95    REF2  =  AFGEN(TF1S, PVC)
               .
               .
               .
170    TWCD  =  . . .
176    CMI2  =  REF2 - TWC
193    TWC   =  MODINT(TWCOO,CMI2, CMI2, TWCD)
194    TWC   =  FCNSW(CMI2, REF2, REF2, TWC)
```

The explanation of the above sequence of coding which implements the second method of the SSTU test is now given.

It is assumed that the temperature TWC is saturated and vaporization is occurring. The vaporization and condensation rates directly affect the absolute pressure around the fluid circuit and the absolute pressure PVC of this particular section determines the saturation temperature. Suppose that the absolute pressure PVC were to increase. Then the algebraic sign of the control-variable CMI2 would become positive. The MCI would resume normal integration of the differential equations. Statement Number 194 utilizes the CSMP function called Function-Switch. The control-variable CMI2 controls the output of Statement Number 193. If the algebraic sign of the control-variable CMI2 is negative or zero, then the value of TWC is replaced by the value of REF2. If CMI2 has a positive sign, then the output of the Function-Switch is equal to TWC. Therefore, once saturation has been reached and vaporization is occurring, TWC cannot drop below saturation unless all heat input is turned off or an increase in the local absolute pressure occurs such that REF2 becomes greater than the temperature TWC.

The UTSS test described in this chapter is used where appropriate throughout the simulation. The second method of making the SSTU test is used only with the preheater and vaporization sections of the system. The first method of the SSTU test is used in all other sections of the fluid circuit.

A flow-diagram of the entire simulation program is given in Figures 13(a) through 13(r).

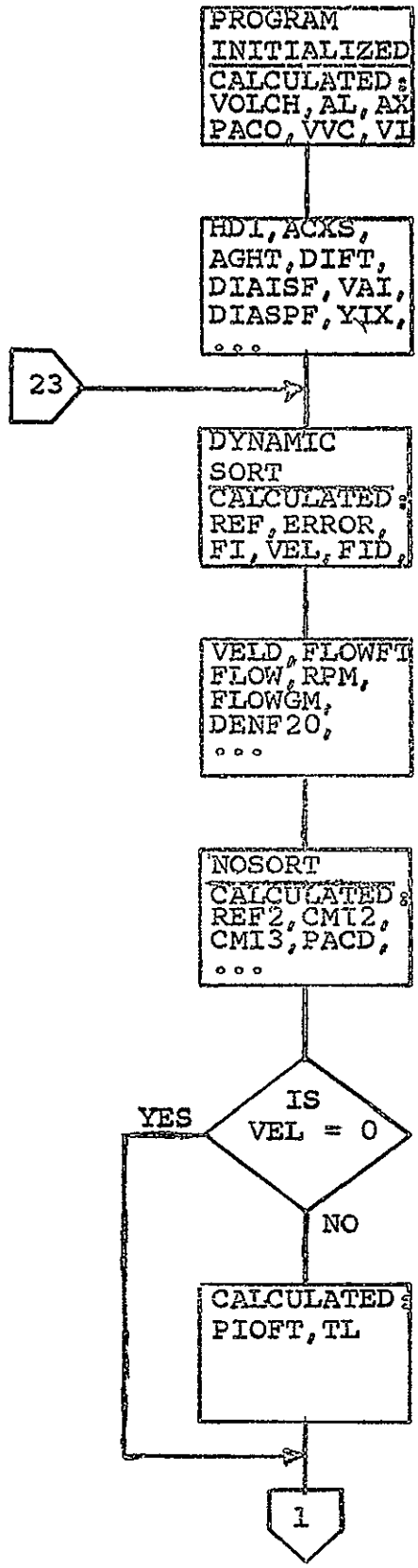

FIGURE 13(a). COMPUTER SIMULATION FLOW-DIAGRAM

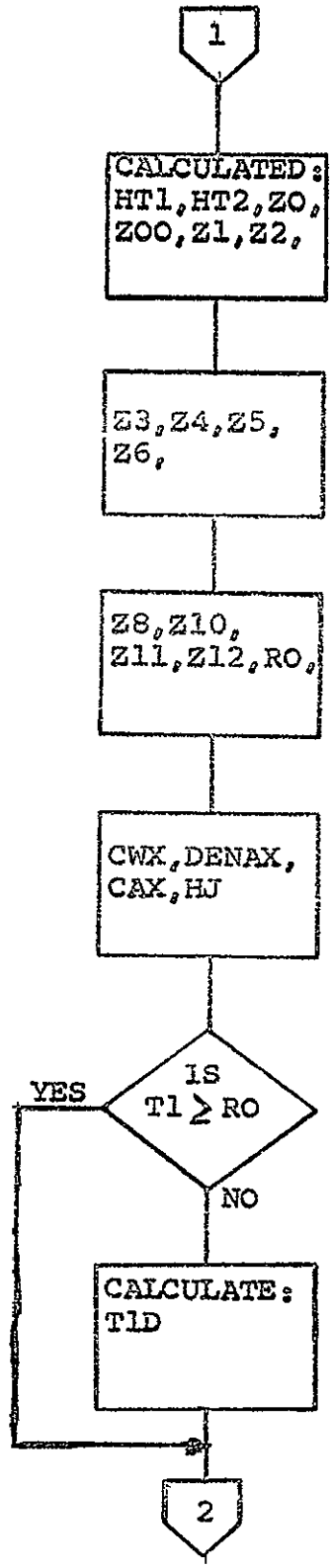

FIGURE 13(b). COMPUTER SIMULATION FLOW-DIAGRAM

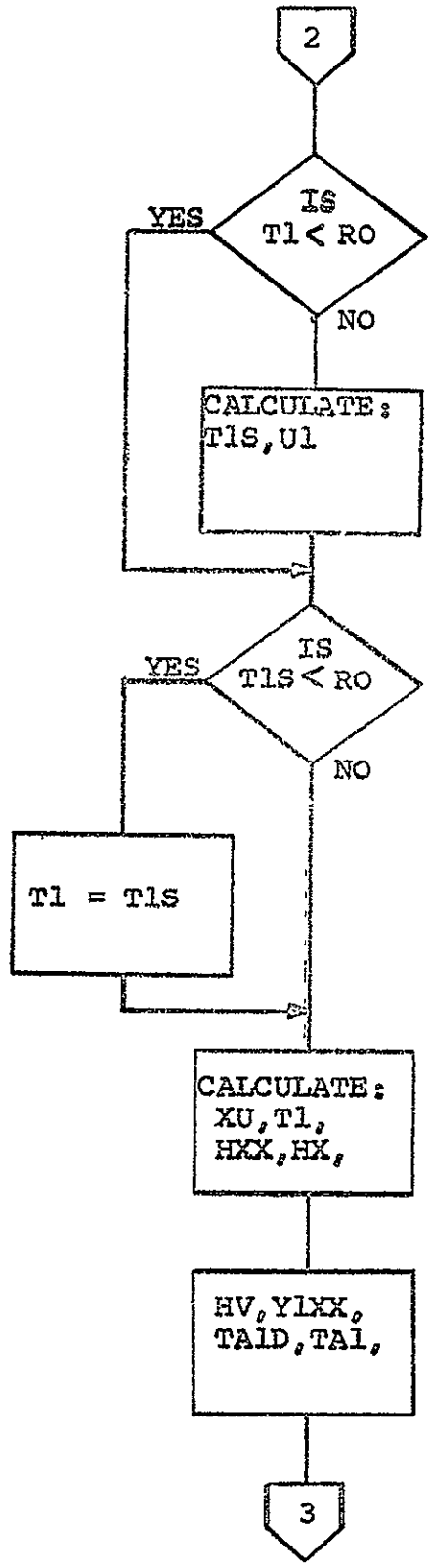

FIGURE 13(c). COMPUTER SIMULATION FLOW-DIAGRAM

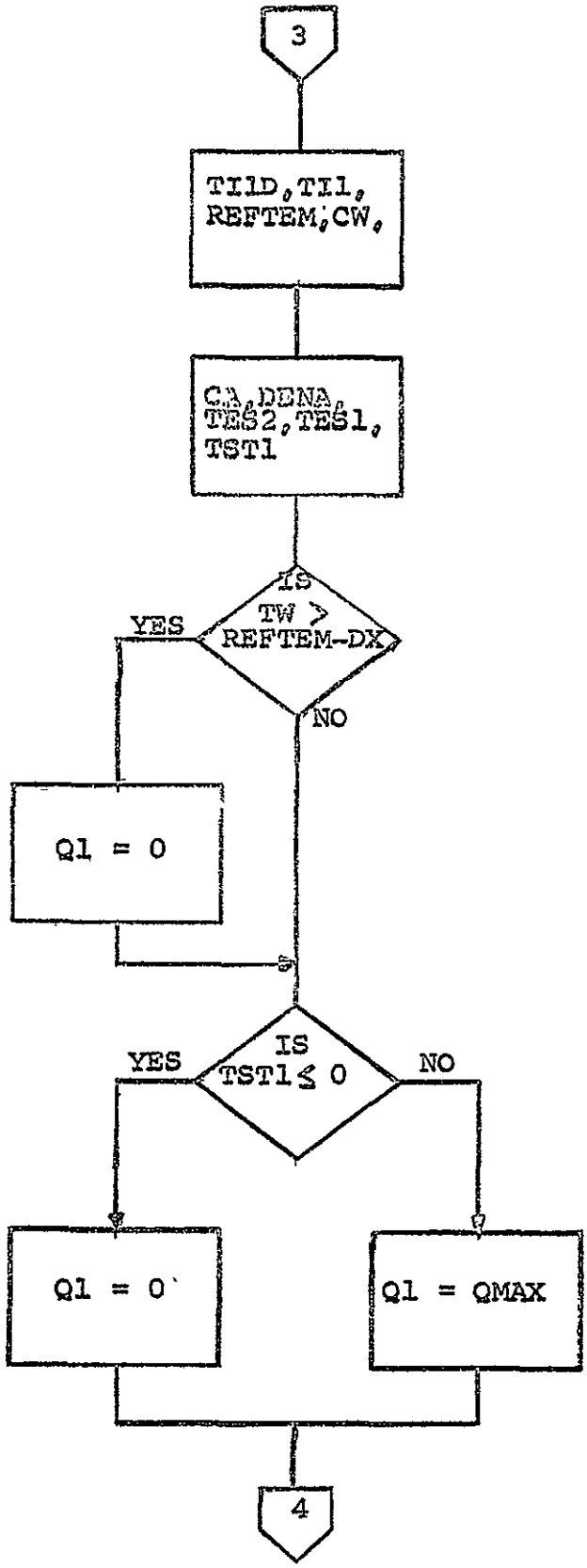

FIGURE 13(d). COMPUTER SIMULATION FLOW-DIAGRAM

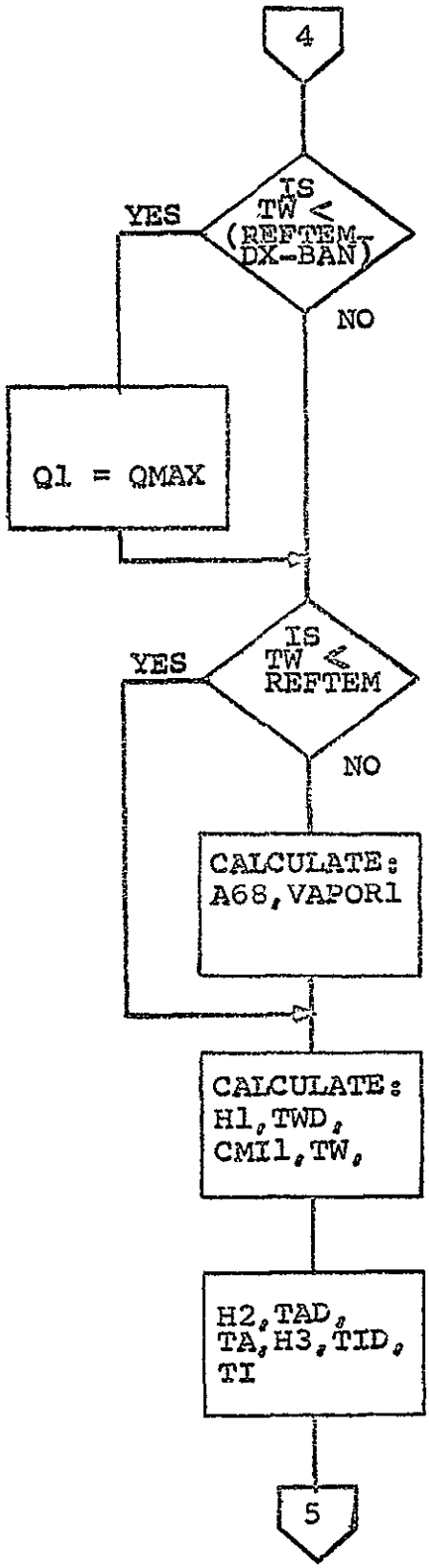

FIGURE 13(e). COMPUTER SIMULATION FLOW-DIAGRAM

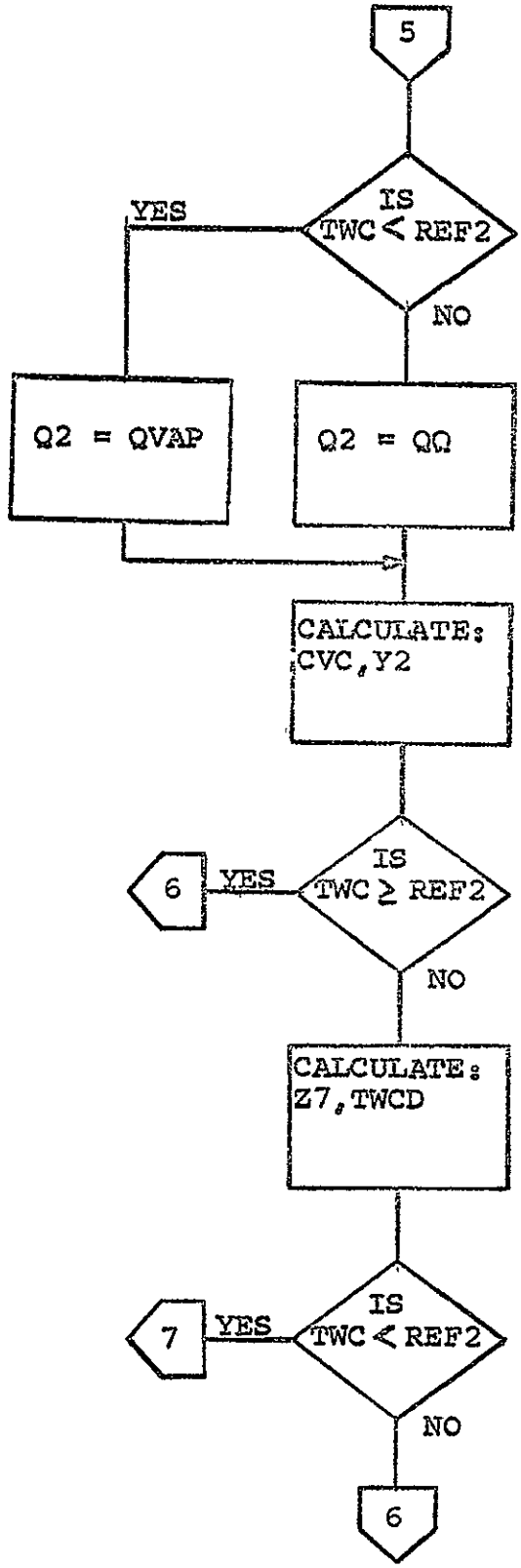

FIGURE 13(f). COMPUTER SIMULATION FLOW-DIAGRAM

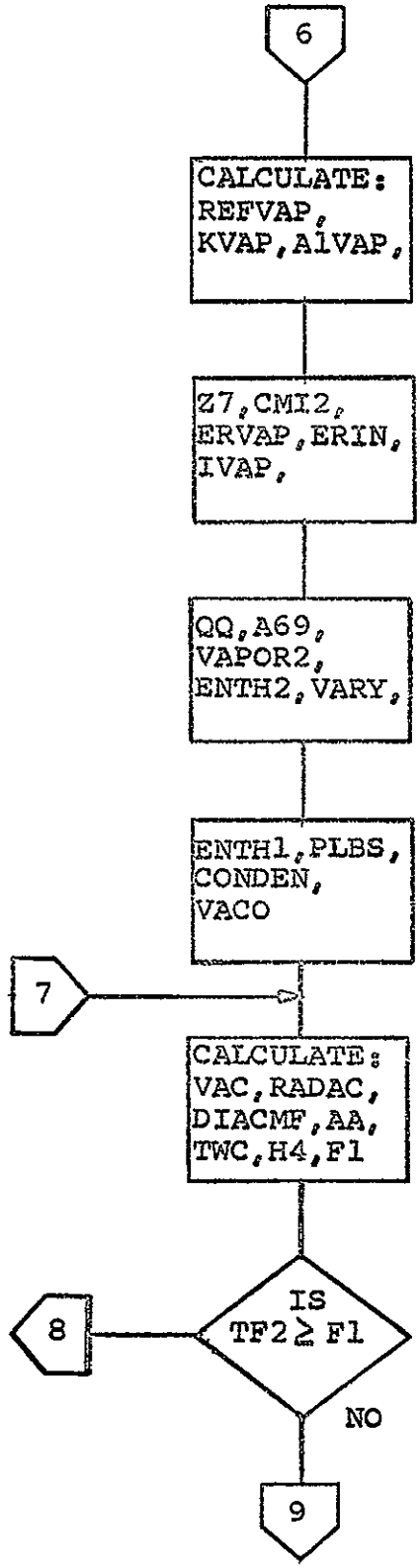

FIGURE 13(g). COMPUTER SIMULATION FLOW-DIAGRAM

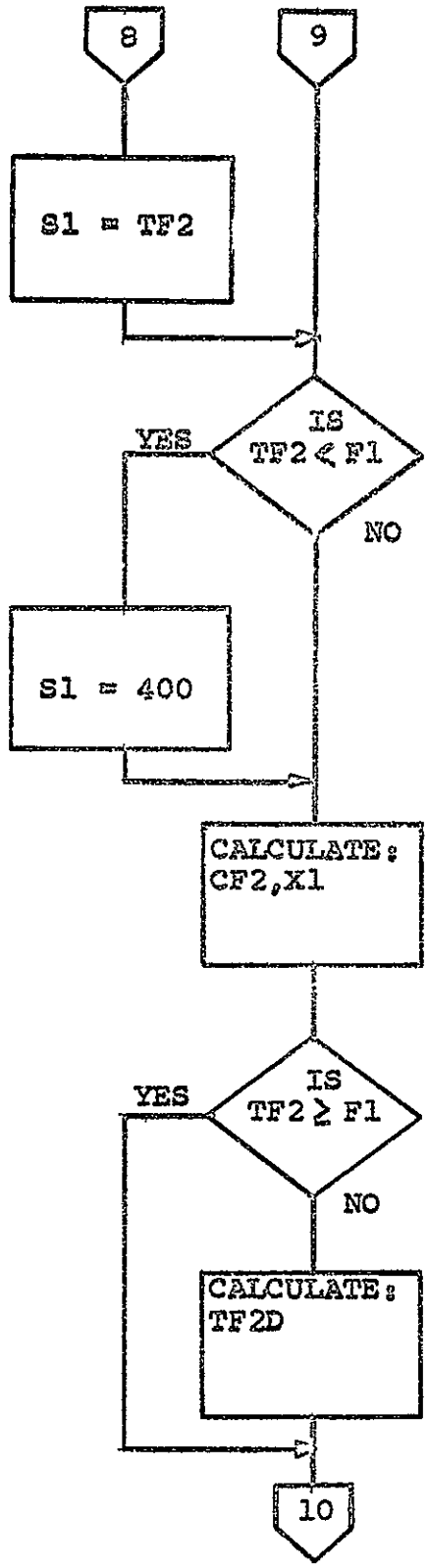

FIGURE 13(h). COMPUTER SIMULATION FLOW-DIAGRAM

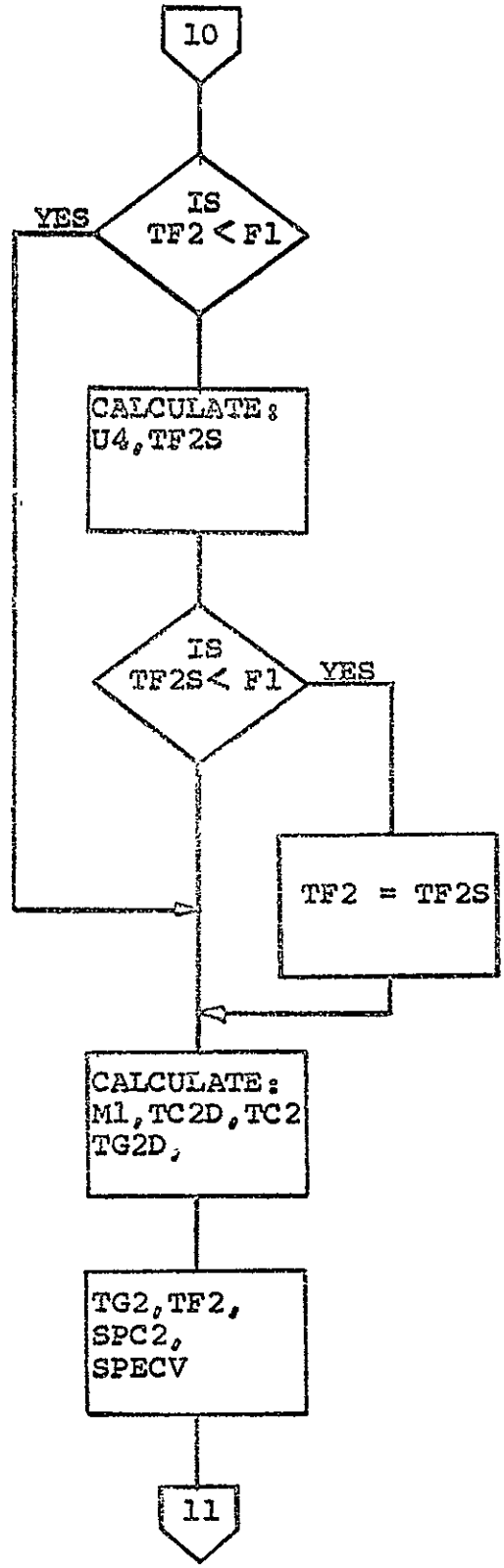

FIGURE 13(i). COMPUTER SIMULATION FLOW-DIAGRAM

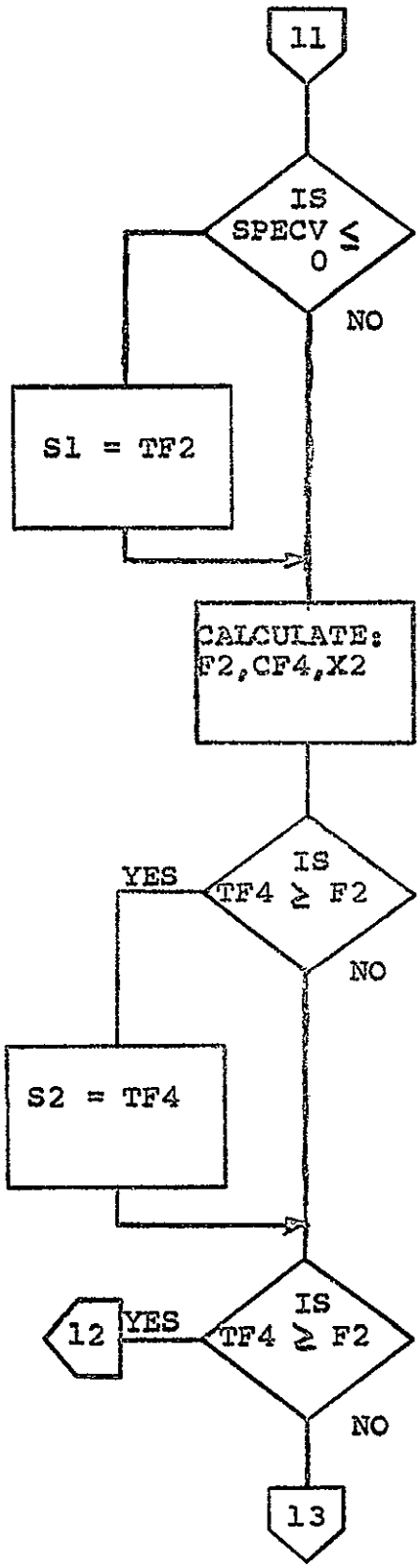

FIGURE 13(j). COMPUTER SIMULATION FLOW-DIAGRAM

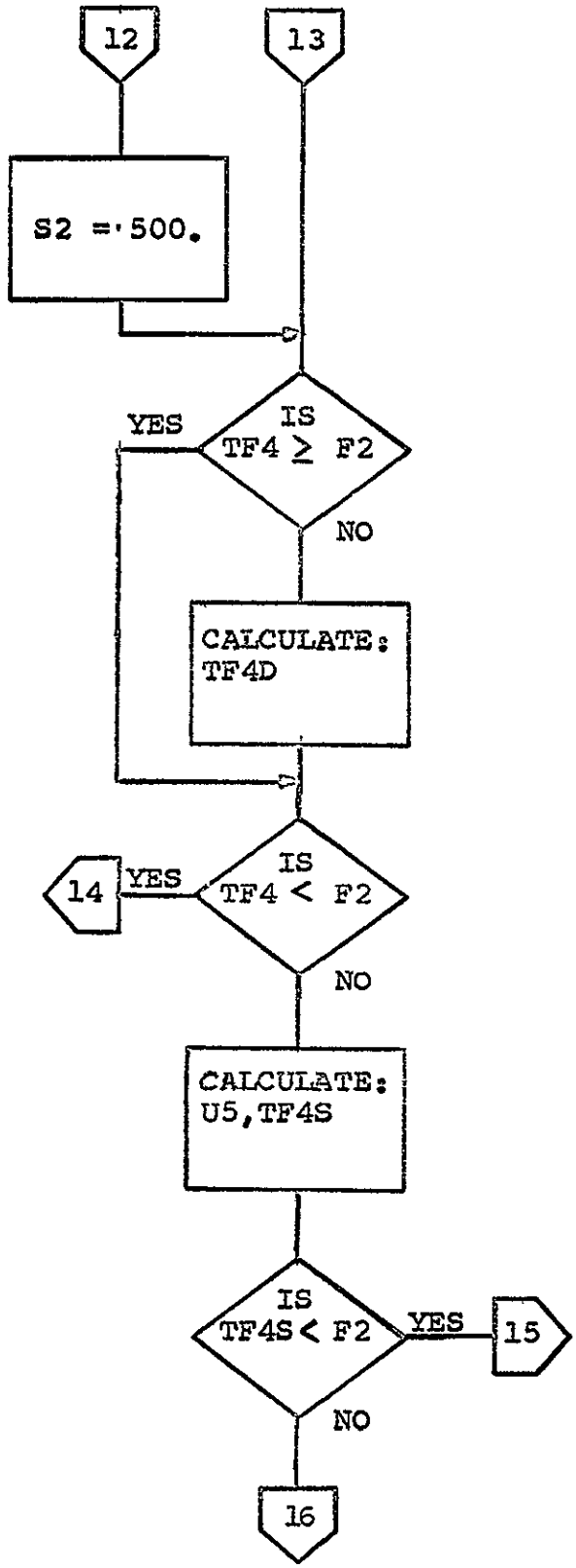

FIGURE 13(k). COMPUTER SIMULATION FLOW-DIAGRAM

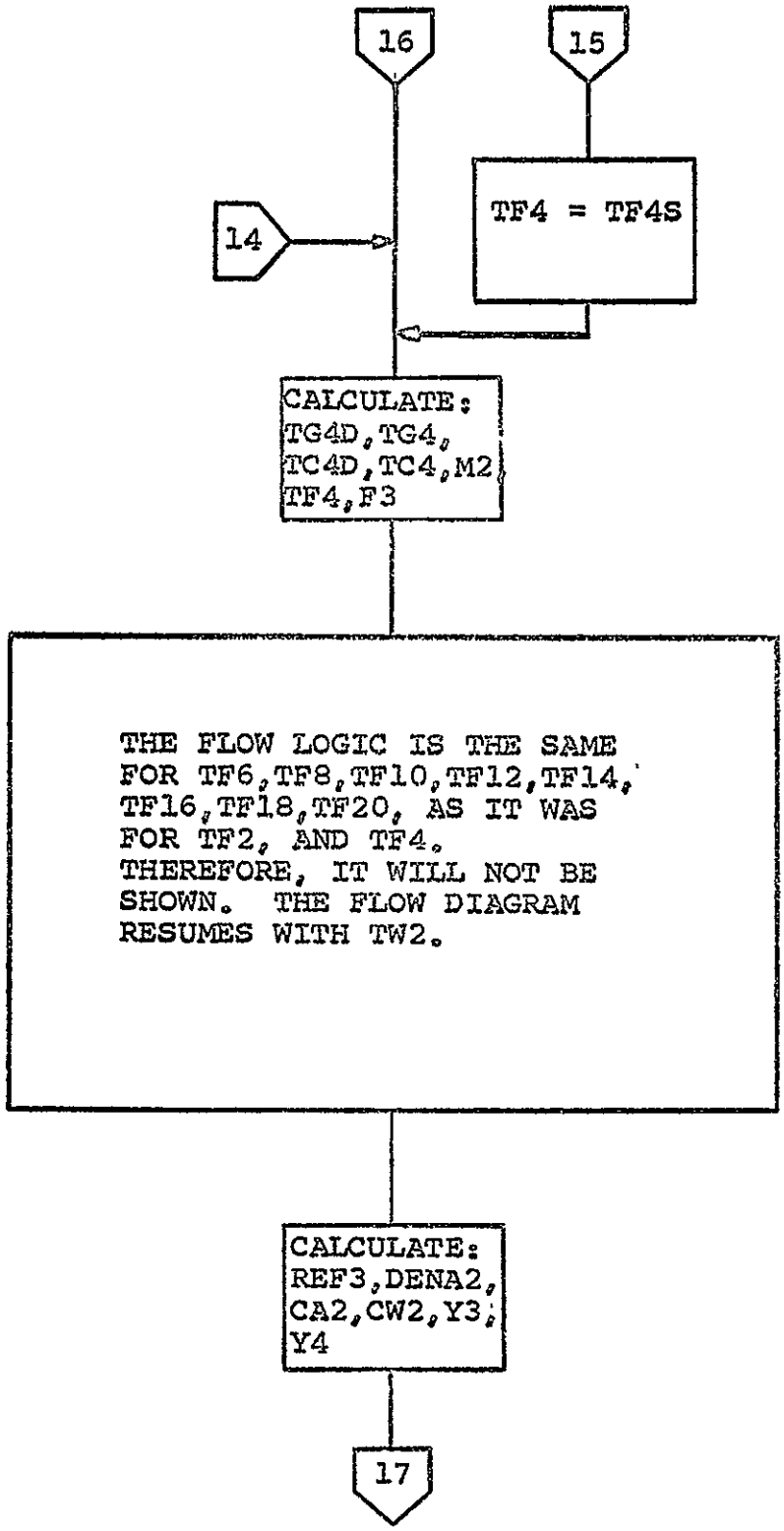

FIGURE 13(1). COMPUTER SIMULATION FLOW-DIAGRAM

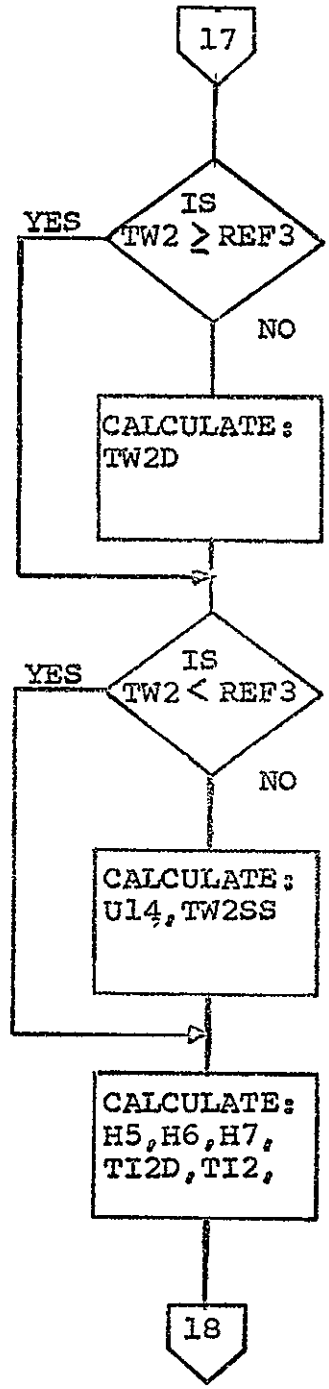

FIGURE 13(m). COMPUTER SIMULATION FLOW-DIAGRAM

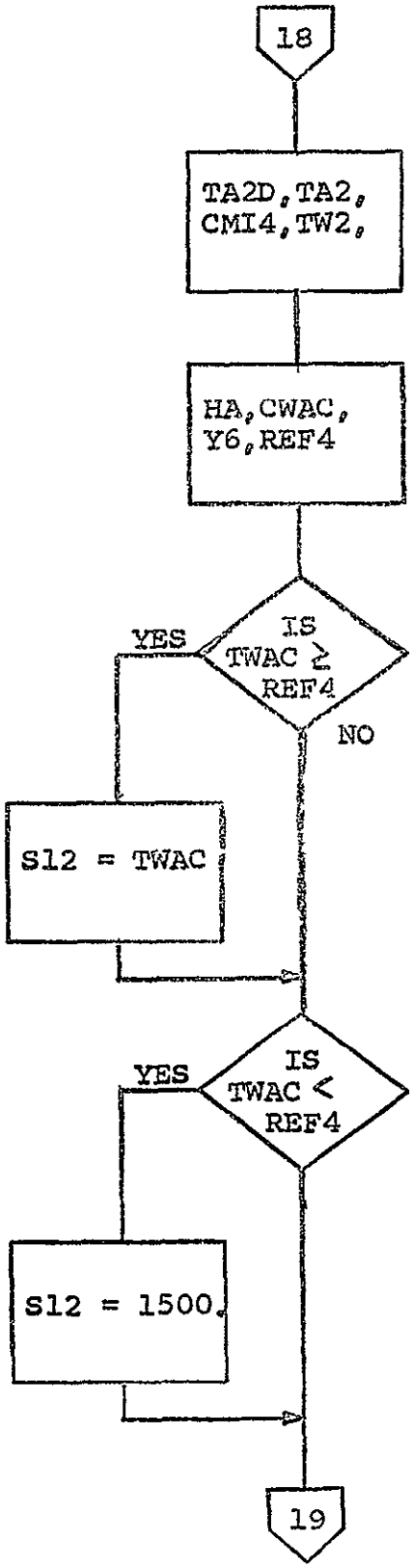

FIGURE 13(n). COMPUTER SIMULATION FLOW-DIAGRAM

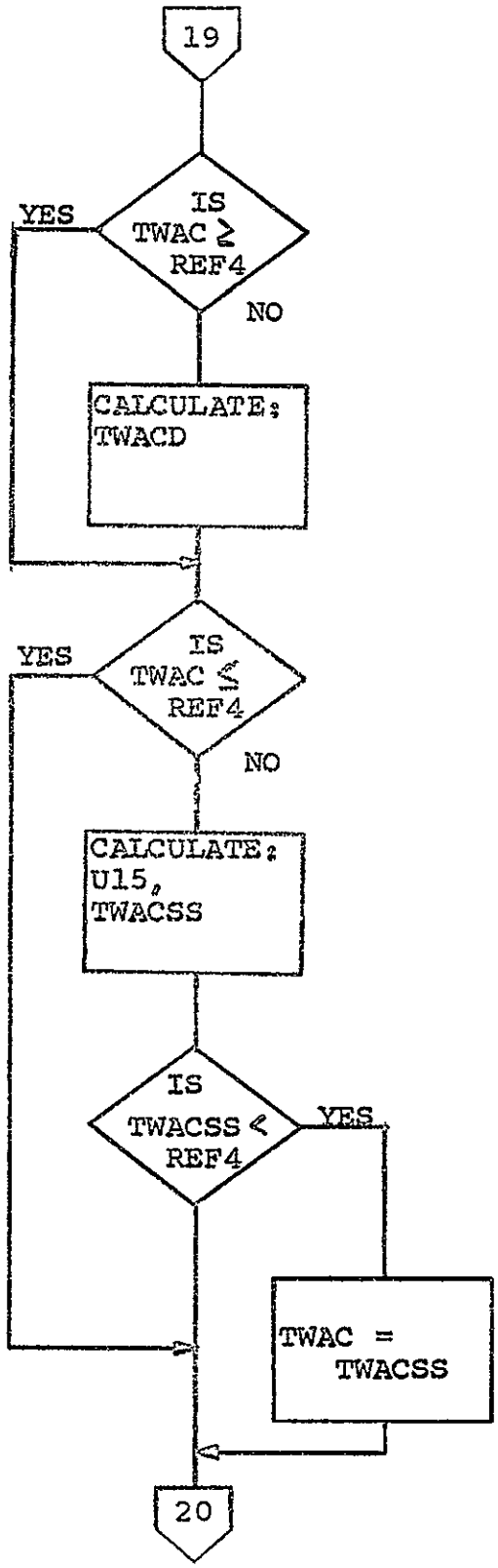

FIGURE 13(o). COMPUTER SIMULATION FLOW-DIAGRAM

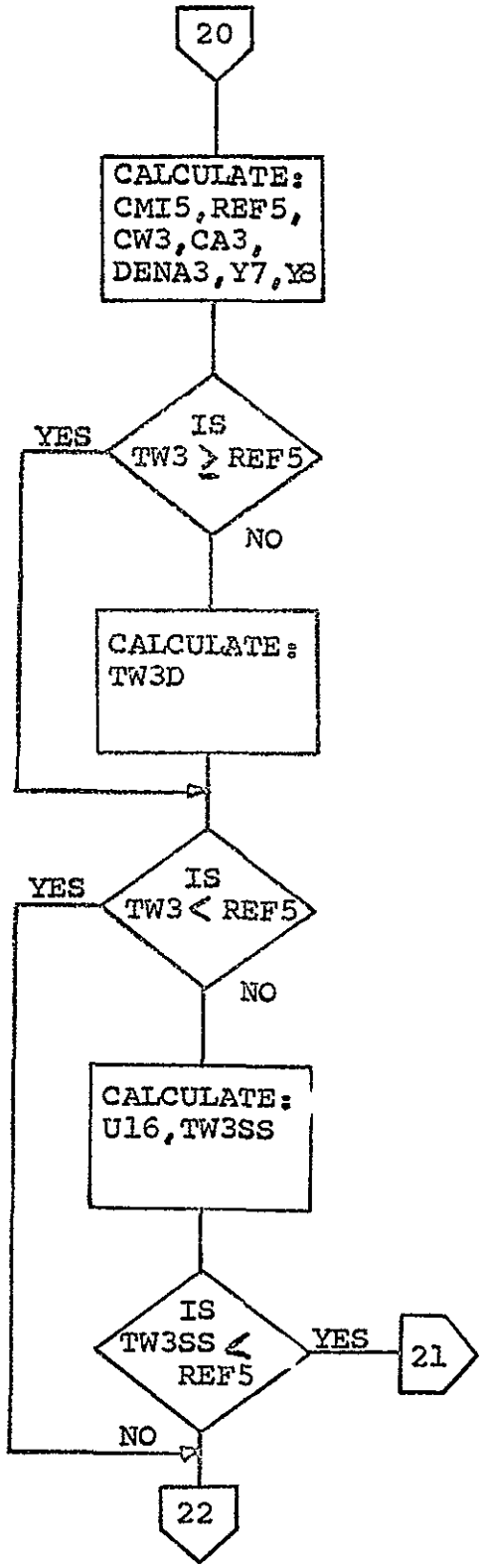

FIGURE 13(p). COMPUTER SIMULATION FLOW-DIAGRAM

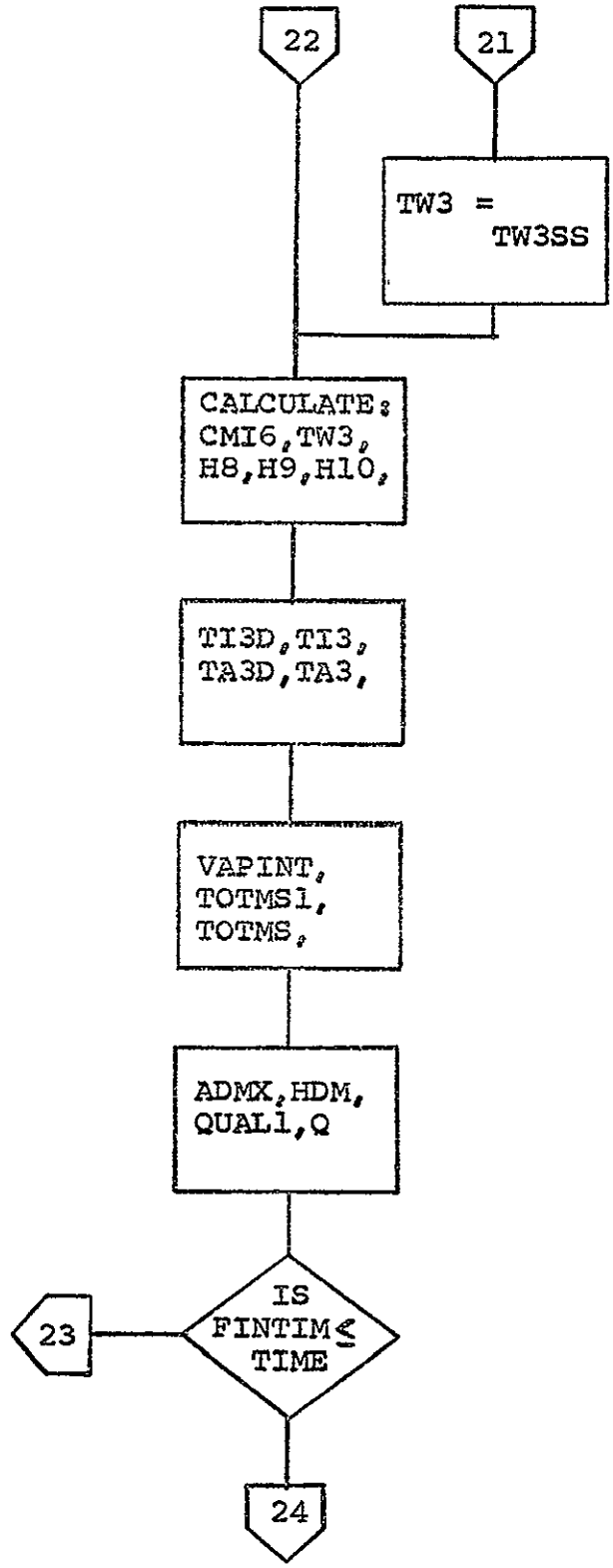

FIGURE 13(q). COMPUTER SIMULATION FLOW-DIAGRAM

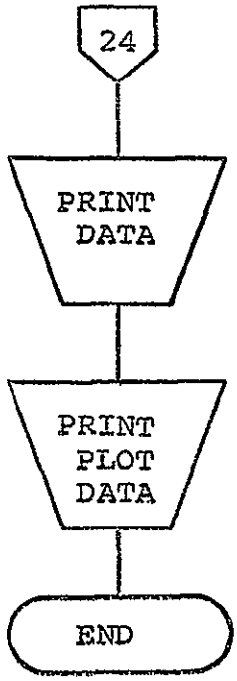

FIGURE 13(r). COMPUTER SIMULATION FLOW-DIAGRAM

CHAPTER IV

DISCUSSION AND DISPLAY OF SIMULATION RESULTS

The system was simulated under several operating conditions, i.e., several flow-rates, a number of different temperature initial conditions, and various values of heat input. Only two runs, runs A and B are included. These runs are representative of the many runs that were simulated, i.e., they approach the experiment conditions in which two-phase flow exist in the porous bed. The simulation runs included in this thesis show the response of the system for different temperature initial conditions throughout the system.

The system contains 15 gallons of water. In runs A and B the flow-rate was 1 gpm; therefore, it will take 15 minutes for all the water in the system to be circulated one time. In run A the system initial temperature conditions were lower than run B. The simulation time of run A was 0.8 minutes which does not allow the water in the fluid circuit to completely circulate. Therefore, run B which started at higher initial temperatures allows the study of system operation at a later time than run A. Thus run A gives the view of the system approaching the desired experiment conditions while run B more closely

approaches this condition.

Run A

Conditions under which run A was made are given:

Heat input: Q1 = 10 BTU/min or zero depending upon the action of the preheater control. Q2 = 40 BTU/min or 50 BTU/min depending on the action of the vaporization control.

Flow-rate: started from zero flow at time equal zero, and achieved 1 gpm in .0025 minutes.

Initial pressures: were equal to the absolute pressure in the accumulator, PAC, which was 15.834 lbf/in^2.

Simulation time: 0.8 minutes

Initial temperatures: water throughout the system was $212^{\circ}F$.

Porous media: $208^{\circ}F$

Channel: $210^{\circ}F$

Insulation: $75^{\circ}F$

Ambient: $70^{\circ}F$

The results of run A are given in Figures 14 through 27. Under the given run conditions for run A, Figure 15 shows that TWC has saturated, and vaporization is occurring as seen in Figure 24. However, no vapor exists past the first

section of the porous bed since vapor cannot exist in those sections in which the surrounding water is not saturated. See Figures 18 through 21. In order for vapor to exist through the porous bed the system has to operate a longer time so that the temperature of the water in the porous bed is brought up to saturation temperature.

Initially the water temperature dropped in every section of the porous bed. Since the initial temperature of each section of the porous media was set at a lower temperature than the surrounding water, it absorbs heat from the water, lowering the temperature of the water until heated water has flowed into the particular section. For example, at a flow-rate of 1 gpm, water leaving the vaporization chamber and proceeding through the bed would arrive at sections 1 through 10 in: .0167 min.; .0278 min.; .0389 min.; .05 min.; .0612 min.; .0725 min.; .0834 min.; .0945 min.; .1055 min.; .1162 min., respectively.

In 0.8 minutes none of the observable sections of the porous bed reached saturation temperature. A saturation condition exists if the temperature curve intersects the reference saturation temperature curve. It appears that an intersection between the temperature curve, TF4, and the reference temperature curve, F2, is imminent. See Figure 18.

It is noted from Figure 25 that the pressure in the accumulator had reached a constant value during the 0.8

minutes of run time. This indicates the vaporization and condensation have become equal; however, the heated water has not been circulated back to the preheater section. When the heated water returns to the preheater section, and its temperature and the temperature of the water of the previous cycle are not equal, then a temperature transient condition will exist.

Run B

The initial temperature conditions for run B are higher than run A and represent the system operation at a later time than run A.

Conditions under which run B was made are given:

Heat input: same as run A.

Flow-rate: same as run A.

Initial pressures: same as run A.

Simulation time: 0.9 minutes

Initial temperatures: Water temperatures:
TW = 214.25°F, TWC = 214.20°F, TF2 = 214.15°F,
TF4 = 214.10°F, TF6 = 214.08°F, TF8 = 214.05°F,
TF10 = 214.0°F, TF12 = 213.98°F, TF14 = 213.95°F,
TF16 = 213.90°F, TF18 = 213.88°F, TF20 = 213.85°F,
TW2 = 213.83°F, TWAC = 213.80°F, TW3 = 213.78°F,
T1 = 213.77°F.

These temperature initial conditions were set to ensure the temperature in any particular section of the system

was less than or equal to the saturation temperature for that section.

Porous media: 216°F

Channel: 216°F

Insulation: 200°F

Ambient: 70°F

The results of run B are given in Figures 28 through 46. With the system initial conditions as given above, vaporization occurred almost immediately as noted by the following: (1) the intersection of the temperature curve, TWC, and the reference temperature curve, REF2. See Figure 29. (2) the increase of pressure, PAC, which is due to vapor displacing water into the accumulator. See Figure 44.

There was no initial decrease of water temperature, within the porous bed, TF2 through TF18, since the porous media was given a higher initial temperature than the water. See Figures 32 through 40.

During the run time, 0.9 minutes, the first four sections of the porous bed became saturated as the heated water and vapor travel down the porous bed. See Figures 32 through 35. It also appears that sections five and six of the porous bed are going to saturate. See Figures 36 and 37.

The temperatures, TWAC and TW3, appear to have reached a constant value indicating the accumulator is receiving sufficient heat from the incoming flow to offset the heat transfer losses incurred in the accumulator. See Figures 41 and 42.

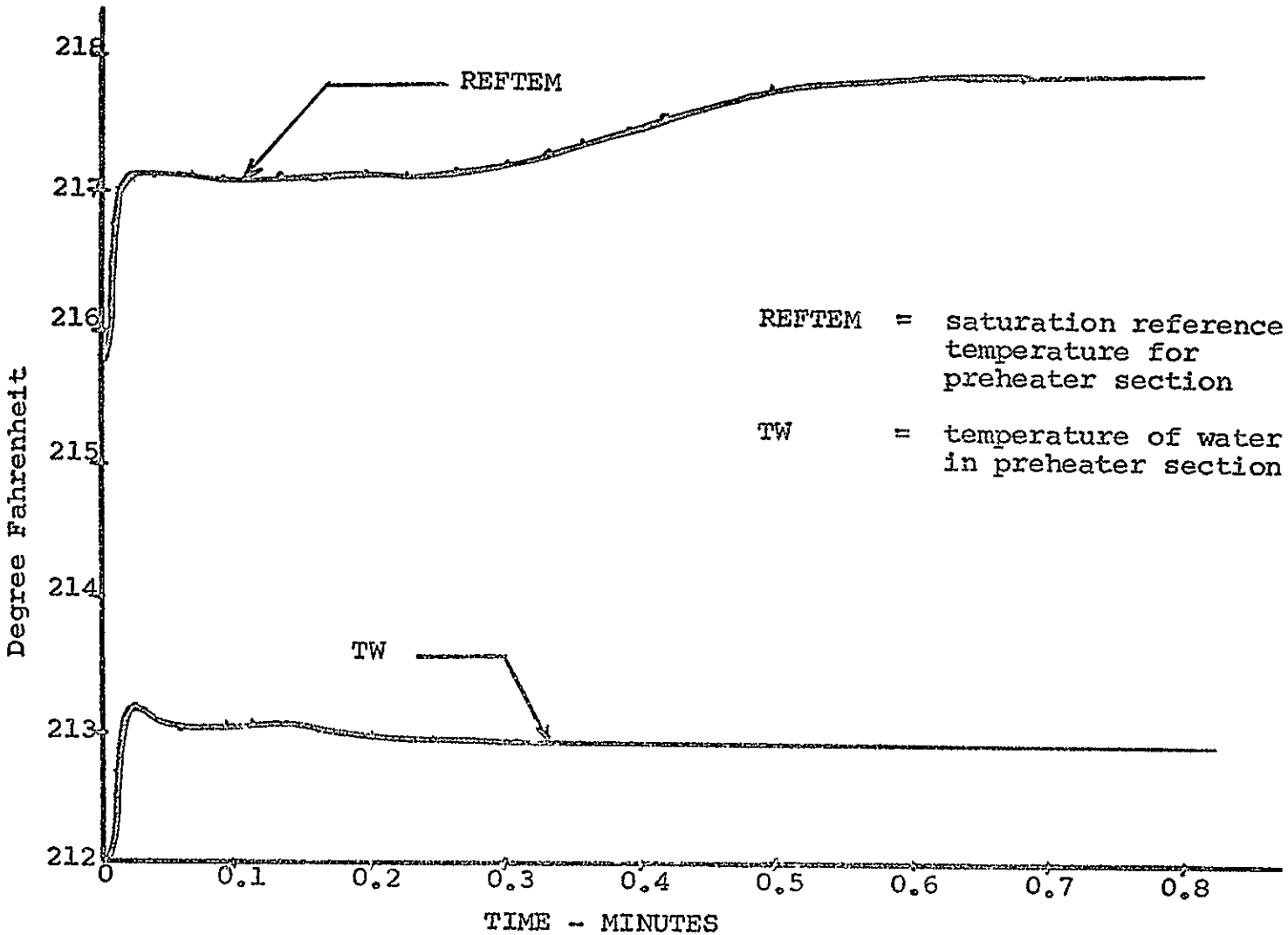

FIGURE 14. RUN A, TIME RESPONSE OF TW AND REFTEM.

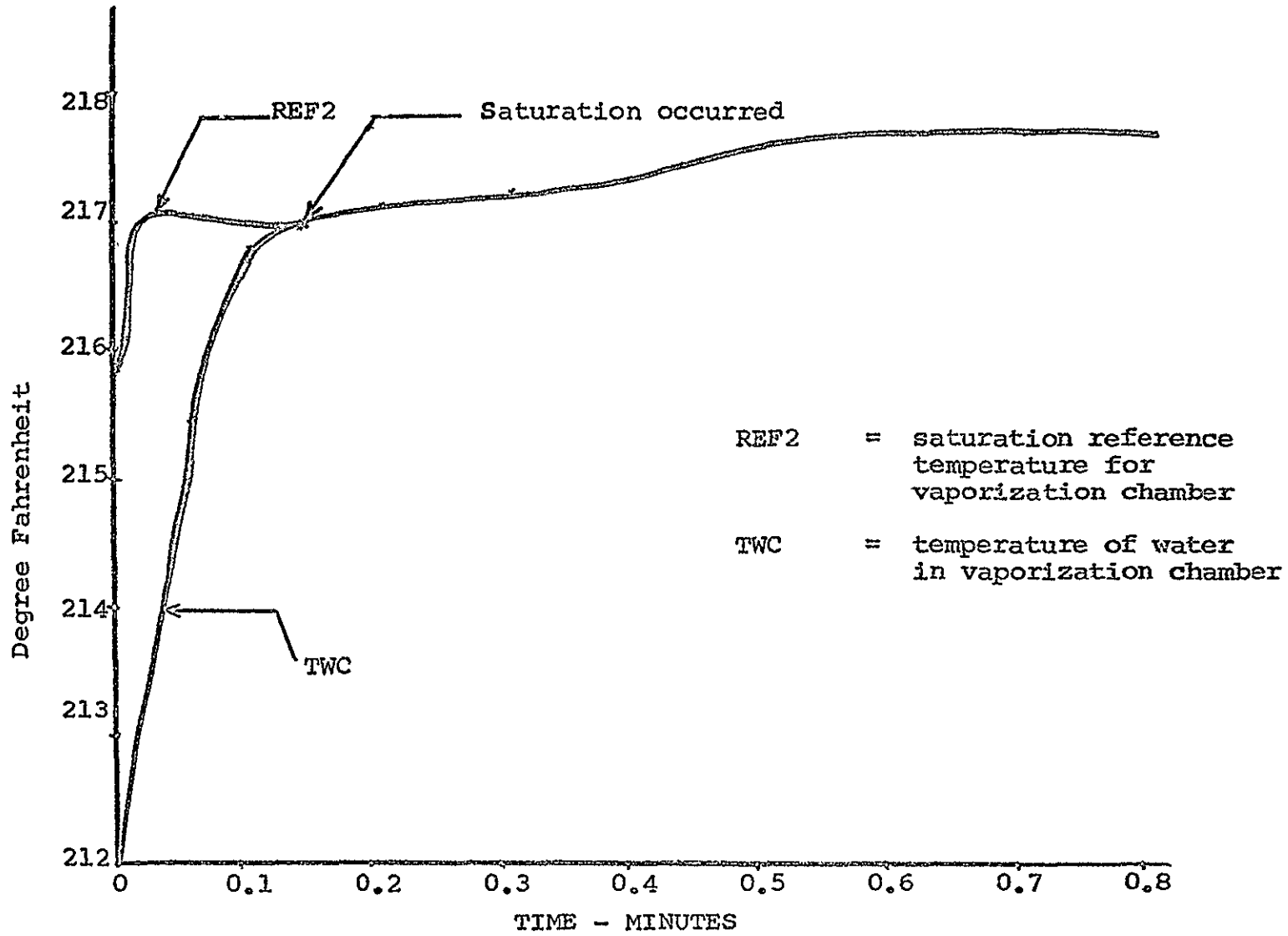

FIGURE 15. RUN A, TIME RESPONSE OF TWC AND REF2.

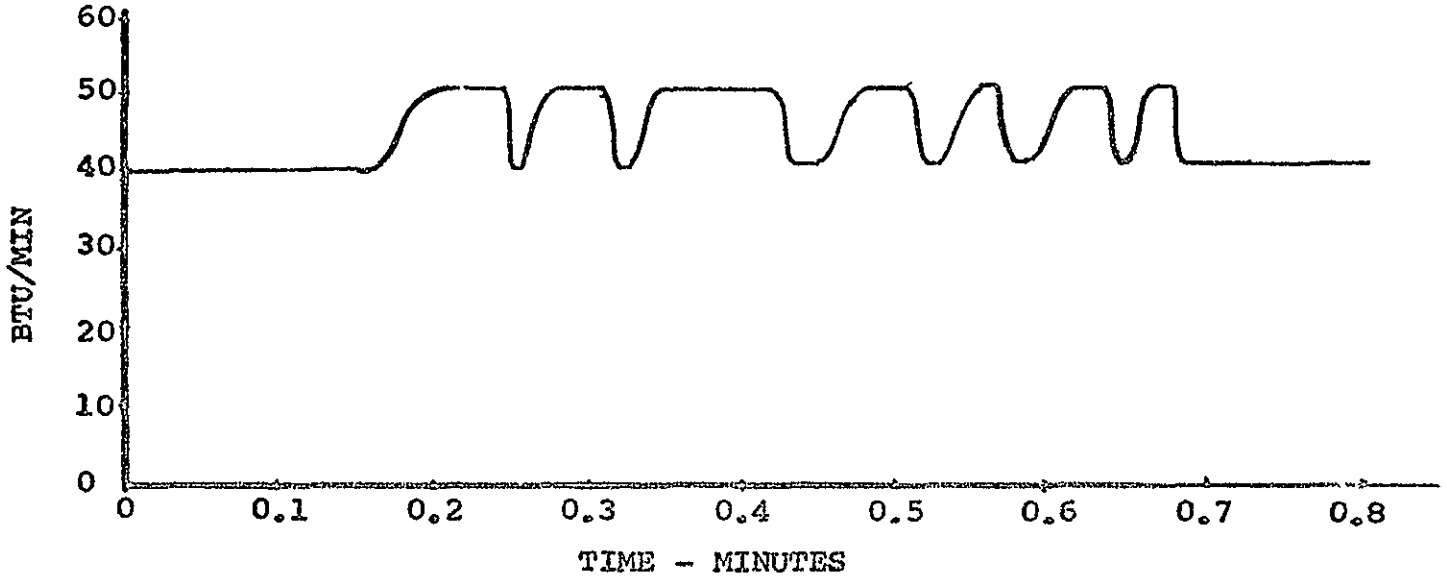

FIGURE 16. RUN A, TIME RESPONSE OF VAPORIZATION HEAT-RATE INPUT.

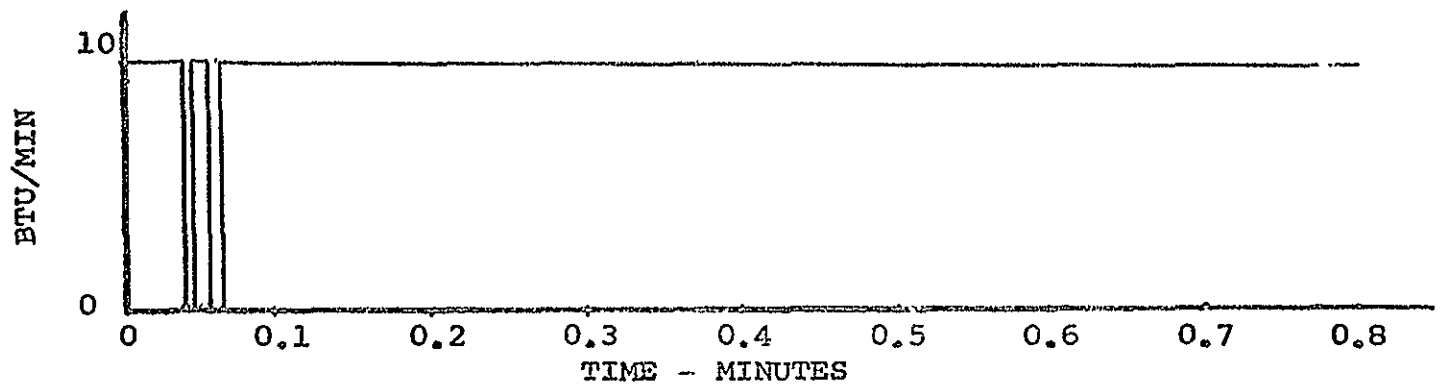

FIGURE 17. RUN A, TIME RESPONSE OF PREHEATER HEAT-RATE INPUT.

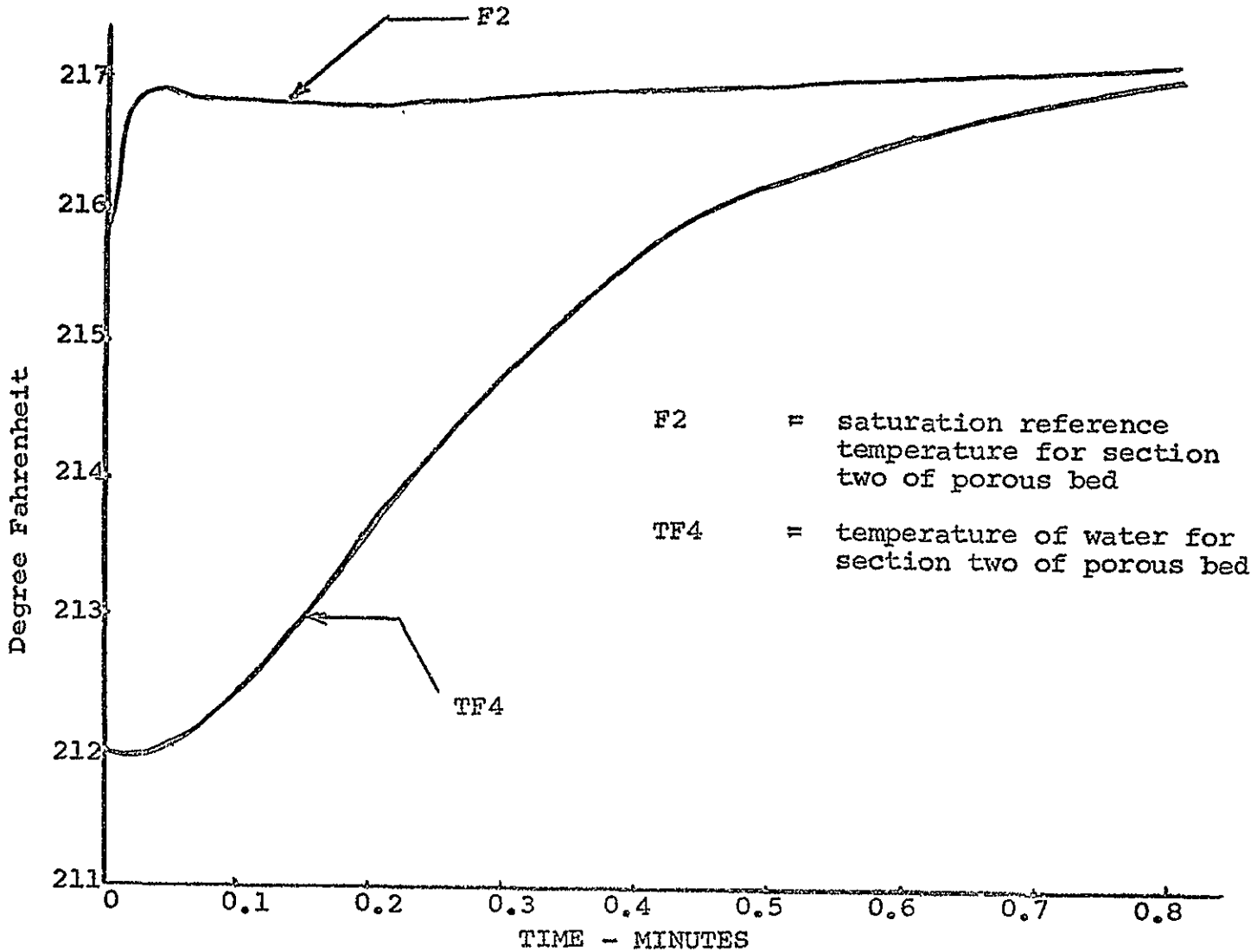

FIGURE 18. RUN A, TIME RESPONSE OF TF4 AND F2.

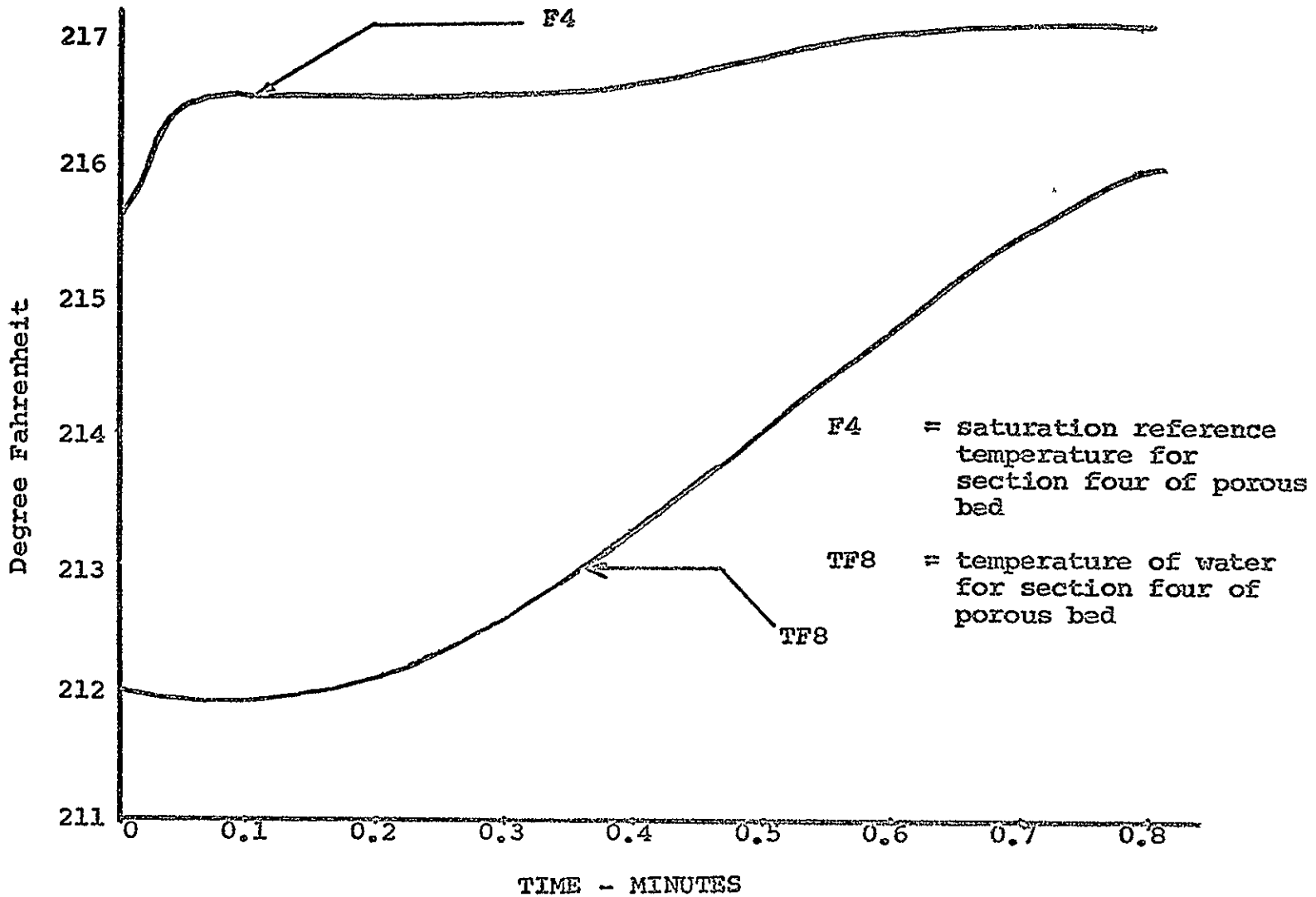

FIGURE 19. RUN A, TIME RESPONSE OF TF8 AND F4.

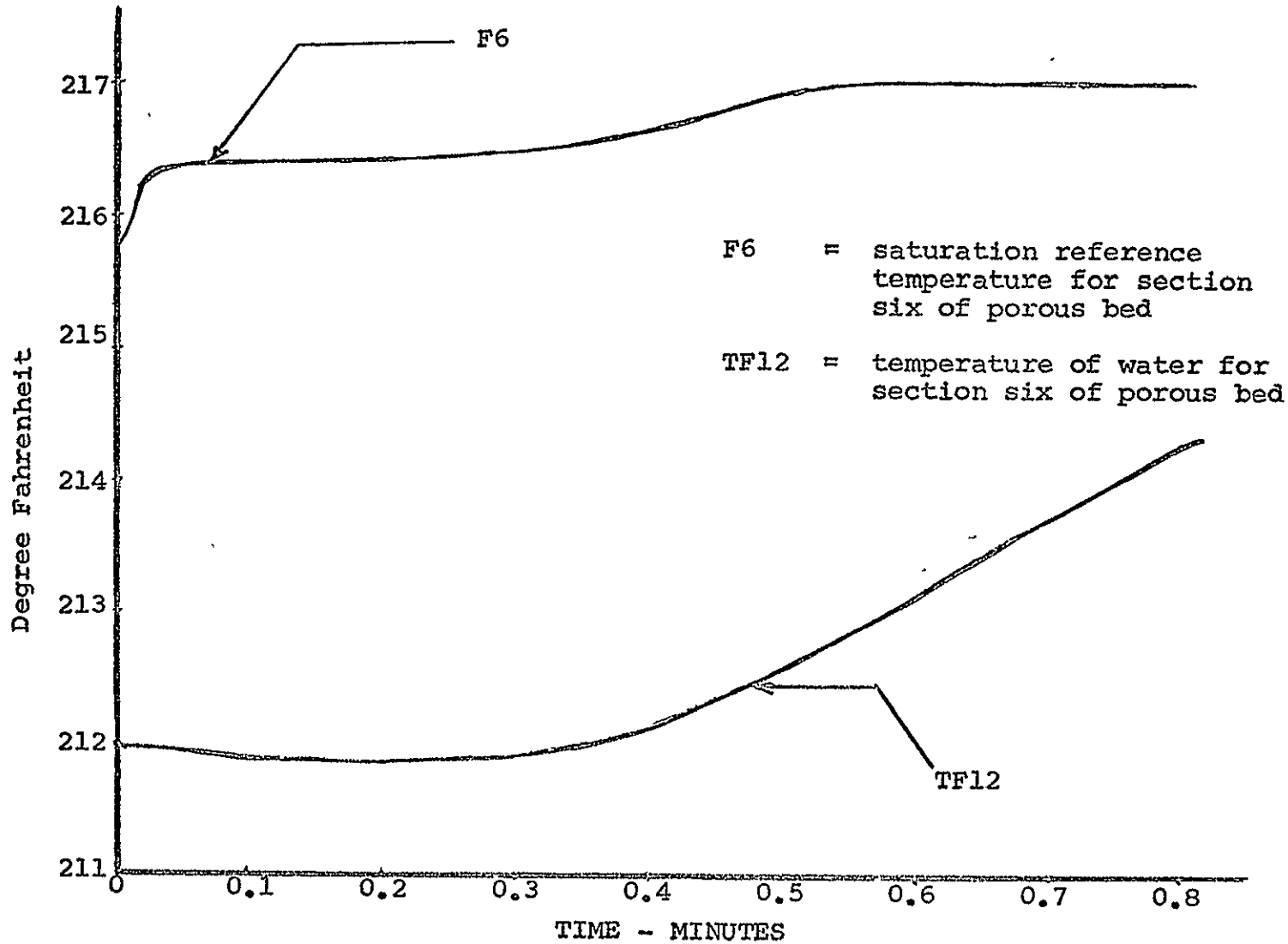

FIGURE 20. RUN A, TIME RESPONSE OF TF12 AND F6.

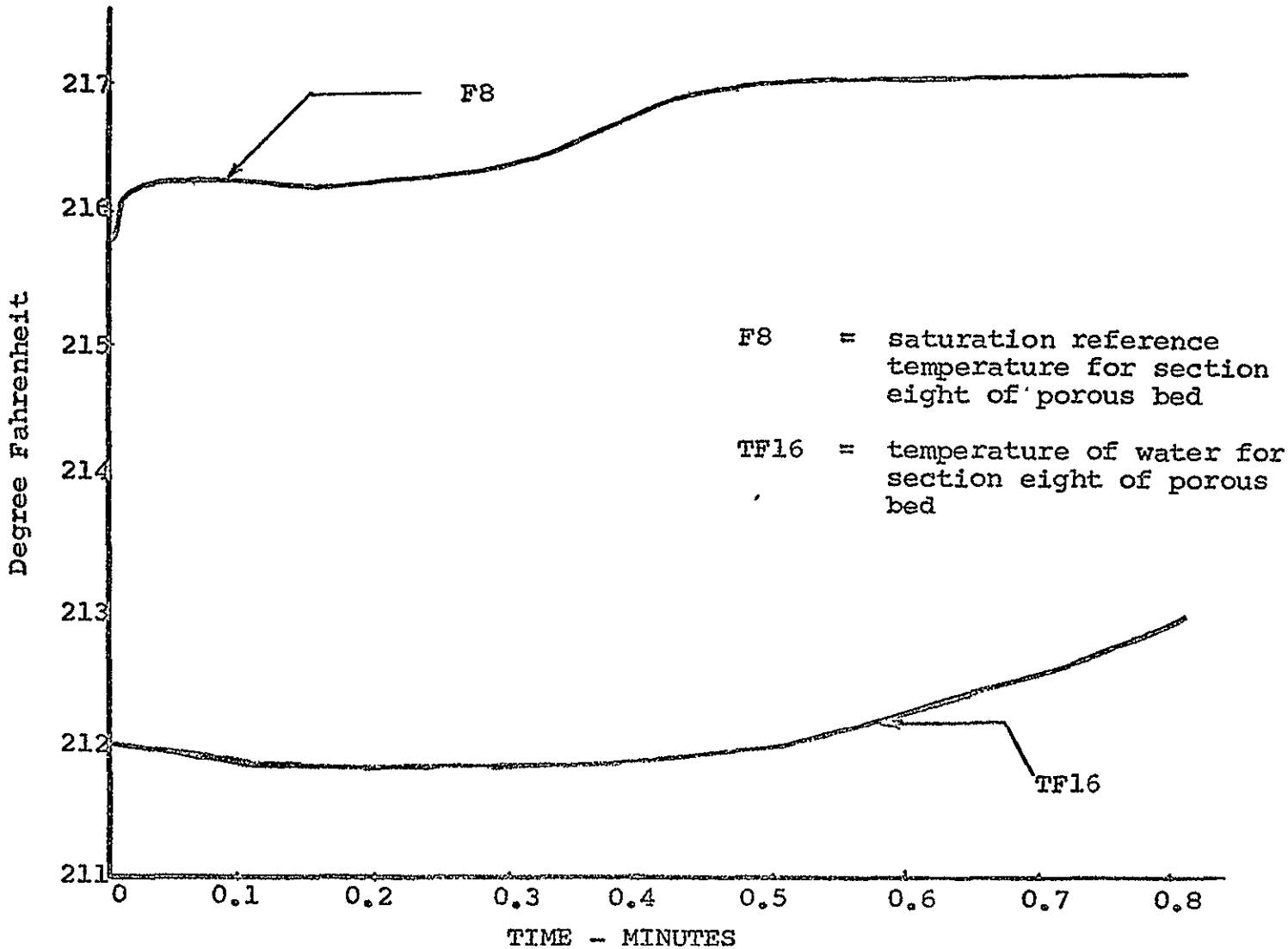

FIGURE 21. RUN A, TIME RESPONSE OF TF16 AND F8.

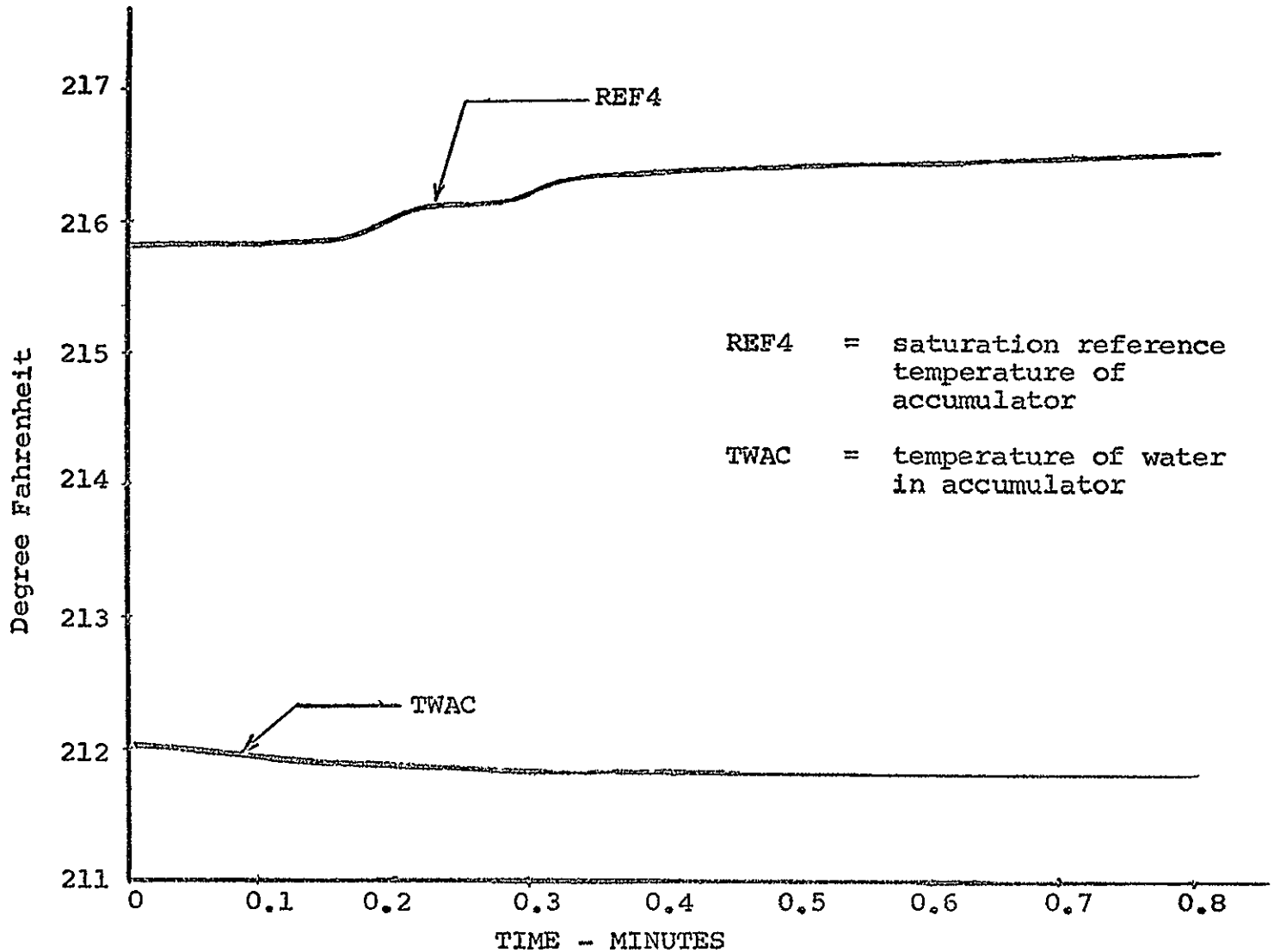

FIGURE 22. RUN A; TIME RESPONSE OF TWAC AND REF4.

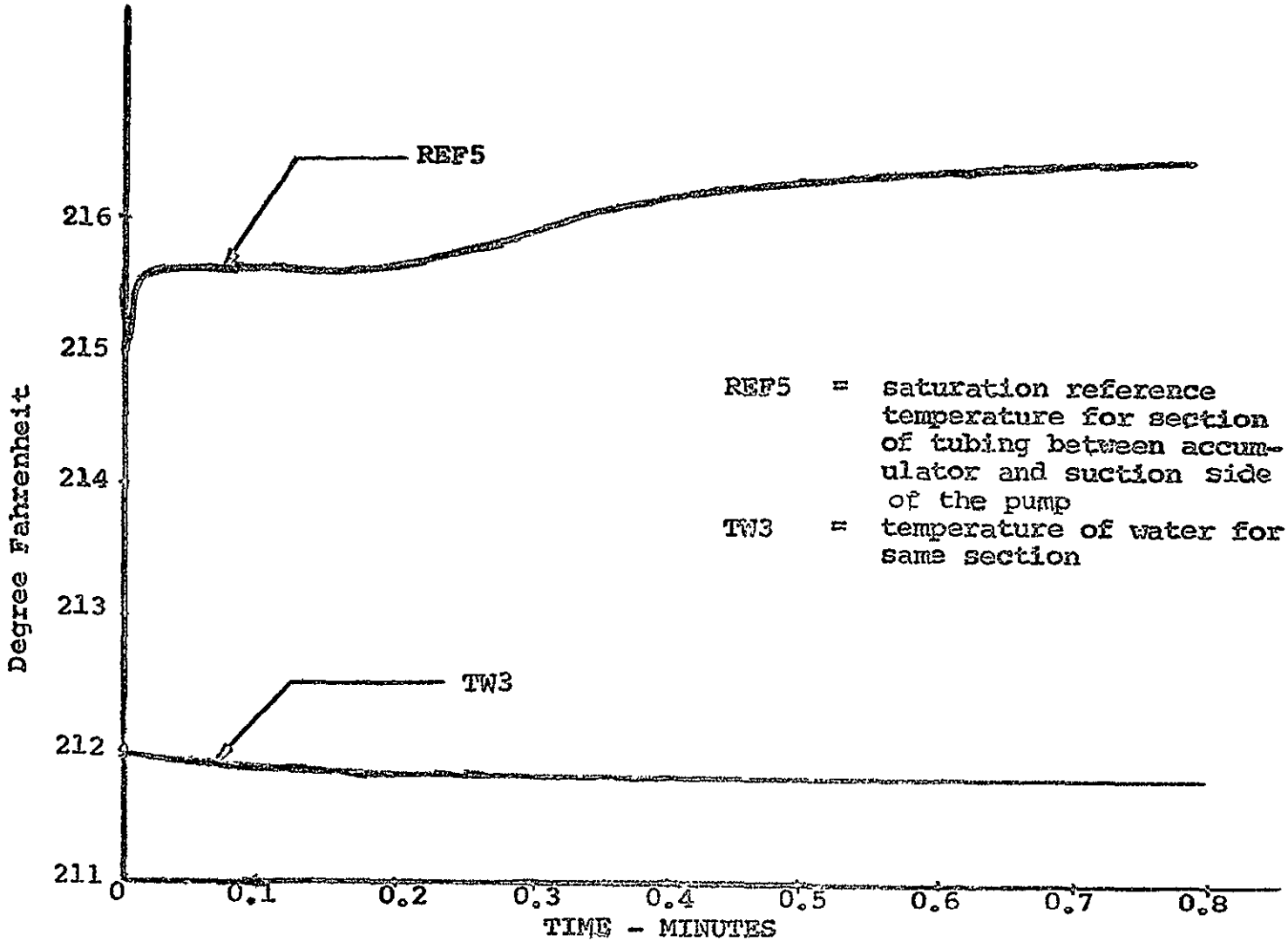

FIGURE 23. RUN A, TIME RESPONSE OF TW3 AND REF5.

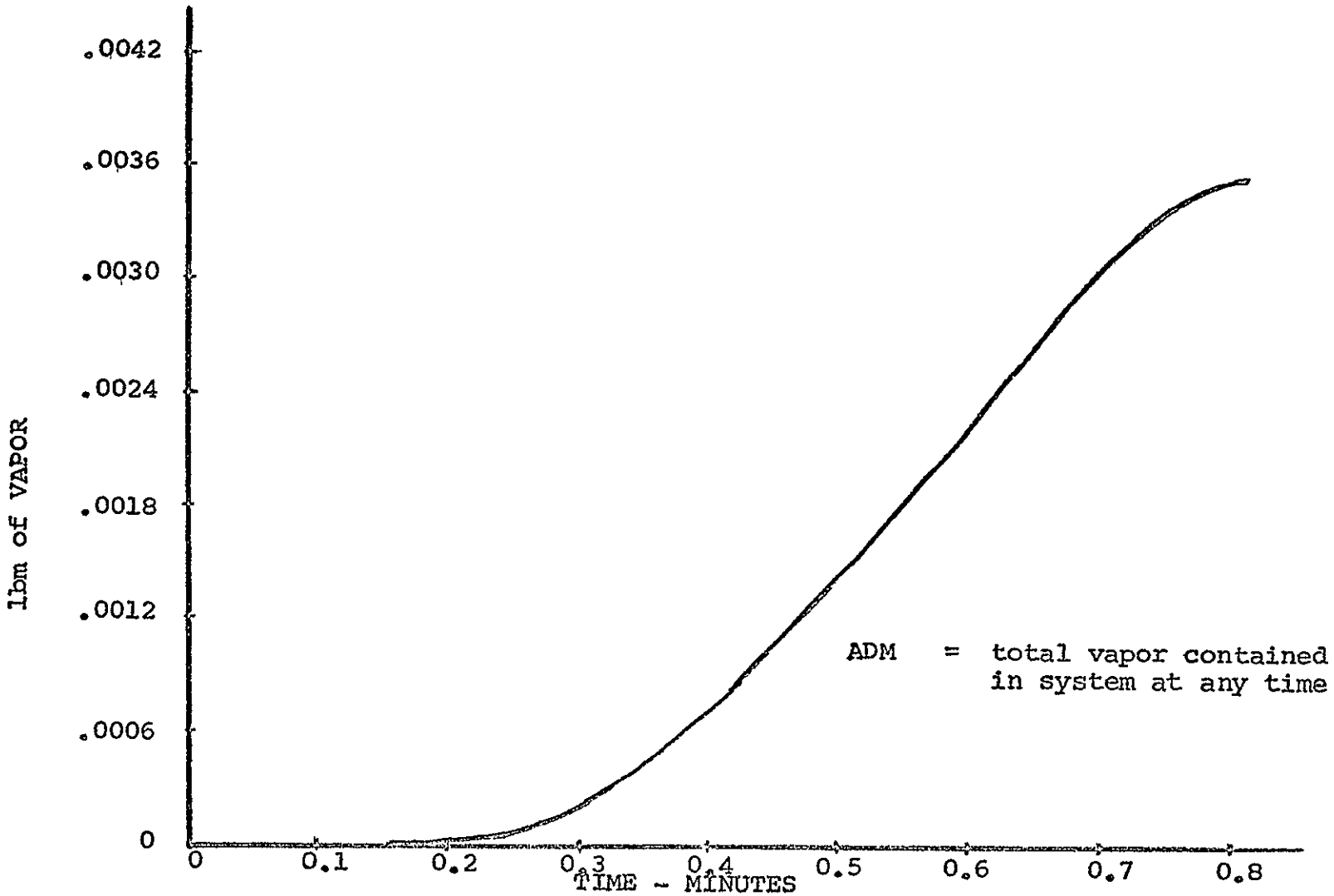

FIGURE 24. RUN A, TIME RESPONSE OF THE VAPOR CONTENT OF ADM.

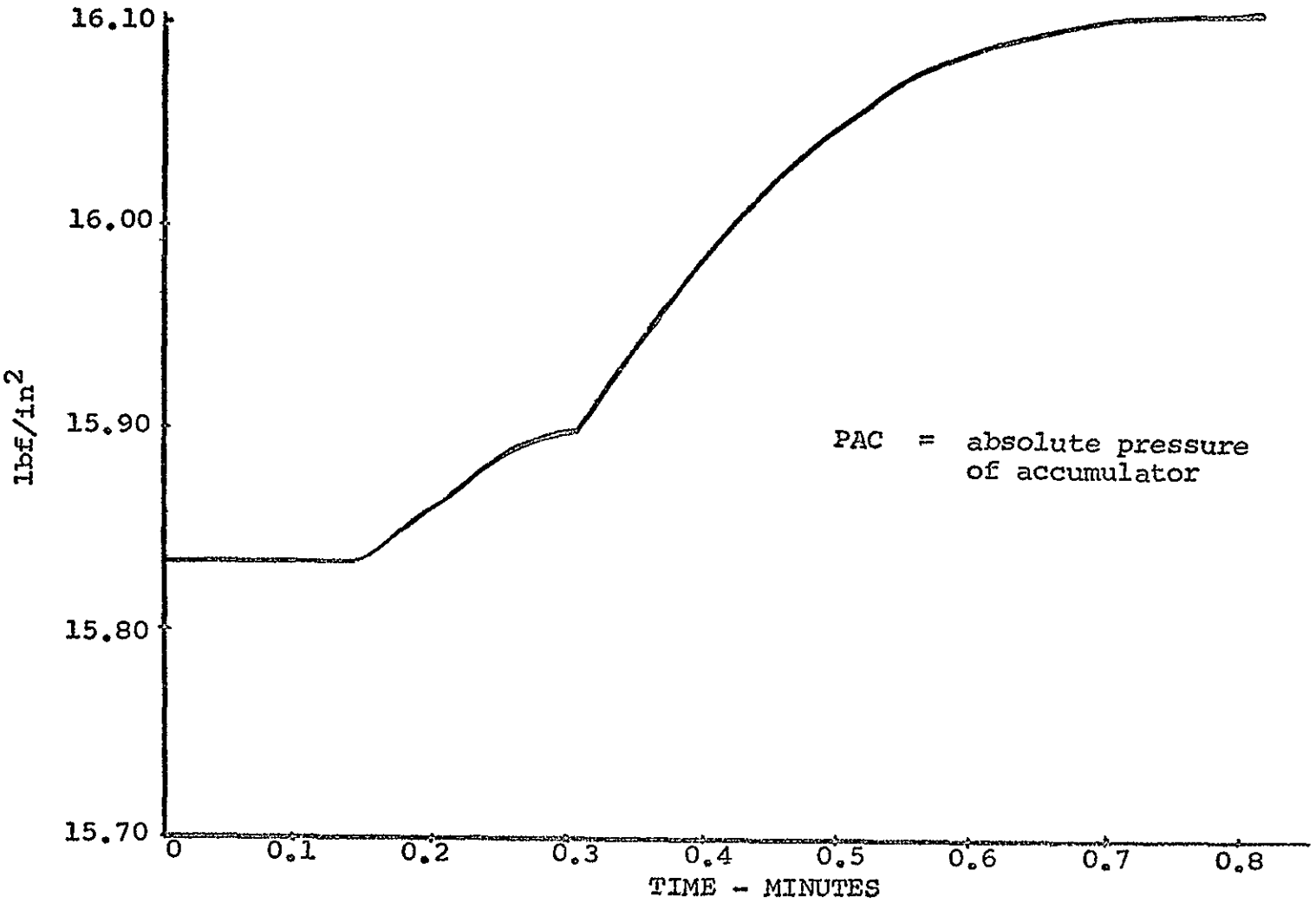

FIGURE 25. RUN A, TIME RESPONSE OF PAC.

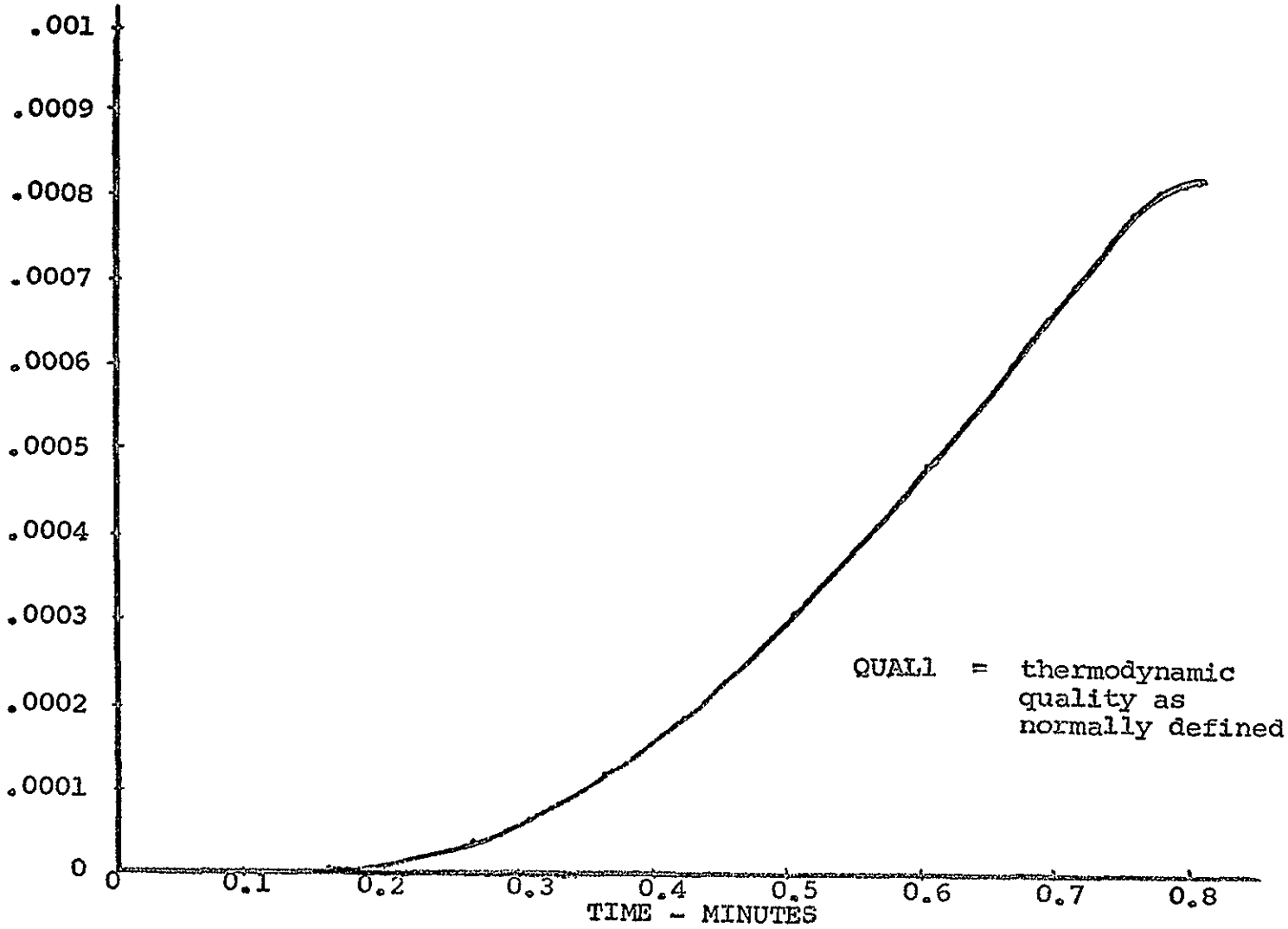

FIGURE 26. RUN A, TIME RESPONSE OF QUAL1.

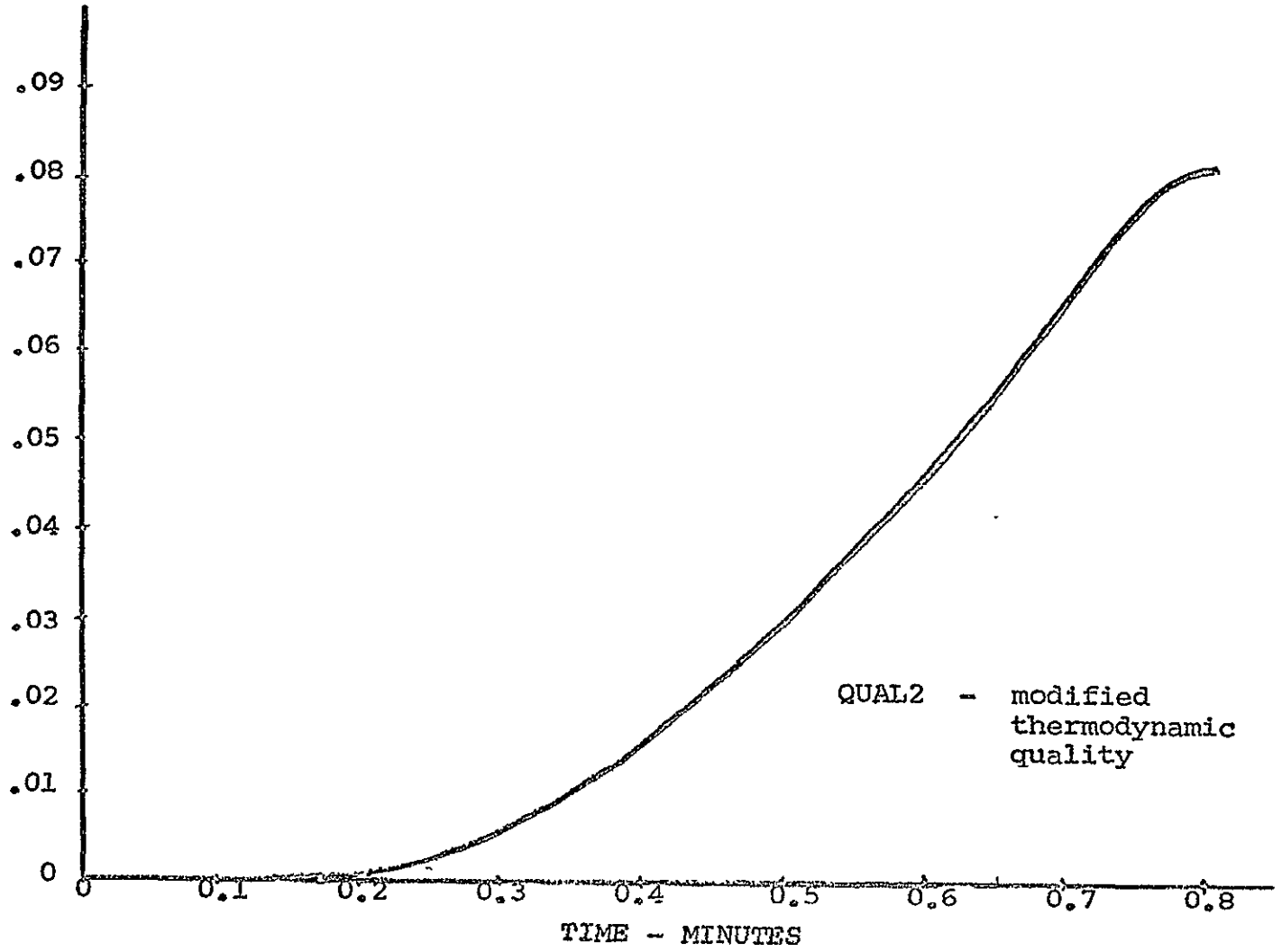

FIGURE 27. RUN A, TIME RESPONSE OF QUAL2.

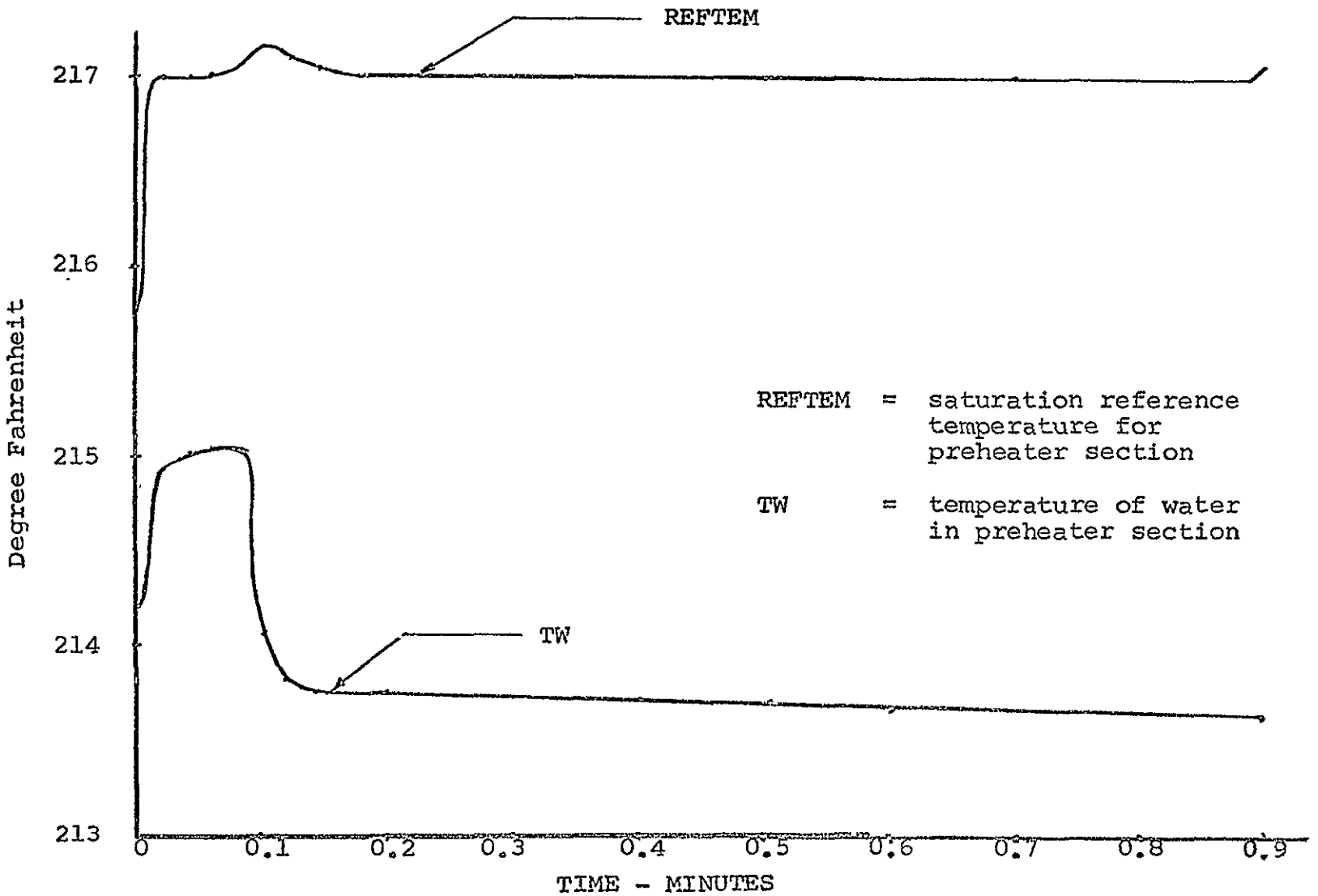

FIGURE 28. RUN B, TIME RESPONSE OF TW AND REFTEM.

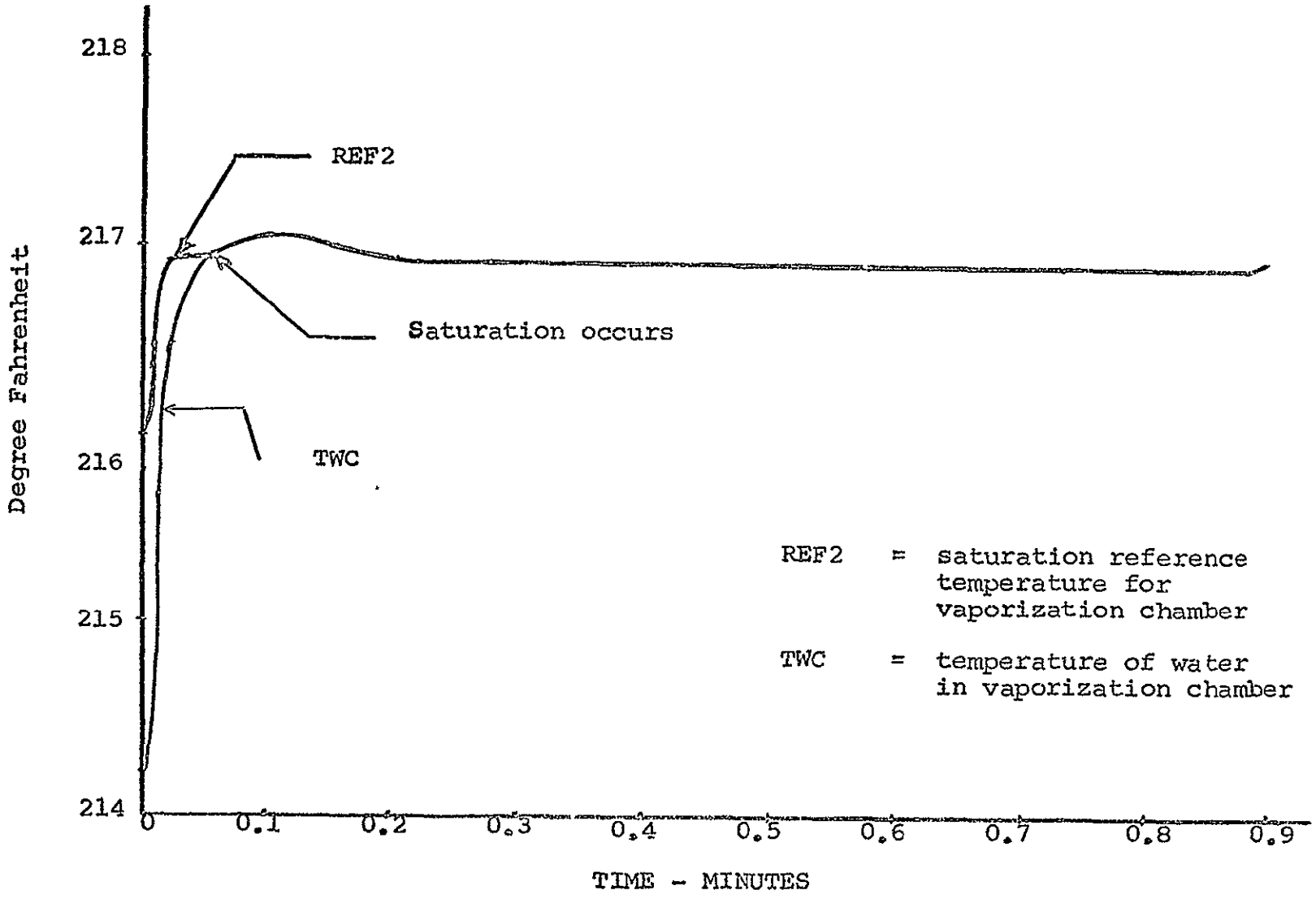

FIGURE 29. RUN B, TIME RESPONSE OF TWC AND REF2.

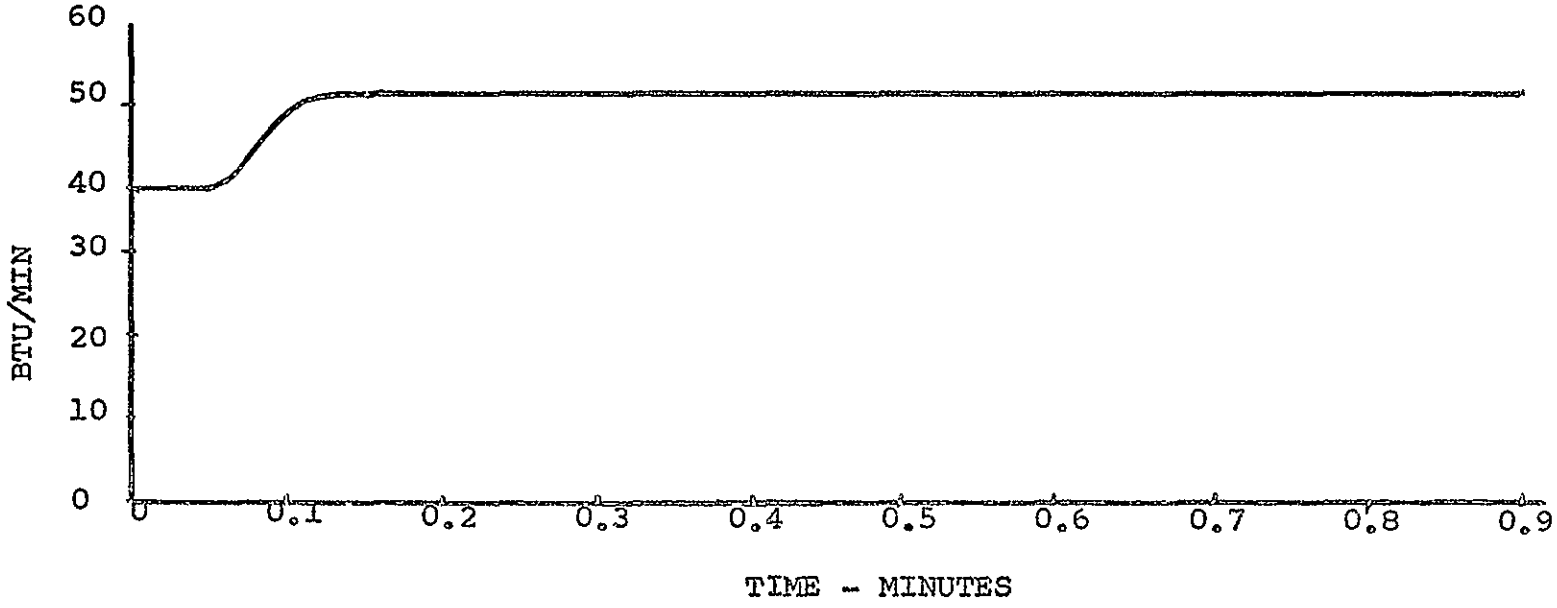

FIGURE 30. RUN B, TIME RESPONSE OF VAPORIZATION HEAT RATE INPUT

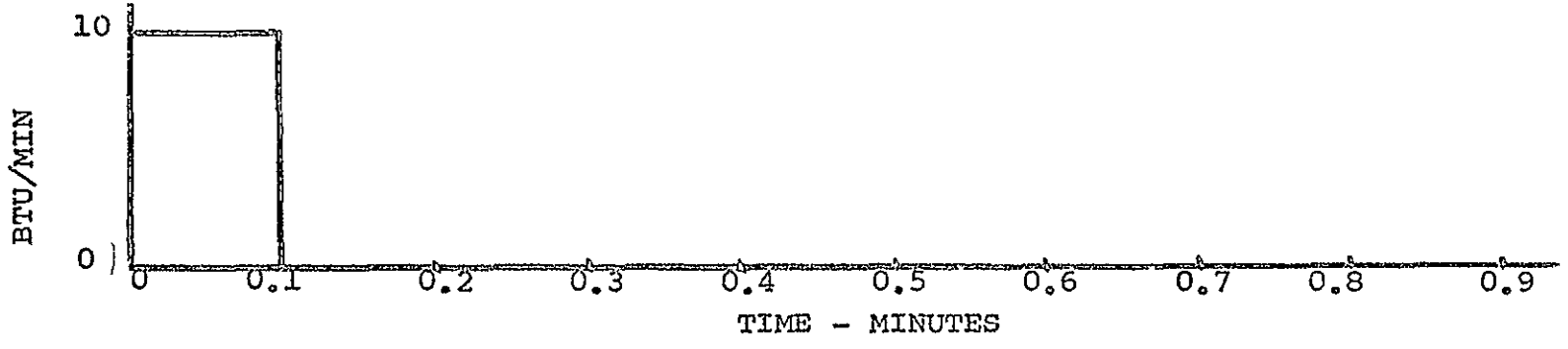

FIGURE 31. RUN B, TIME RESPONSE OF PREHEATER HEAT RATE INPUT

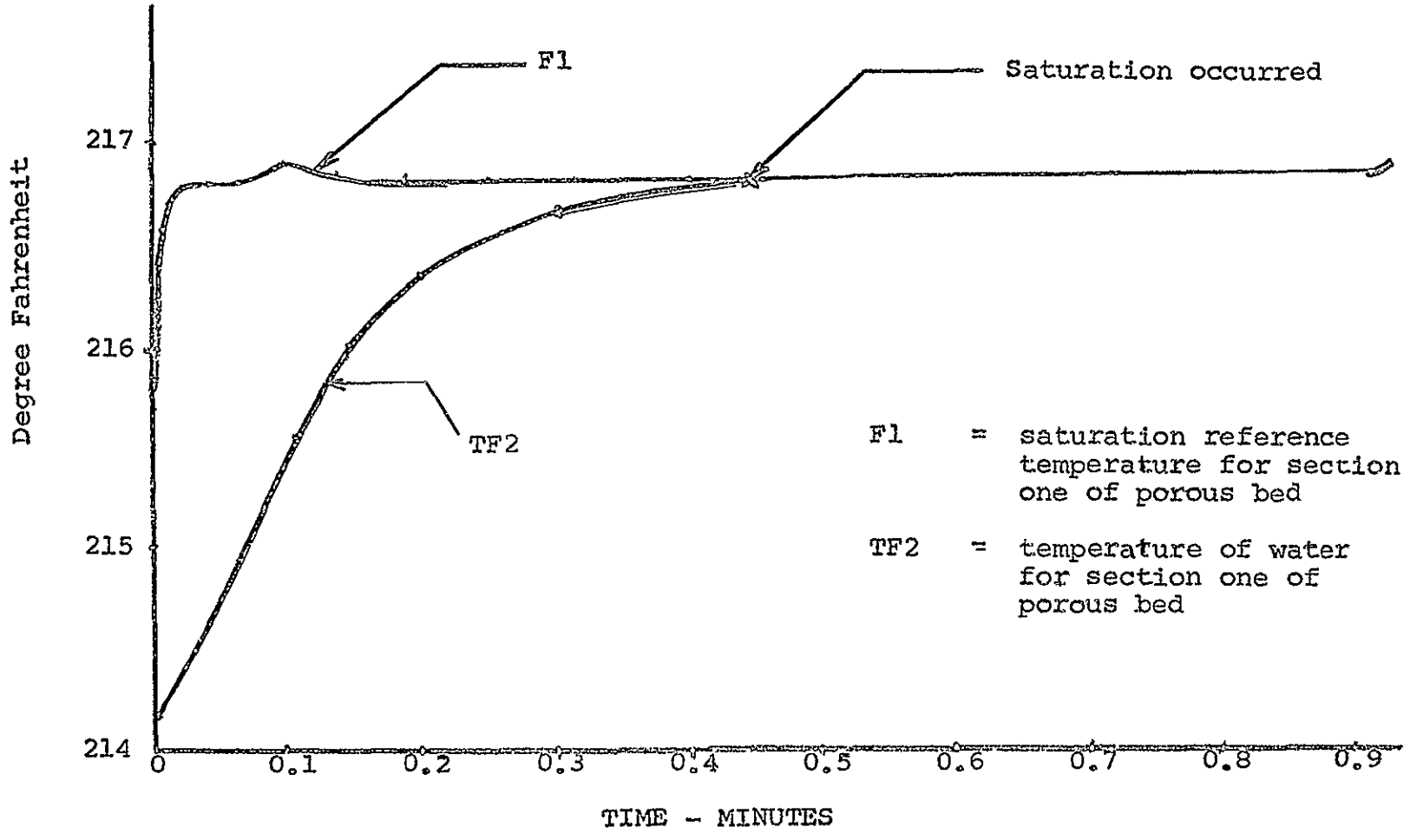

FIGURE 32. RUN B, TIME RESPONSE OF TF2 AND F1.

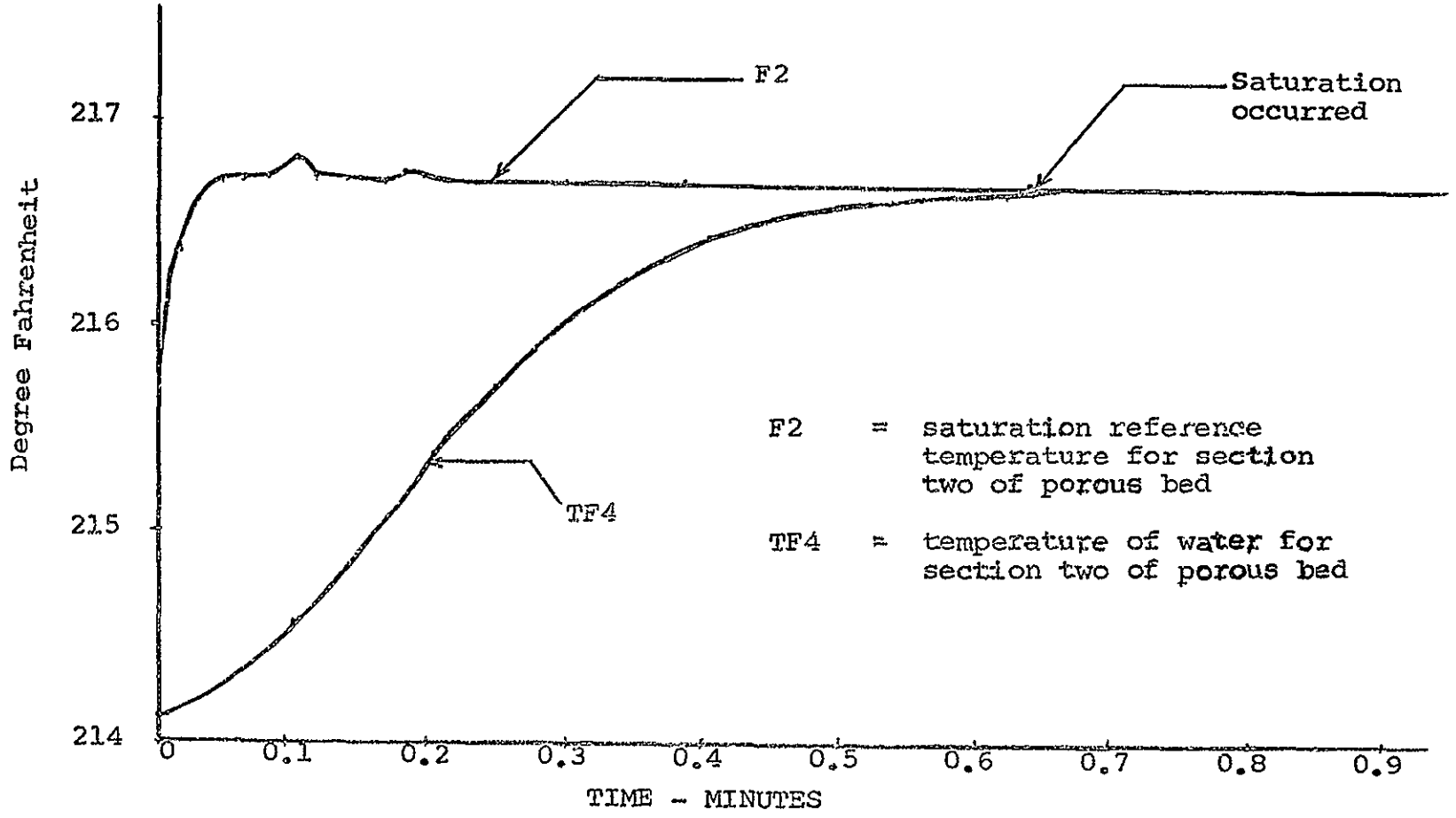

FIGURE 33. RUN B, TIME RESPONSE OF TF4 AND F2.

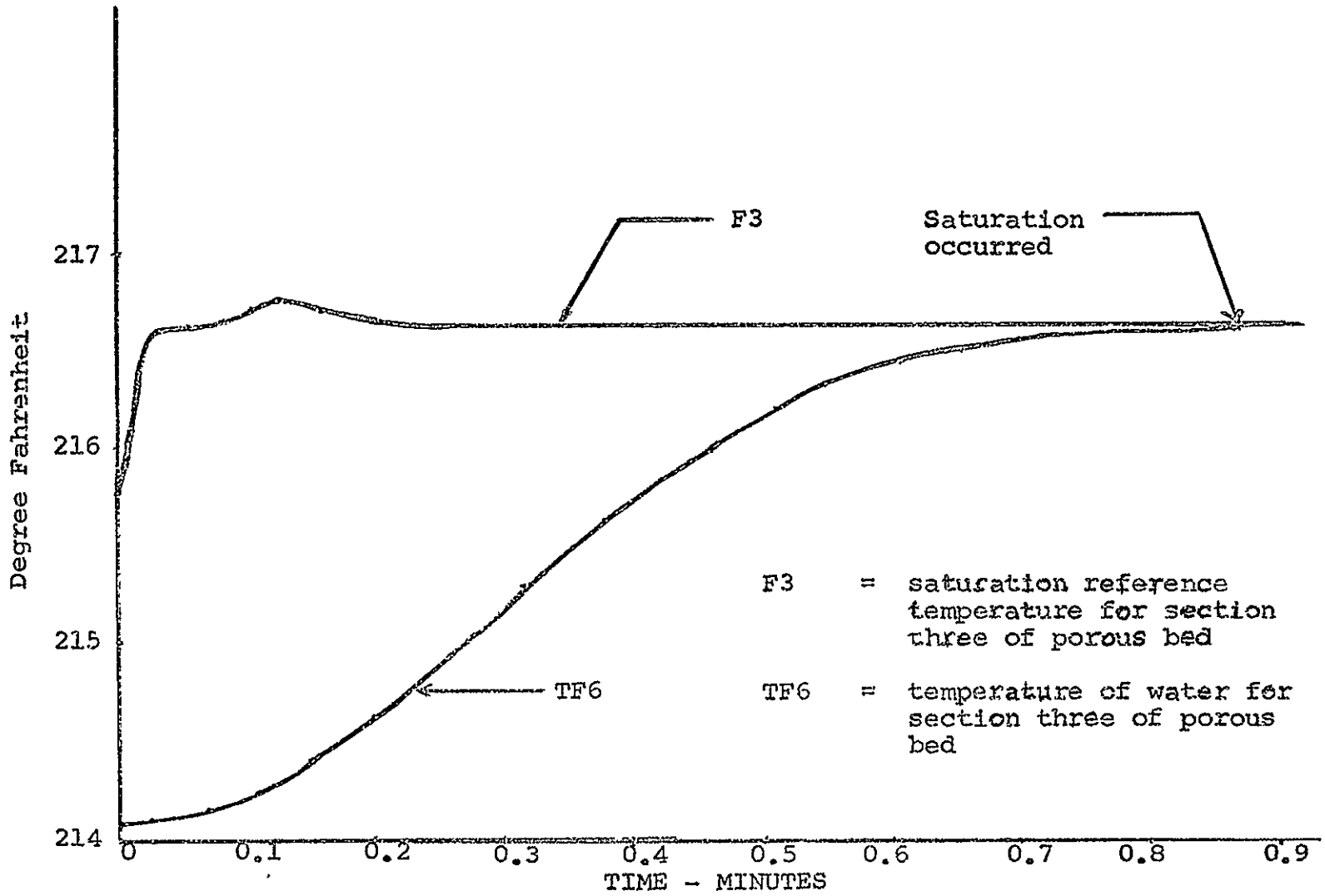

FIGURE 34. RUN B, TIME RESPONSE OF TF6 AND F3.

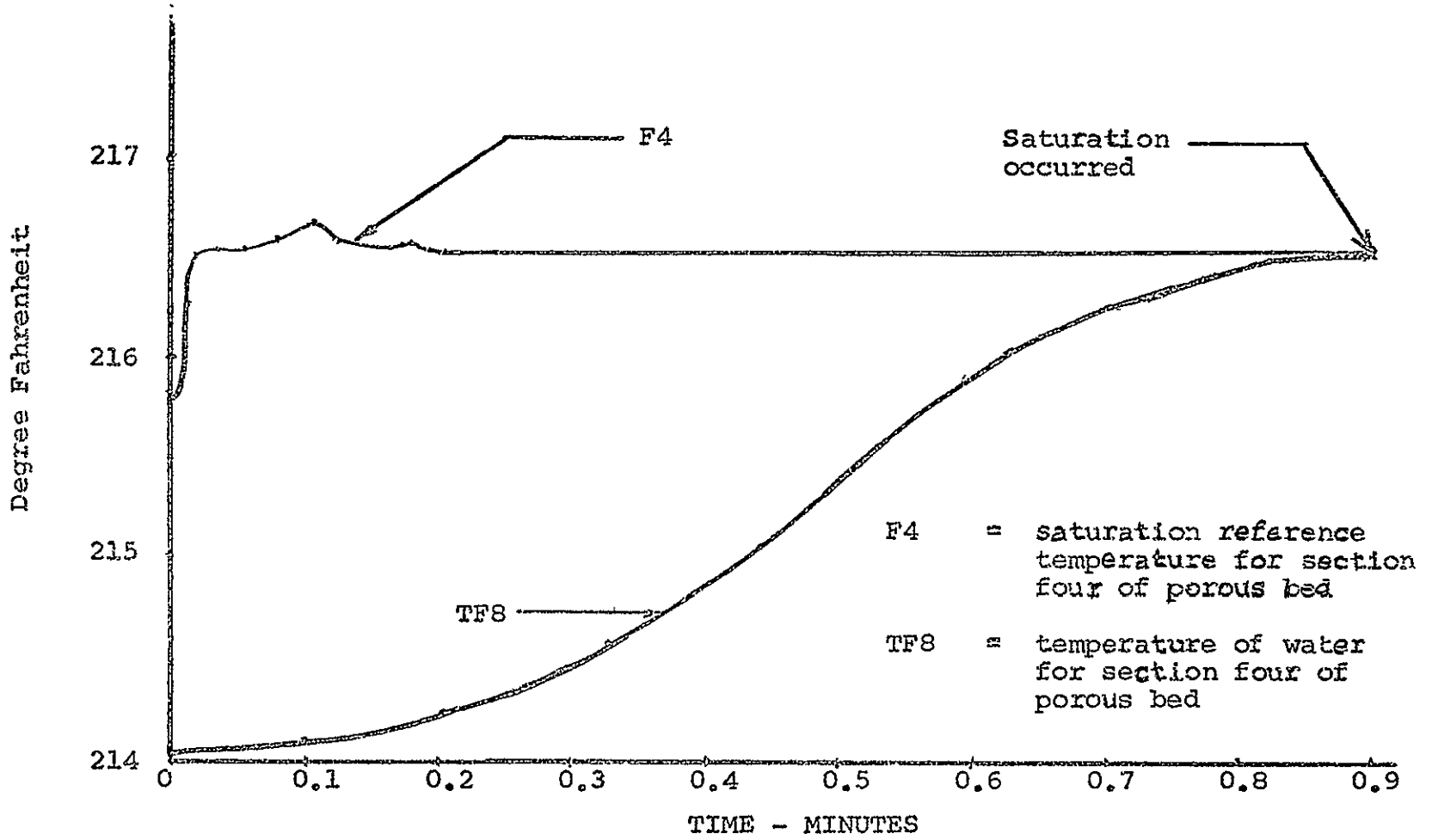

FIGURE 35. RUN B, TIME RESPONSE OF TF8 AND F4.

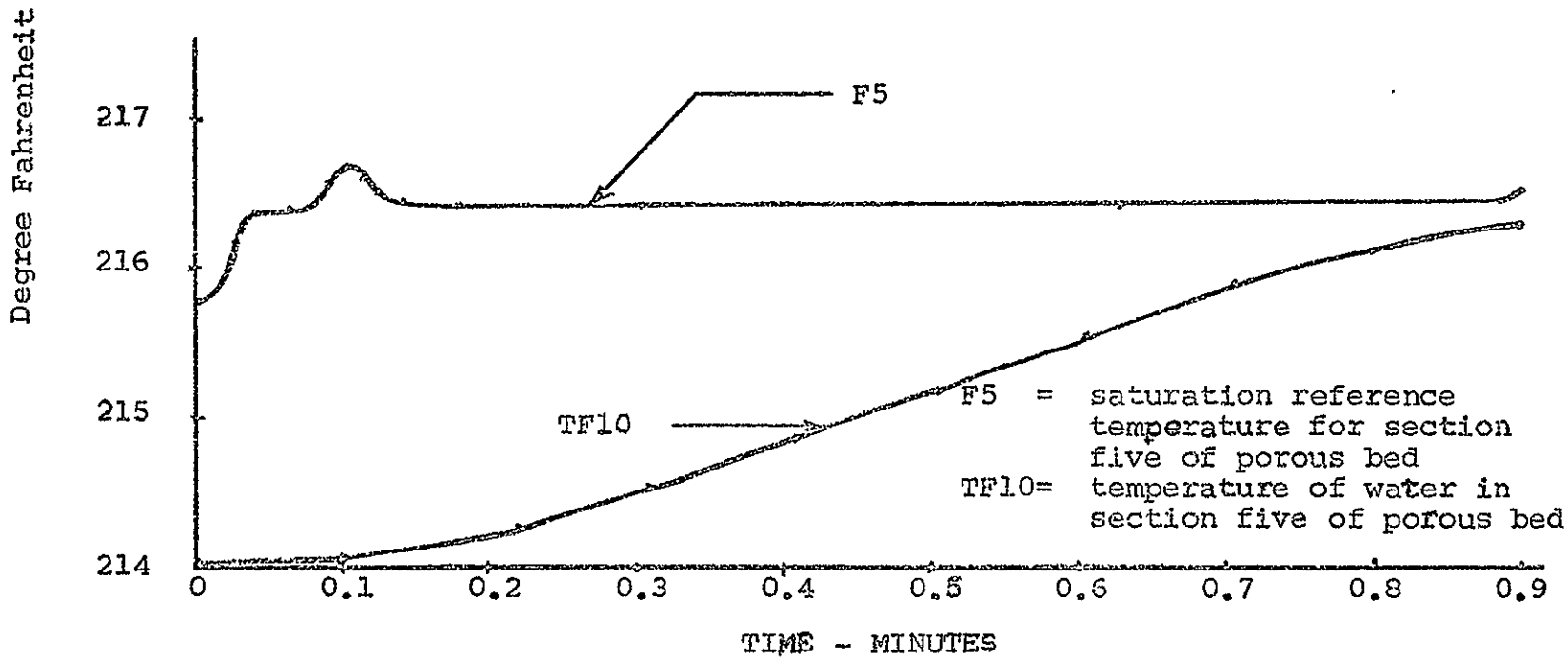

FIGURE 36. RUN B, TIME RESPONSE OF TF10 AND F5.

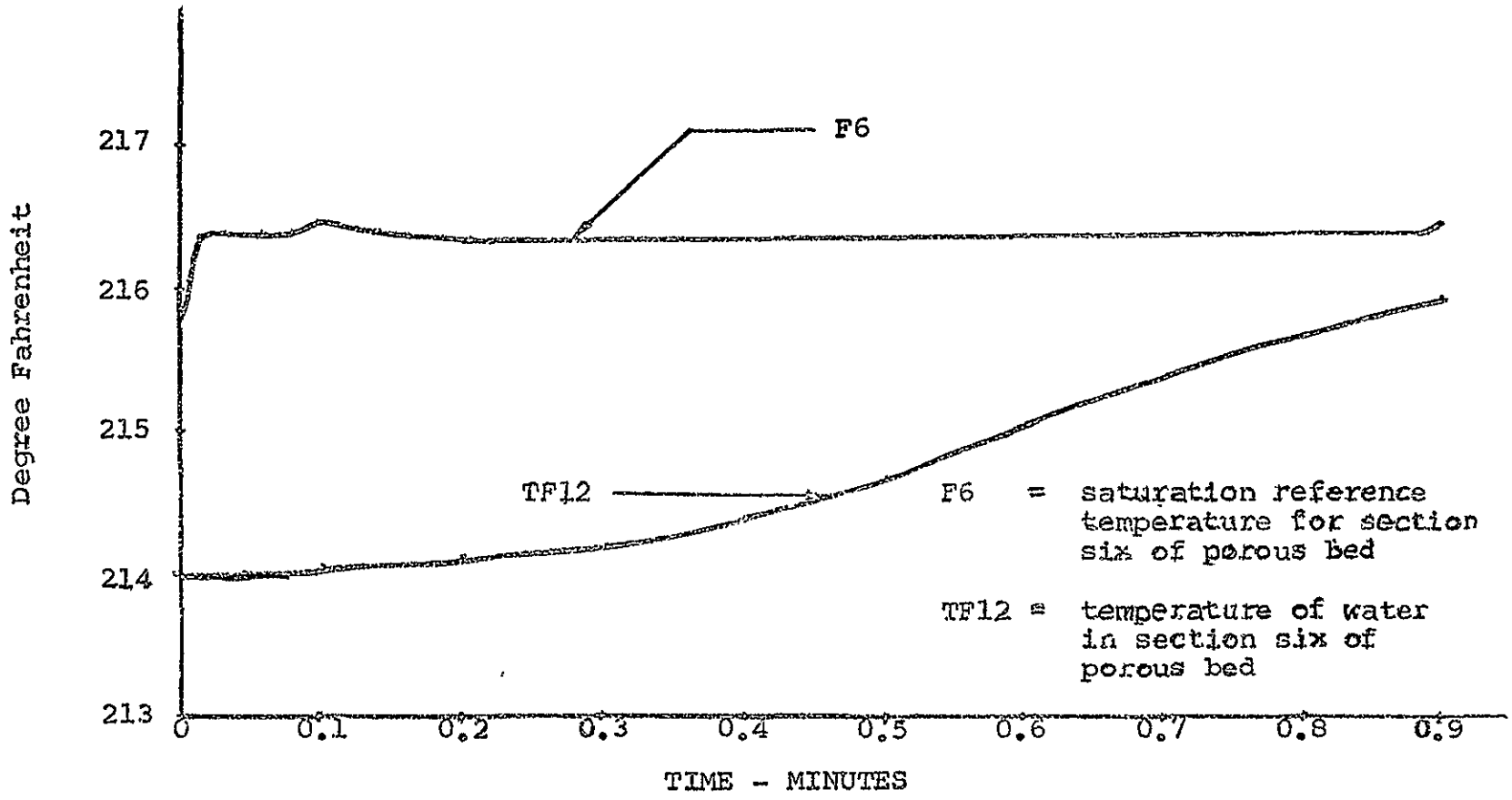

FIGURE 37. RUN B, TIME RESPONSE OF TF12 AND F6.

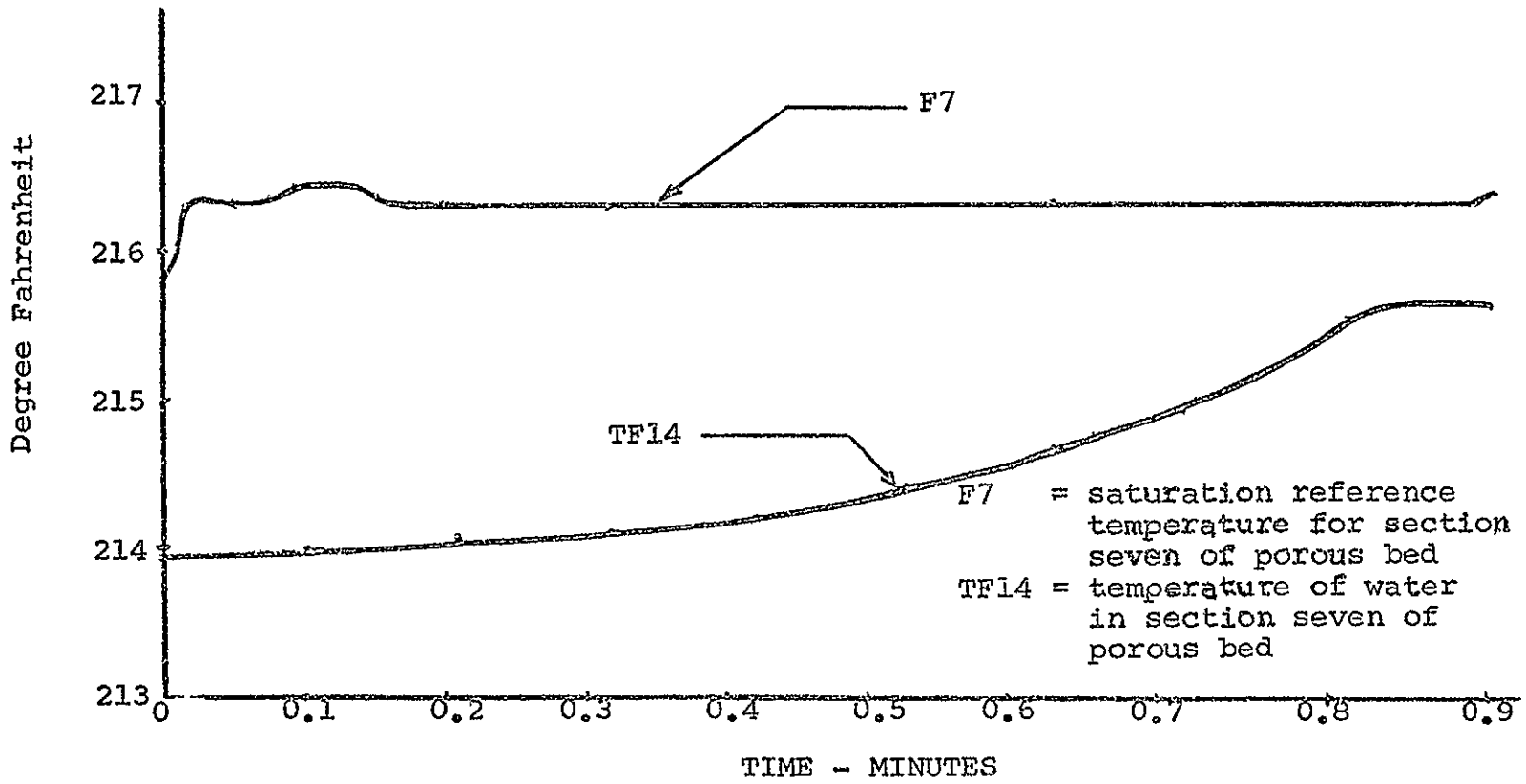

FIGURE 38. RUN B, TIME RESPONSE OF TF14 AND F7.

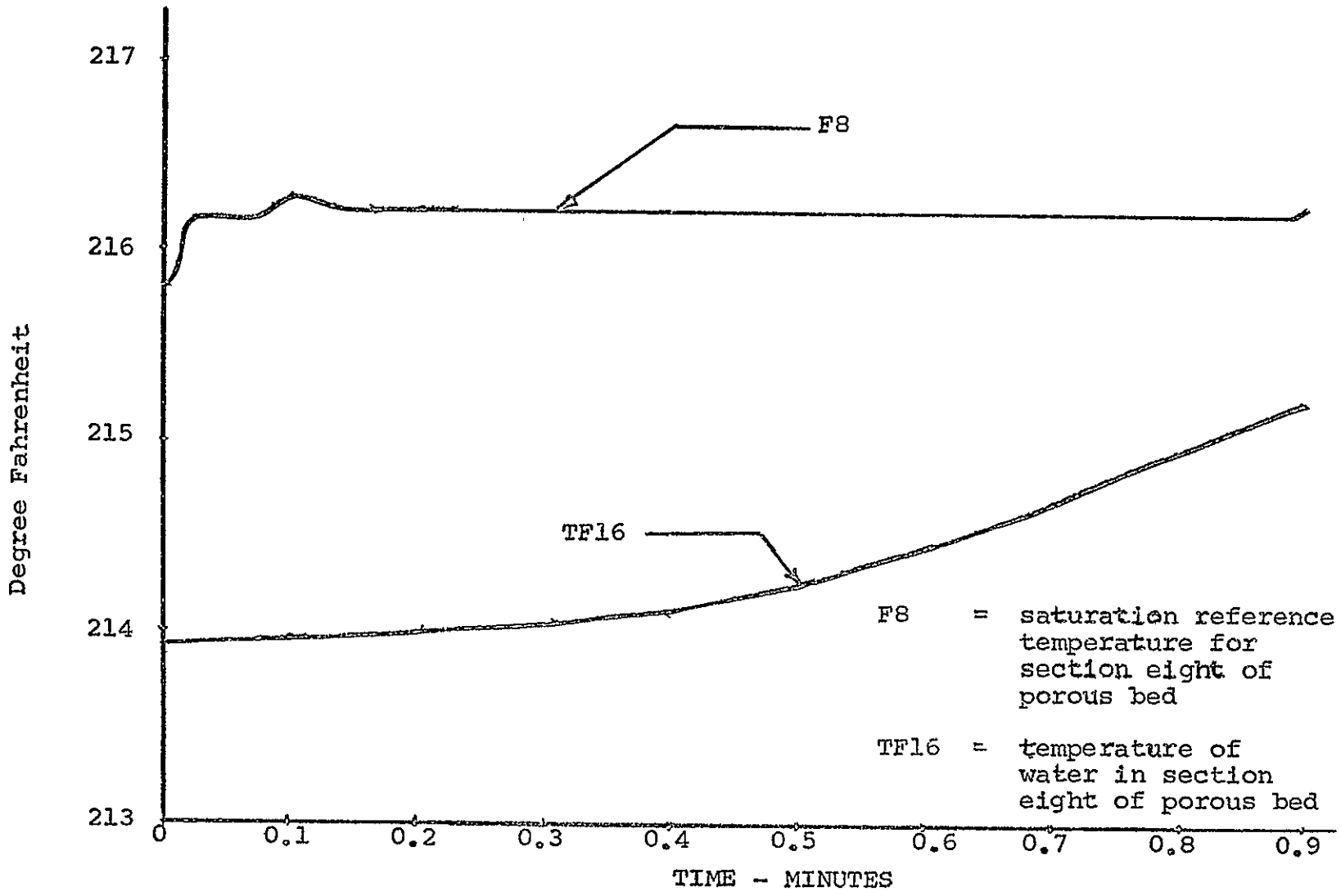

FIGURE 39. RUN B, TIME RESPONSE OF TF16 AND F8.

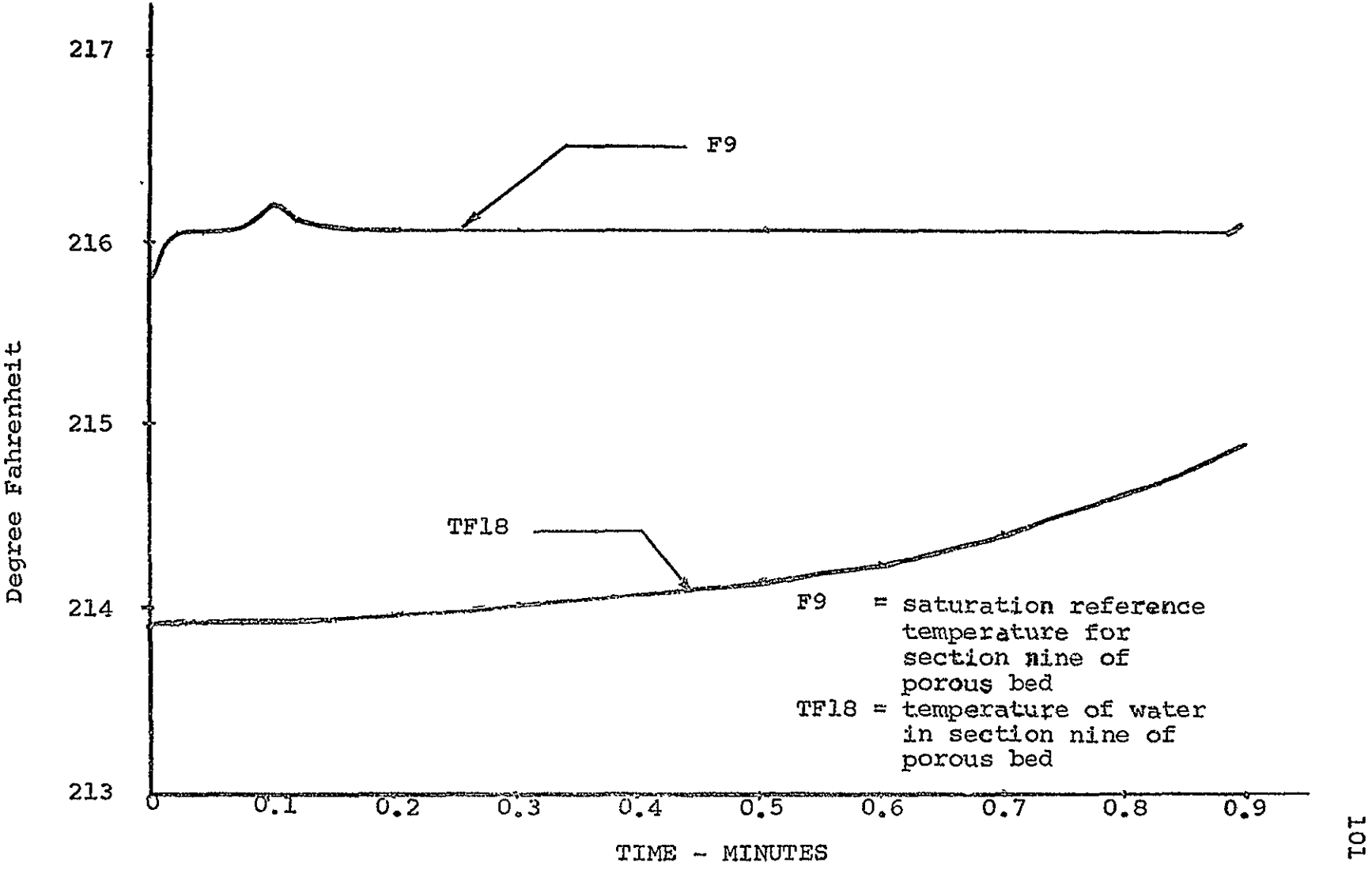

FIGURE 40. RUN B, TIME RESPONSE OF TF18 AND F9.

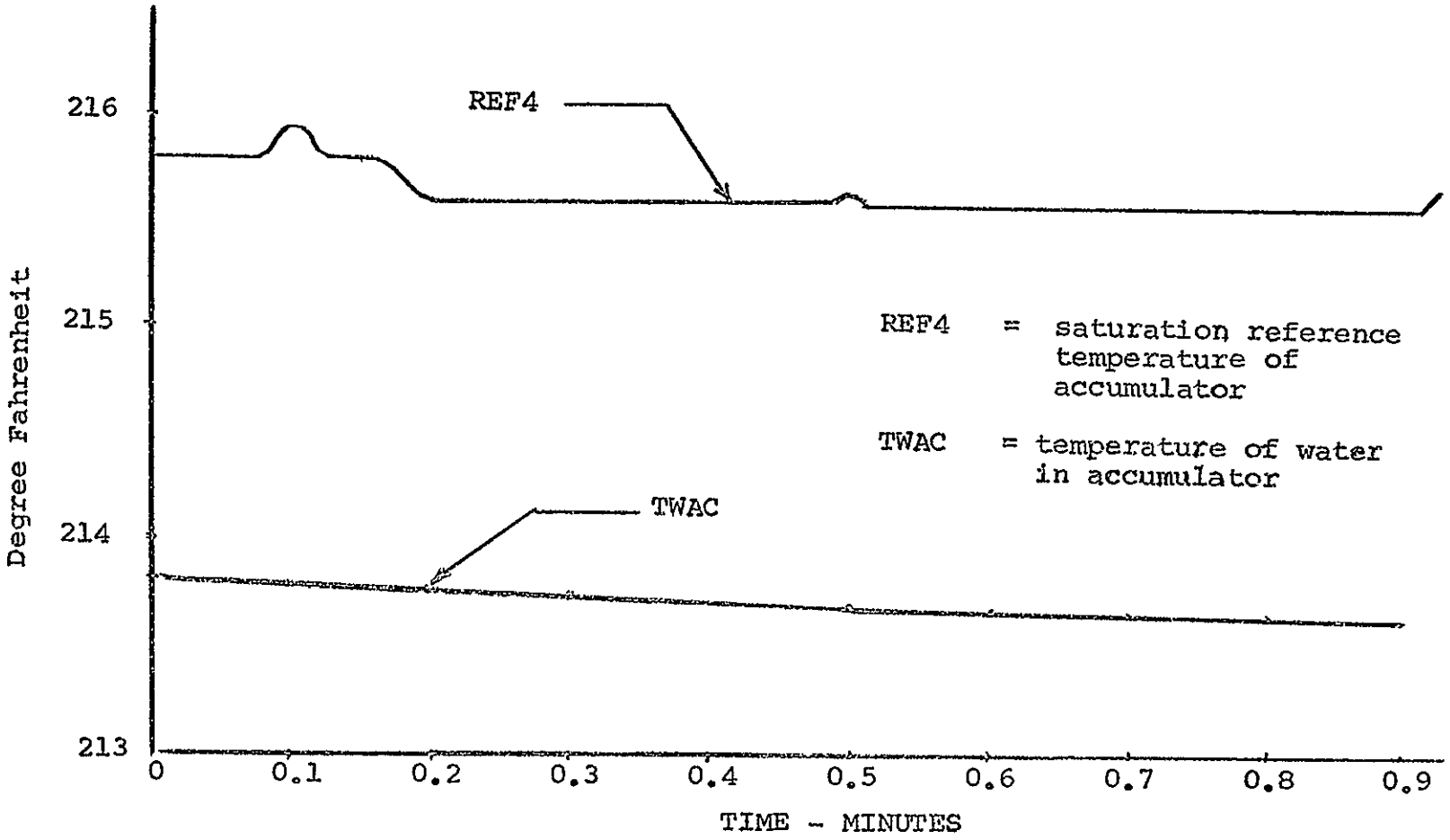

FIGURE 41. RUN B, TIME RESPONSE OF TWAC AND REF4

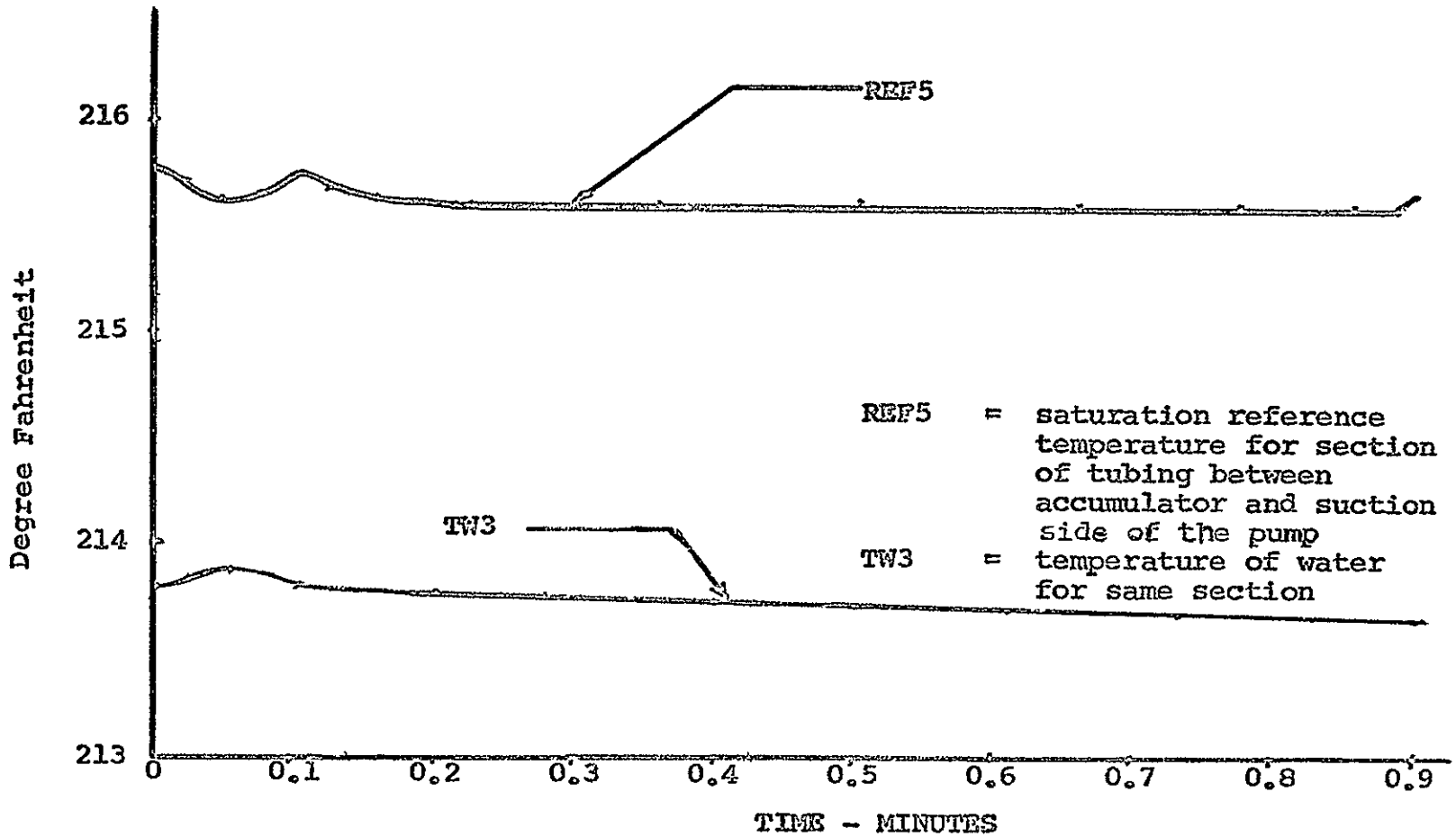

FIGURE 42. RUN B, TIME RESPONSE OF TW3 AND REF5.

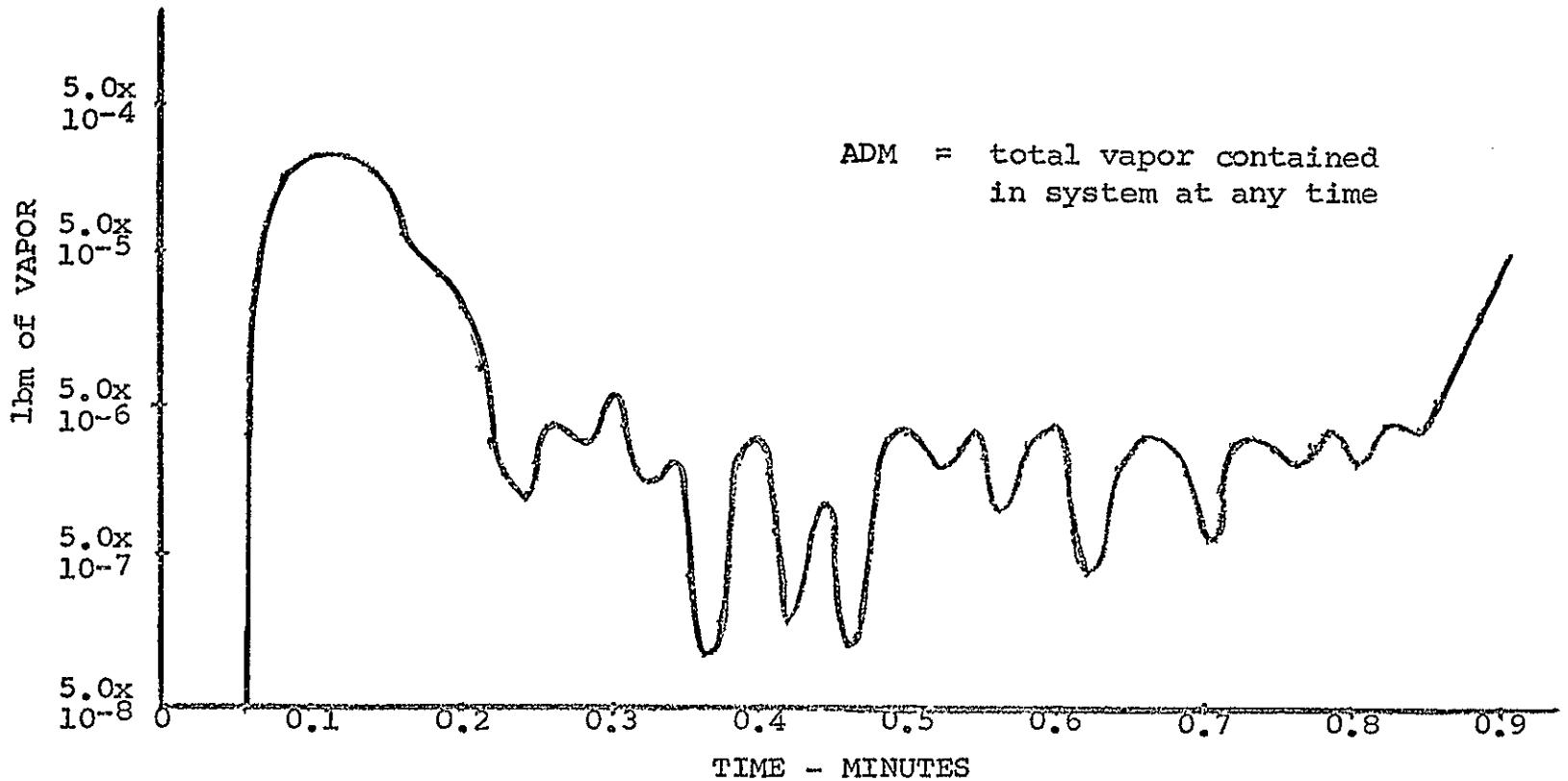

FIGURE 43. RUN B, TIME RESPONSE OF THE VAPOR CONTENT OF ADM.

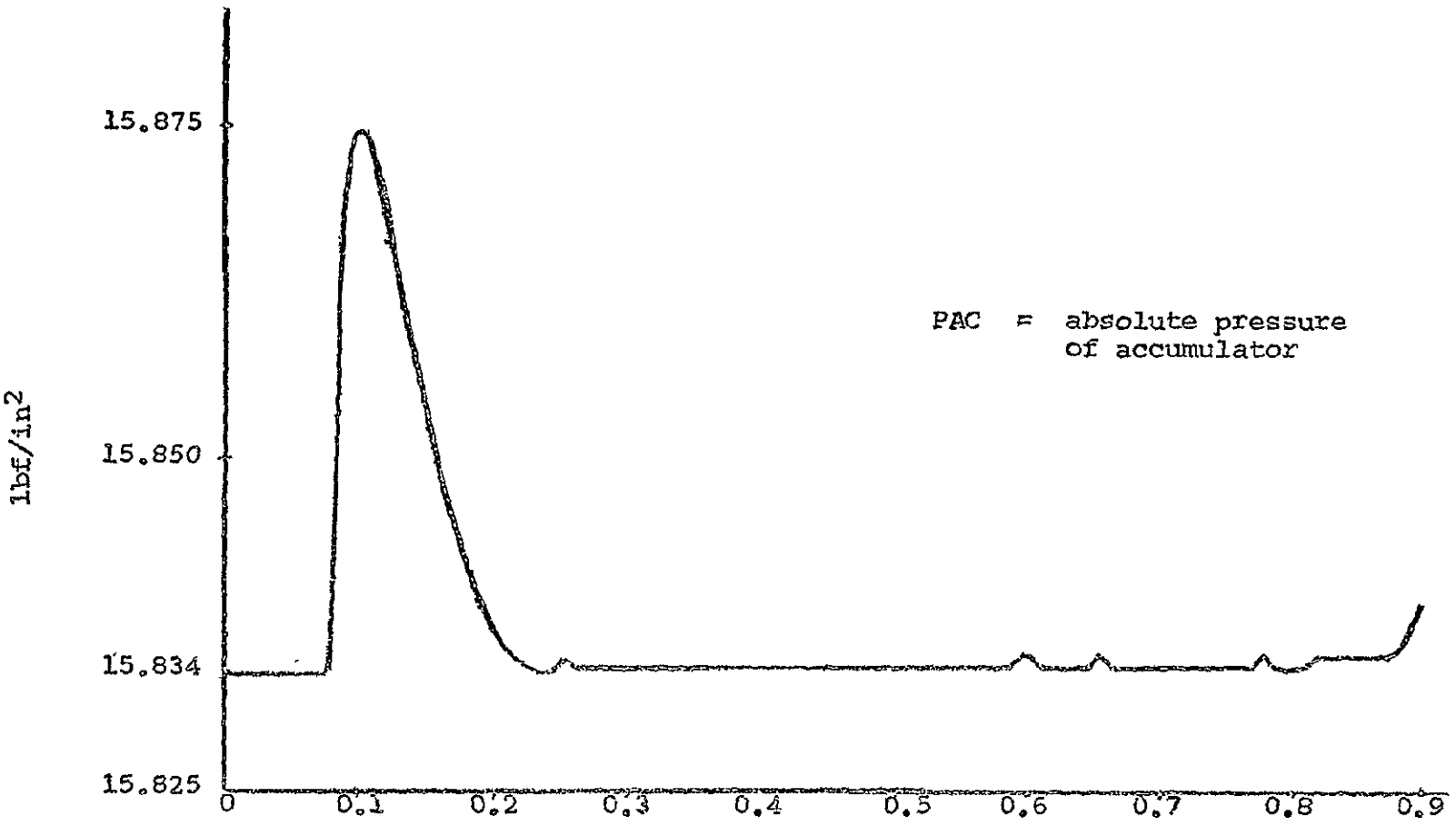

FIGURE 44. RUN B, TIME RESPONSE OF PAC.

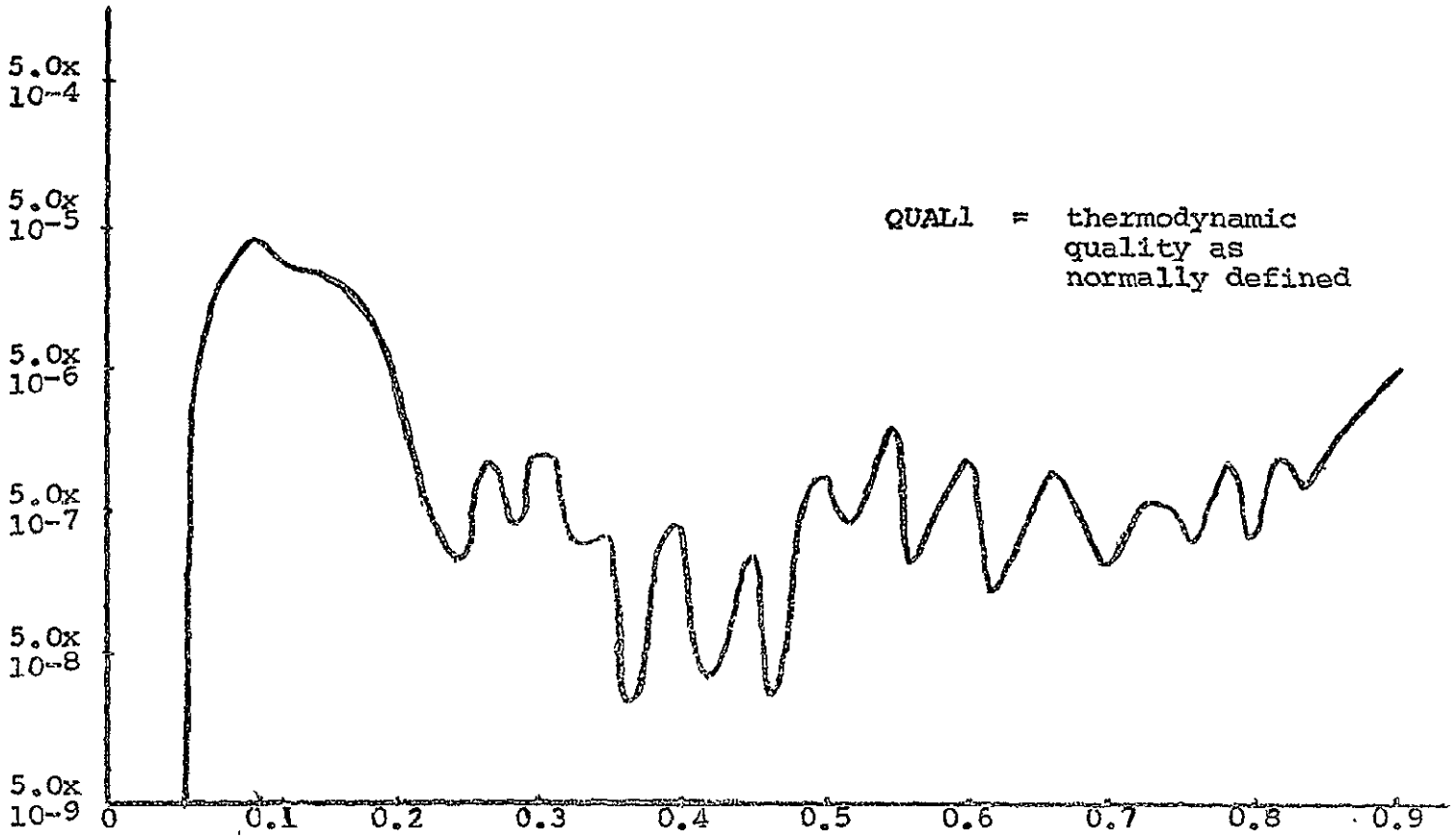

FIGURE 45. RUN B, TIME RESPONSE OF QUAL1.

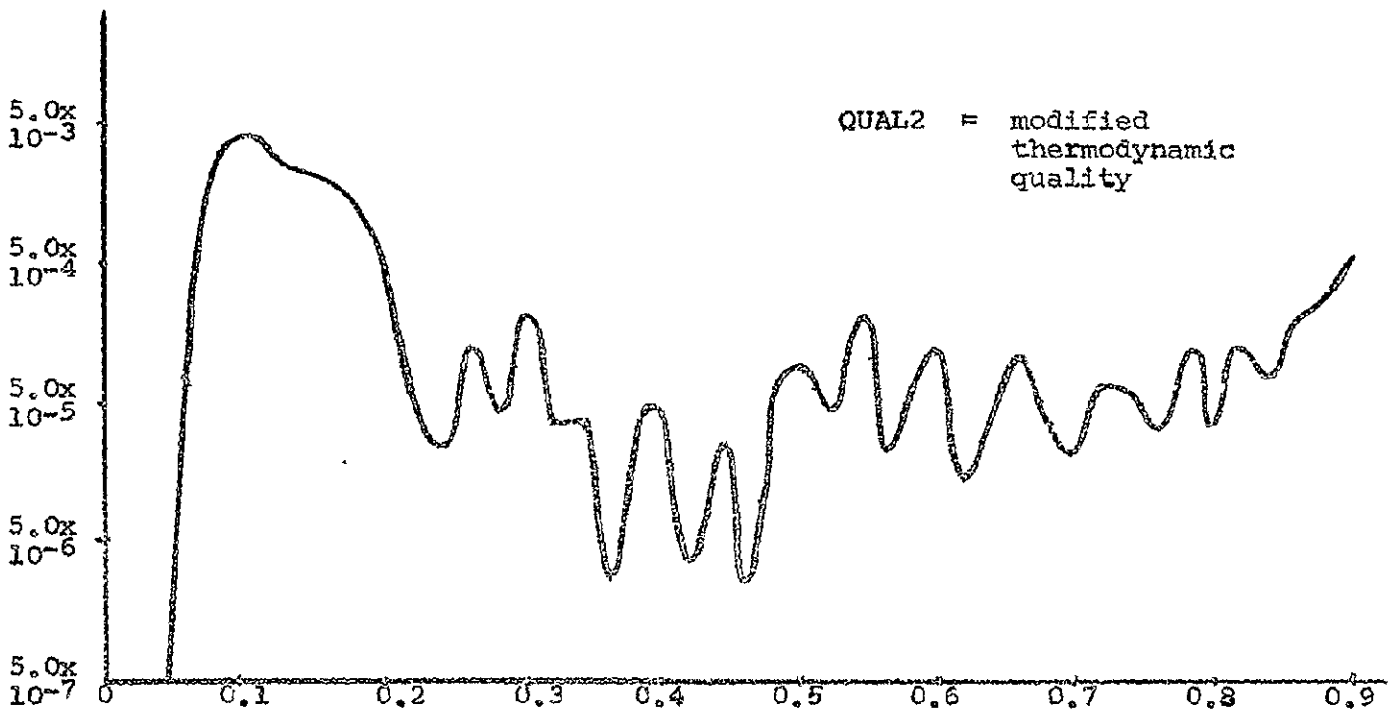

FIGURE 46. RUN B, TIME RESPONSE OF QUAL2.

CHAPTER V

CONCLUSIONS AND RECOMMENDATIONS

An idealized mathematical model of the proposed flight experiment was developed in Chapter II. The resulting system of differential and algebraic equations was then prepared in a form that was representative of the proposed system and was digitally simulated utilizing IBM's Continuous System Modeling Program. The simulation program and several of the programming techniques were developed in Chapter III. In Chapter IV the foundation for later recommendations was laid.

Throughout the thesis an effort was made to maintain a system's viewpoint while also developing the capability for studying the proposed system in considerable detail.

From the simulation of this system several comments can be made with regard to digital simulation utilizing CSMP.

CSMP is capable of handling systems which require a complex mathematical formulation to describe its functional characteristics. The implementing of physical constraints which are a function of the system state are relatively easy to incorporate into a CSMP simulation. For example, in this simulation it was required to switch-in and switch-out the appropriate equations depending upon whether the

system was in a saturated state or an unsaturated state. The price paid for these capabilities is in total computation time. For example, in order to obtain 0.9 minutes of real time simulation, it required 50 minutes of machine computation time. The mathematical description used to describe the system utilized 51 integrators and 58 function generators. It is well known that the digital computer is notoriously slow in performing numerical integration. The user of CSMP has six different integration methods from which to select. These integration methods differ in degree of complexity, and consequently, in the degree of accuracy obtainable, and the time required to perform the numerical integration. Therefore, if computation time is of prime importance, the mathematical description should be simplified, i.e., reduce the number of integrators in the simulation. Also, the use of the simpler integration methods should be investigated. The final selection of integration method will most likely depend upon a trade off between accuracy and computation time.

In the system simulated, the channel and the accumulator were the only portions of the system not thermally insulated. Due to the requirements of the experiment, the channel cannot be insulated, but no such restriction is placed on the accumulator. Therefore, the heat losses sustained in the simulated system may be considered to be maximum.

Based upon all the simulation runs and upon calculations made using 60 BTU/min heat input rate (maximum available), the proposed system is capable of producing and maintaining vapor in the porous bed.

A check was made of the coefficients of the temperature differential equations. For example, at saturation the derivative term on the left hand side of Equation 48 is constrained to be equal to zero. Then Equation 48 becomes an algebraic equation and can be solved explicitly for the temperature of the water in terms of the equation coefficients and other system temperatures. Also at saturation the water temperature is a function of pressure, and is given by Equation 49. The results obtained from comparing Equations 48 and 49 under saturated conditions compared with $3^{\circ}F$. This would indicate the coefficients of Equation 48 and similar equations are essentially correct.

From the system equations as given in Chapter II, and the results of the simulation runs, the following comments and recommendations are given:

1. The system should be preheated under pressure on the ground and sealed, because of the 60 BTU/min maximum heat input rate. By heating the system under pressure more heat energy can be stored. This is done to compensate for heat losses occurring between the time the experimental package is sealed aboard the space craft and time for the first experiment to be run.

2. The system is extremely sensitive to pressure changes due to vaporization. It may be necessary to include a separate pressure control system. This feature may possibly be incorporated into the vaporization control system after redefining the control law for this control system.

3. The design of the accumulator for this system is an important consideration. A trade off must be made between a highly pressure sensitive system and the values obtained in the measurement of the average system quality, and the use of pressure feedback to the vaporization control. If the accumulator is properly designed, then the method of vaporization control proposed in this thesis is feasible.

4. If possible, several flow-rates in the range of .5 - 1.0 gpm should be selected for the experiment. This would allow the designer of the preheater control system to set the dead-band around the thermodynamic equilibrium points as determined from the system simulation.

The digital simulation of the idealized mathematical model is sufficiently general to allow the system designers to subject the simulated system to various operating conditions as they see desirable. This would certainly aid them in the selection of physical components and the design of the various control systems.

REFERENCES

[1]Schultz, Donald G. and Melsa, James L. State Functions and Linear Control Systems, McGraw-Hill Book Company, Inc., New York, 1967, pp. 355-421

[2]Murphy, Gordon J. Basic Automatic Control Theory, D. Van Nostrand Company, Inc., Princeton, New Jersey, Second Edition, 1966, pp. 414-426.

[3]Reethof, G. "Hydraulic Components," Mechanical Design and Systems Handbook, ed. Harold A. Rothbart, Mc-Graw-Hill Book Company, Inc., New York, 1964, Section 37, pp. 1-20.

[4]Finch, Volney C. Pump Handbook, The National Press, No publishing address, 1948, p. 23.

[5]Wilson, Warren E. Positive-Displacement Pumps and Fluid Motors, Pitman Publishing Corporation, New York, 1950, pp. 25-30.

[6]Collins, Royal Eugene. Flow of Fluids Through Porous Materials, Reinhold Publishing Corporation, New York, 1961, p. 3.

[7]Evers, James Leonard. An Investigation of Two-Phase Flow Through Porous Media, Ph.D. Dissertation, University of Alabama, 1969, p. 22.

[8]Lewis, Ernest E. and Stern, Hansjoerg. Design of Hydraulic Control Systems, McGraw-Hill Book Company, Inc., New York, 1962, pp. 145-152.

[9]Brown, Charles Leonard. Basic Thermodynamics, McGraw-Hill Book Company, Inc., New York, 1951, p. 41.

[10]Merritt, Herbert E. Hydraulic Control Systems, John Wiley and Sons, Inc., New York, 1967, pp. 25-53.

[11]IBM System/360 Continuous System Modeling Program (360A-CX-16X) User's Manual - H20-0367-2.

[12]Resnick, Robert and Halliday, David. Physics - For Student of Science and Engineering Part I, John Wiley and Sons, Inc., New York, Sixth Printing, October, 1963, p. 468.

BIBLIOGRAPHY

Brown, Aubrey I. and Marco, Salvatore M. Introduction to Heat Transfer, McGraw-Hill Book Company, Inc., New York, Second Edition, 1951.

Elgerd, Olle J. Control Systems Theory, McGraw-Hill Book Company, Inc., New York, 1967.

Gibson, John E. and Tuteur, Franz B. Control System Components, McGraw-Hill Book Company, Inc., New York, 1958.

Gourishankar, Vembu. Electromechanical Energy Conversion, International Textbook Company, Scranton, Pennsylvania, 1965.

Holman, J. P. Heat Transfer, McGraw-Hill Book Company, Inc., New York, 1963.

Hughes, William F. and Brighton, John A. Fluid Dynamics, "Schaum's Outline Series," Schaum Publishing Company, New York, 1967.

Keenan, Joseph H. and Keyes, Frederick G. Thermodynamic Properties of Steam, John Wiley and Sons, Inc., New York, 1936.

Koenig, Herman E., Tokad, Kesavan and Hedges. Analysis of Discrete Physical Systems, McGraw-Hill Book Company, New York, 1967.

Kuo, Benjamin C. Automatic Control Systems, Prentice-Hall, Inc., 1962.

Reynolds, William C. Thermodynamics, McGraw-Hill Book Company, New York, 1965.

Pippenger, John J. and Hicks, Tyler G. Industrial Hydraulics, McGraw-Hill Book Company, New York, 1962.

Shinskey, F. G. Process Control Systems, McGraw-Hill Book Company, New York, 1967.

Streeter, Victor L. Fluid Mechanics, McGraw-Hill Book Company, New York, Fourth Edition, 1966.

Walters, Ronald. Hydraulic and Electro-Hydraulic Servo Systems, CRC Press, Division of The Chemical Rubber Company, Cleveland, Ohio, 1967.

Williams, Theodore J. and Lauher, Verlin A. Automatic Control of Chemical and Petroleum Processes, Gulf Publishing Company, Houston, Texas, 1961.